Abstract

BORTZ, DAVID MATTHEW. Modeling, Analysis, and Estimation of an *in vitro* HIV Infection Using Functional Differential Equations (Under the direction of H. Thomas Banks).

This dissertation focuses on developing mathematical and computational tools for use as an aid in understanding the cellular population dynamics of an *in vitro* HIV experiment. We carefully develop a functional differential equation model which incorporates mathematical mechanisms that account for both the biological delays and the parameter uncertainty inherent in the system. We present the theoretical foundations for our methodology which then allow us to develop a numerical approximation scheme and perform parameter identifications (even on the delay distributions) and sensitivity analyses. We summarize the results of a numerical investigation of the delays followed by the results from the nonlinear least squares inverse problem. We then present a statistical significance argument for the importance of the delay mechanism as well as the results of a sample sensitivity analysis of the system with respect to select parameters.

MODELING, ANALYSIS, AND ESTIMATION OF AN *IN VITRO* HIV INFECTION USING FUNCTIONAL DIFFERENTIAL EQUATIONS

BY

DAVID MATTHEW BORTZ

A DISSERTATION SUBMITTED TO THE GRADUATE FACULTY OF
NORTH CAROLINA STATE UNIVERSITY
IN PARTIAL FULFILLMENT OF THE
REQUIREMENTS FOR THE DEGREE OF
DOCTOR OF PHILOSOPHY

APPLIED MATHEMATICS

COMPUTATIONAL MATHEMATICS CONCENTRATION

RALEIGH, NORTH CAROLINA

AUGUST 2002

APPROVED BY:

H. THOMAS BANKS CHAIR OF ADVISORY COMMITTEE	MARIE DAVIDIAN
KAZUFUMI ITO	HIEN T. TRAN

To Laura Hinchman, beloved grandmother, storyteller, and friend.

Biography

The author was born in January of 1975 on the wind-swept plains of central Texas and grew up in the slightly less wind-swept cornfields of midwestern Illinois. He was raised (along with his charming younger sister) by loving parents who read to him regularly from the revered tomes of Maurice Sendak, Shel Silverstein, and Dr. Seuss. In a peripatetic education, that in some way, perhaps foreshadowed his later wanderings, the author attended no fewer than seven different institutions of learning between kindergarten and twelfth grade. In June of 1992, he graduated from Galesburg High School, to this day remaining unabashedly proud both for getting kicked off the Student Council and of his memorable (if somewhat questionable) impersonation of Franklin Roosevelt.

Following a short and relatively uneventful digression to a small midwestern liberal arts college, the author (now with ponytail) found himself with a deep-seated wanderlust. Thus, in January of 1995, he returned to his roots, journeying a thousand miles from the cornfields of his youth, landing deep in the heart of Texas. During the next two and half years of halcyon college days, the author reveled in, as some guidebook called it, the “intelligent and quirky” environment, all the while experiencing a disconcerting urge to own cowboy boots and dance

the Texas Two-step. In May of 1997, he graduated from Rice University with a Bachelor of Arts in Computational and Applied Mathematics having learned, among other things, the wisdom in always possessing a teaspoon and an open mind.

The author then began his graduate studies at North Carolina State University and during his time in Raleigh was a mathematical apprentice to an evangelical numerical analyst, a former ski bum, and a fast talking hurricane with a penchant for quoting Lewis Carroll during control theory lectures. Following the appropriate gestation period, which included some radiant, yet ephemeral, purple hair and the acquisition of two earrings, the author finally defended his dissertation in August of 2002.

In spite of the prospect of more midwestern winters, he has accepted a position as an Assistant Professor in the Department of Mathematics at the University of Michigan-Ann Arbor. And therefore, beginning in the Fall of 2002, the author will *finally* have a *real job* (much to the relief of his parents and grandparents).

Acknowledgments

As with any endeavor of this nature, my studies did not occur in a vacuum and thus there are a multitude of individuals to whom I am greatly indebted. First and foremost, as my advisor and mathematical father figure, Dr. Banks has played a pivotal role in my education and without him, this dissertation would not have been possible. I am and will be forever grateful for his guidance and advice.

Over the course of my tenure as a graduate student at NCSU there have been many who have aided me on this long strange trip including: Alan Cain, Marie Davidian, Sarah Holte, Kazufumi Ito, Tim Kelley, and Hien Tran, and I am immensely grateful to each of them.

I thank my parents for all their love, support, and understanding over the last 27 and a half years. Most importantly, I thank them for not hanging up during a certain phone conversation that began, “Mom, Dad, I’m going to transfer to Rice.” I thank my sister Sarah for scintillating conversations over brunch, the best birthday and Christmas presents, and knowing where the wild things are. This dissertation is dedicated to my maternal grandmother, Laura Hinchman, who has always been a source of inspiration for me, both as a role model and hero.

I would also like to thank those individuals whose brilliant and tireless efforts at crafting

free software have helped to make my computer truly a joy to use: Matthias Ettrich (LyX [62]), Donald Knuth (TEX [52]), Larry McVoy (BitKeeper [15]), Richard Stallman (GNU [32]), and Linus Torvalds (Linux [57]).

Finally, in a particular and very specific order (the analysis and interpretation of which I leave as an exercise to the reader), I present a list of email address aliases of those to whom I am grateful for their friendship: fig (who fixes life when it is broken), noahr (fellow collaborator on seals, seagulls, and Dilbert Spaces), tenny (a friend who knows the importance of a good porch), glee (future Hollywood bigshot), kkdyer (one of the classiest people I know), ckuster (fellow Linux zealot and frisbee golf partner; mortal enemy on the Island of Catan), sandy (fellow knoxie and Babylon 5 fan), julie (who hopefully received wise and sagely advice from Elvis the Oracle), z (hrmmmmmmm), v (bear left, right frog), may (friend of George O. and partner in Debian zealotry; other mortal enemy on the Island of Catan), kara (aka Eco Spice), rachel (hi Mimi ☺), kevin & mindy (hey pacque way!), jneal (life is indeed short, far too short), rory (who likes my blue, but not-so-suede shoes), and brenda (one of the great philosopher-secretaries of our time). These kind souls have helped me maintain an understanding of the truth that (as Oscar Wilde would have said)

Life is far too important to be taken seriously.

Contents

List of Tables

List of Figures

Chapter 1

Introduction

Viruses are obligate intra-cellular parasites with a multitude of pathways for infecting and reproducing within their target hosts. The Human Immunodeficiency Virus (HIV) is a lentivirus that is the etiological agent for the slow, progressive, and fatal Acquired Immunodeficiency Syndrome (AIDS) to which there is currently no known cure. According to a Joint United Nations Programme on HIV/AIDS June 2000 report, there were approximately 34.3 million individuals infected with HIV/AIDS worldwide at the end of 1999, including 24.5 million in sub-Saharan Africa [80]. Thus, HIV-related illness and death is and will continue to be an important clinical and public health issue as well as an international security, stability, and development issue. Clearly it is imperative that we attain a greater understanding of HIV/AIDS viral infection dynamics.

1.1 Overview

In this chapter, we present a basic overview of HIV and its pathogenesis along with a survey of recent mathematical methods used to study the virus. We also present brief histories of two useful tools that we will employ in our approach. In Chapter 2, we present the development of a mathematical model designed to describe the viral infection dynamics of an HIV *in vitro* experiment [82]. An important and nontrivial aspect of modeling the HIV pathogenesis is deciding how to mathematically describe the delay between viral infection and production, and indeed a significant portion of Chapter 2 is devoted to this topic. Following the development of this model, in Chapter 3 we present a rigorous mathematical analysis including: an existence and uniqueness proof for a solution to the model (Section 3.1.1), a numerical scheme based upon an Abstract Evolution Equation approach (Section 3.1.2), and well-posedness results for the inverse problem (Section 3.2) as well as the sensitivity equations (Section 3.3). With this mathematical framework, we then present in Chapter 4 the results of applying these tools toward understanding the aforementioned *in vitro* experiment. The primary goal of this dissertation is to showcase the power and utility of theses advanced mathematical methods and approaches as an aid in the developing of new insights into HIV pathogenesis.

1.2 Background

1.2.1 The Human Immunodeficiency Virus

For HIV, the core of the virus is composed of single-stranded viral RNA and protein components. As depicted in Figure 1.2.1, when an HIV virion comes into contact with an uninfected target cell, the viral envelope glycoproteins fuse to the cell's lipid bilayer at a CD4 receptor site and the viral core is injected into the cell. Once inside, the protein components enable transcription and integration of the viral RNA into viral DNA and then incorporation into the cellular DNA (provirus). With its altered cellular DNA, the cell produces capsids and protein envelopes and transcribes multiple copies of viral RNA. The cell assembles a virion by then encasing the viral RNA in a capsid followed by a protein envelope. The new HIV virion pushes out through the cell membrane budding off in chains of virions (though sometimes single virions do float away into the plasma). Clearly the time from viral infection to viral production (sometimes called the *eclipse phase* [70]) is not instantaneous, and (as indicated in the figure) it is estimated that the first viral release occurs approximately 24 hours after the initial infection [28, 66]. As mentioned before, the development of mathematical models and the associated numerical techniques that incorporate these delays into models for HIV infection dynamics is a primary motivation for our efforts here.

Within the HIV modeling community, there is considerable debate upon the proper compartment definitions. It is not our goal to advocate one model over another and as such we will simply choose one with which we illustrate our methodology. The multi-compartment model

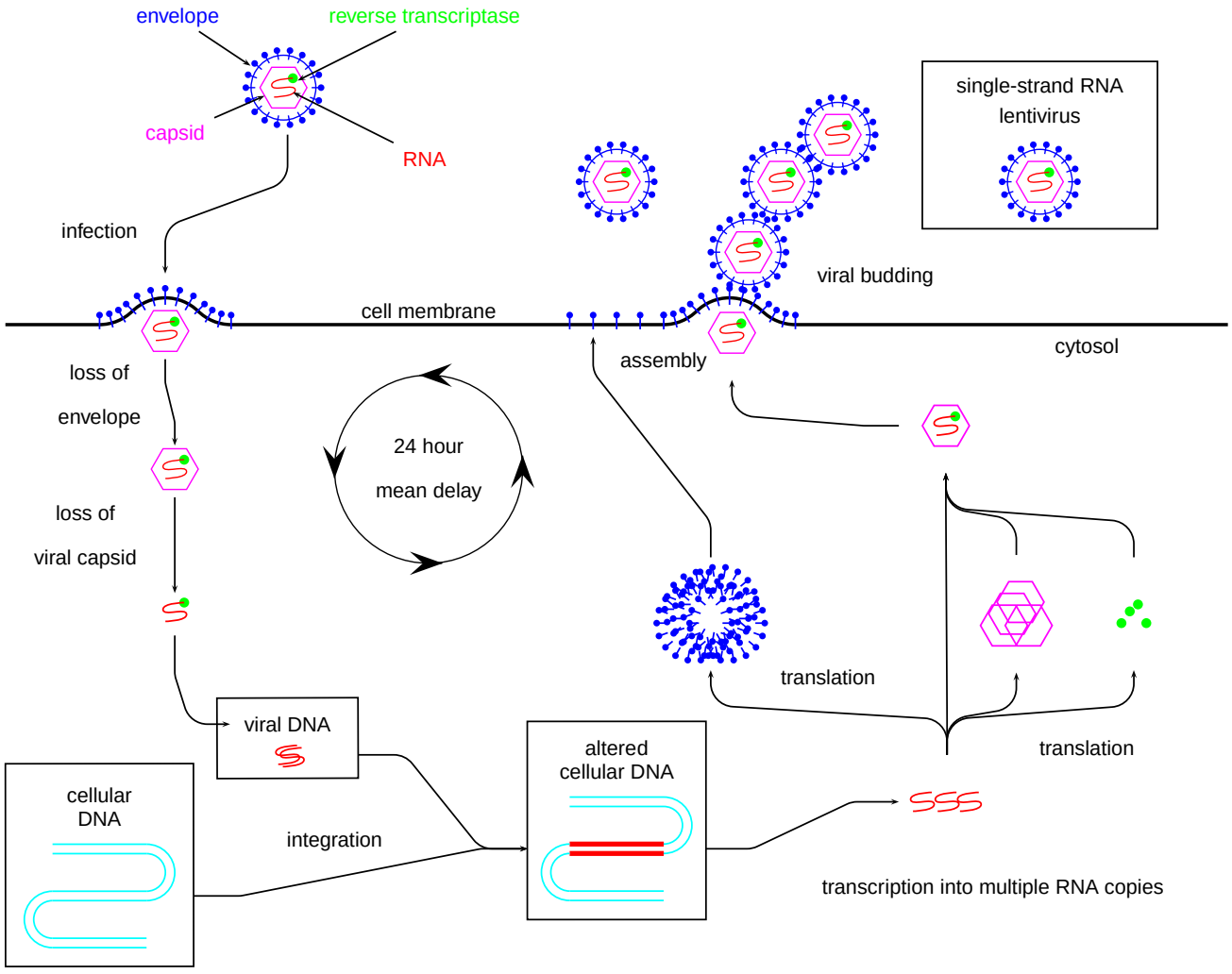

Figure 1.2.1: HIV Infection Pathway

that we use (and discuss in detail in Section 2.1) describes the moment a virion contacts the appropriate receptor site as the beginning of *acute infection*. If the acutely infected cell survives through its first viral release, roughly 3 hours later the physiological characteristics of the cell change and it is subsequently classified as a *chronically infected* cell. Note that in the chronic stage, it is possible for the cells to continue to divide and to produce virions, albeit at a much slower rate than acutely infected or non-infected cells.

1.2.2 Mathematical Models of HIV

Over the past 7 years, the use of mathematical models as an aid in understanding features of HIV and other virus infection dynamics has been substantial. Several papers published in the mid nineties provided strong evidence for the high rate of HIV-1 replication and clearance in infected individuals [43, 78, 94]. By the end of the decade, the general consensus was that *in vivo*, on the order of 10^{10} virions are assembled and cleared every day [65, 76, 81]. In many of these papers, the viral clearance rate c was identified by modeling the disease pathogenesis with a system of deterministic differential equations, numerically calculating a solution, and then fitting the results with experimental data (using a nonlinear least squares (NLS) approach), e.g., see [76, 78, 81]. The existence of such a high replication/clearance rate implies a high mutation rate, thus indicating that pharmacological mono-therapy will ultimately fail, since the virus can rapidly manifest a resistance to any one drug. More importantly, this knowledge directly contributed to the current practice of simultaneously administering multiple drugs to HIV positive individuals in an effort to counteract the high mutation rate of the virus.

Following its success in helping to identify this significant feature of the HIV pathogenesis, the use of mathematical modeling and parameter identification in the study of HIV experienced a dramatic increase. In particular, in the wake of the publication of [78], there were papers covering everything from additional and/or alternative compartment formulations [19, 53, 67, 69, 73, 79, 83, 95, 99, 100] to arguments for and against the use of delay differential equations in modeling the eclipse phase [38, 39, 42, 58, 66, 70, 71, 72] (including those that addressed the solution stability [23, 71, 72, 87]). As mentioned before, our approach is to develop tools which, hopefully, will allow one to develop new insights into HIV pathogenesis. Indeed, there is a precedence for this approach, as is evidenced by previous papers within the HIV modeling literature that make use of stochastic analysis and inference [48, 88, 89, 92, 97, 101], control theory [50, 96], and nonlinear analysis [40, 93]. Note that the above survey is not intended to be comprehensive, as there already exist thorough reviews of the field presented in [74, 75, 77].

Within the context of delay equations, many of the aforementioned papers focused heavily on the inter-relationship between the parameters describing the drug efficacy η, the length of the eclipse phase τ, the infected T-cell death rate δ, and the virion clearance rate c [38, 42, 58, 66, 70, 71, 72, 87]. One approach to numerically simulating these systems with delays is sometimes referred to as the *method of stages* and is described in [21, 47, 58, 59, 66, 72]. Indeed, several researchers have used this technique to simulate delay ODE models of HIV and argue that the inclusion of delays in the viral production of infected cells dramatically changes estimates of specific parameters. For example, Grossman, et. al., [38] argue that including a delay in the model for the death of infected cells leads to different conclusions regarding

residual transmission of infection (during antiviral pharmaceutical therapy), while Lloyd [58] argues that an absence of delays in the model leads to (as we now know suspiciously) optimistic conclusions about treatment efficacy. Clearly an accurate model for the delay is important, and in Section 2.1, we carefully describe a way to properly develop a model for the delay that accounts for many of its biological aspects.

All of the cited papers which include delays in their models represent them using a gamma distribution (or Erlang distribution [47]) to describe a distribution of delays, and thus can reduce the resulting system of integro-differential equations to a system of (non-delayed) ordinary differential equations. This non-delayed system can easily be simulated using standard numerical integration techniques (e.g., Runge-Kutta) in standard mathematical software. An alternative method (an implementation of which is presented in Section 3.1.2) that first converts a delay system into an abstract evolution equation (before numerical simulation) is described in [3, 8, 10]. This approach allows for simulation of systems with general delay kernels describing the delay distributions, and does not require that the model be reduced to a system of non-delayed ODEs.

As is clear from this discussion, there is no dearth of interesting mathematical topics to address. However, we will concentrate on the mathematical modeling of the viral dynamics (primarily focusing on the mathematical aspects and biological nature of the delays), along with developing appropriate tools for solving both the forward and the inverse problem.

1.2.3 Delay Equation Survey

In the course of developing our model, we employ a delay to mathematically represent the temporal lag between the initial viral infection and the first release of new virions. The study of delay equations has a long history in fields as disparate as economics [34] and ecology [45], with some early applications in engineering found in research concerning the stability of naval vessels [64]. Furthermore, there has also been extensive use of delay equations in modeling biological systems and indeed both May's and Murray's classic texts ([63] and [68] respectively) have a significant sections devoted to delay equations. For the interested reader, there are solid introductory texts [12, 26] (including those that focus heavily on applications to biological systems [24, 54]) and thorough (if somewhat theoretical) advanced texts [25, 37, 41].

1.2.4 Sensitivity Analysis Survey

For *any* system of differential equations designed to model real world phenomena, whether it be biological, chemical, or physical, a common goal is to understand the manner in which the system's constitutive parameters influence its solution. These parameters are designed to correspond to aspects of the phenomena under investigation (e.g., HIV pathogenesis), and thus it is desirable to predict how changes in the parameters will affect the solution. Indeed, there are several papers in the HIV modeling field which focus heavily on the topic (good examples include [83, 85]). One way to address this question is to perform a *sensitivity analysis*, a mathematical tool developed in the context of modern control theory and commonly used in mechanical, aerospace, electrical, and structural engineering. The precursor of this technique

can be traced back to an 1833 electrostatics experiment designed to measure the inductance of certain metals [20]. However, significant activity in this area only arose in the middle part of this century, concomitant with the development of modern control theory in the late 1930's. In our analysis, we will be employing the *semirelative* sensitivity function, though there are other possibilities, such as the *logarithmic* sensitivity function advocated by Bode in his book on electrical network analysis [16]. We direct the interested reader to the following introductory texts [30, 31], advanced texts [51, 90, 91, 98], and surveys of the field [1, 22]. We also note that the sensitivity analysis described here should not be confused with a statistical technique of the same name and based on Latin Hypercube Sampling [46].

Chapter 2

Model Development

2.1 Basic Development

At the 2000 Industrial Mathematics Modeling Workshop for Graduate Students at NCSU S. E. Holte of the Fred Hutchinson Cancer Research Center presented a problem concerning HIV pathogenesis. The problem focused on studying an experiment with two strains (Vpr+/-) of the retrovirus. The expression of the Vpr protein by HIV arrests the cell in the G2 phase of reproduction (immediately before mitosis), preventing division of the infected cell and thus restricting cell proliferation [27]. Mutants of the HIV strain exhibiting an inactive Vpr gene (Vpr-), have been found in *in vitro* cultures, where they consistently outgrew the Vpr+ strain, yet the genotypes of nearly all *in vivo* isolates were encoded for a functional Vpr gene [36]. Our research was initially driven by a desire to aid developing a deeper understanding of this phenomena.

Previous work on the competitive relationship between the *in vitro* and *in vivo* dominant

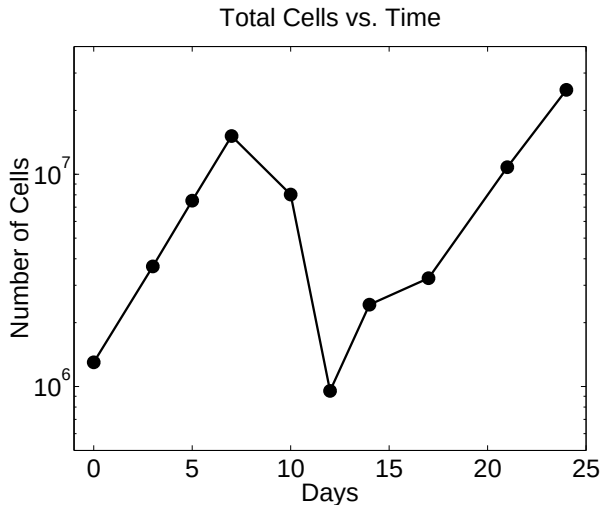

Figure 2.1.1: Log plot of experimental data (10 observations) from [82].

strains of the virus is presented in the context of a difference equation model (depicted below in equation (2.1.2)) in [44]. However, we were not confident in the mathematical description of this complex system developed during the workshop (a summary of which is presented in [18]) and thus in all our subsequent efforts, we focus on studying (with suitable mathematical modeling tools) a simpler *in vitro* experiment with only one strain (Vpr-) of the retrovirus. The data from this study [82] is depicted on a log plot (note the exponential growth) in Figure 2.1.1 and consists of measurements of the total number of cells in a culture at various times after infection with HIV. Furthermore, we were concerned about the appropriateness of using a non-delayed difference equation model to represent an experiment of this type and thus transformed the model to a differential equation (eventually including both delays and random effects).

As mentioned in Section 1.2.1, there is considerable debate among the HIV modeling community with regard to the best compartment definitions. The variables and their respective compartments we have chosen to employ are depicted in Table 2.1, while the corresponding

parameters are depicted in Table 2.2. We began our studies with the system of difference equations (based upon those in [44]) for the Vpr- strain

$$\begin{aligned} V_{n+1} &= e^{-c}V_n + n_A A_n + n_C C_n \\ A_{n+1} &= e^{\left(r-\delta_A-\delta X_n\right)}A_n + \left(1-e^{-pV_n}\right)T_n \\ C_{n+1} &= e^{\left(r-\delta_C-\delta X_n\right)}C_n + (1-e^{-\gamma})A_n \\ T_{n+1} &= e^{(r-\delta_u-\delta X_n-pV_n)}T_n + S\,, \end{aligned} \tag{2.1.1}$$

where n is a positive integer and then transformed them to a system of ordinary differential equations

$$\begin{aligned} \dot{V}(t) &= -cV(t) + n_A A(t) + n_C C(t) - pV(t)T(t) \\ \dot{A}(t) &= \left(r_v - \delta_A - \gamma - \delta X(t)\right)A(t) + pV(t)T(t) \\ \dot{C}(t) &= \left(r_v - \delta_C - \delta X(t)\right)C(t) + \gamma A(t) \\ \dot{T}(t) &= \left(r_u - \delta_u - \delta X(t) - pV(t)\right)T(t) + S\,, \end{aligned} \tag{2.1.2}$$

for t the continuous independent time variable with $0 \le t \le t_f$ and t_f finite. Note that in the first equation, we also added the $-pV(t)T(t)$ term, which is designed to account for the biological fact that upon infecting a cell, a virion is unable to infect additional target cells.

Notation	*Description*
V	Infectious viral population
A	Acutely infected cells
C	Chronically infected cells
T	Uninfected or target cells
X	Total cell population (infected and uninfected) $(A+C+T)$

Table 2.1: *in vitro* model compartments

Models possessing this term are inherently different from many *in vivo* models in which the (large) number of target cells is assumed to be constant. If over the time scale of interest, the T variable were a constant T_0 (such as in [66, 71, 77]), the equation would then be

$$\dot{V}(t) = -\left(c + pT_0\right)V(t) + n_A A(t) + n_C C(t)$$

and we could define a new coefficient $c' = c + pT_0$ for the $V(t)$ term. For our *in vitro* model, we do not have this situation, as the target cell population is not replenished and thus not held constant in the experiment. In other computational results (not reported on here), we omitted the $-pV(t)T(t)$ term from the first equation of the delay system (which is fully developed in the next section and then used throughout the rest of our research) and were also able to attain reasonable fits for our limited data set (albeit with different parameters in the models) along with statistically significant results analogous to those reported in Section 4.2.

We also call attention in (2.1.2) to the form of the nonlinear terms (e.g., $pV(t)T(t)$). Terms such as $pV(t)T(t)$ are obviously only first approximations to the density dependent (on V and T) component of the rate of new infections. A more realistic model requires that this term,

Notation	*Description*
c	Infectious viral clearance rate
n_A	Infectious viral production rate for acutely infected cells
n_C	Infectious viral production rate for chronically infected cells
γ	Rate at which acutely infected cells become chronically infected
r_v	Birth-rate for virally infected cells
r_u	Birth-rate for uninfected cells
δ_A	Death-rate for acutely infected cells
δ_C	Death-rate for chronically infected cells
δ_u	Death-rate for uninfected cells
δ	Density dependent overall cell death-rate
p	Rate of infection
S	Constant rate of target cell replacement

Table 2.2: *in vitro* model parameters

dependent on both $V(t)$ and $T(t)$, be bounded in the limit, i.e., saturation should be modeled in the nonlinear term so that in the limit it is (at least) affine in V or T. While we use this term in our analysis below, for well posedness considerations the term pVT is more appropriately replaced by a function $p(V,T)$ where $(V,T) \mapsto p(V,T)$ is globally Lipschitz (see [3] for the standard form of this assumption). However, for our initial purposes in modeling discussions, the simpler term will suffice.

2.2 Model Derivation

It is biologically unrealistic to expect an entire population of cells to simultaneously change infection characteristics, whether that be from non-infected to productively infected or from acutely infected to chronically infected. In this section we closely examine the various delays

encountered during the viral pathogenesis and present a derivation from first principles (with assumptions based on the biology) that supports a version of system (2.1.2) that treats the delays as random variables.

Let us first consider the delay between initial acute infection and initial chronic infection of a cell and assume that this change occurs $\bar{\mu}_2$ $(\bar{\mu}_2 > 0)$ hours after initial viral infection.[1] Suppose that the delay between initial acute infection and chronic infection varies across the cell population (thus mathematically characterizing the inter-cellular variability) according to a probabilistic distribution $\bar{P}_2(\tau)$ for $\tau \in [0,\infty)$. We denote by $C(t;\tau)$ the subpopulation consisting of chronically infected cells that either maintained their acute infection characteristics for τ time units or are the progeny of those same cells. In other words, for some $\tau > 0$, there exists a subpopulation $C(t;\tau)$ of the chronically infected cells which either spent τ hours as acutely infected cells (before converting to chronically infected cells) or are descendants of cells that spent exactly τ hours as acutely infected cells. Thus, the rate of change in this subpopulation of cells is governed by

$$\dot{C}(t;\tau) \quad = \quad \big(r_v - \delta_C - \delta X(t)\big) C(t;\tau) + \gamma A(t-\tau)\,,$$

where

$$X(t) = A(t) + C(t) + T(t)$$

[1] The choice of the notation $\bar{\mu}_2$ will (hopefully) become clearer after the derivation is complete.

and the expected value of the population of chronic cells is given by integrating over the distribution $\bar{P}_2$, over all possible delays, obtaining

$$C(t) \quad = \quad \mathscr{E}_2\left[C(t;\tau)\right] \quad = \quad \int_0^\infty C(t;\tau)d\bar{P}_2(\tau)\,. \tag{2.2.1}$$

From a probability theory point of view, we are treating the quantity τ as a random variable. Therefore, the rate of change in the total population of chronic cells is governed by

$$\begin{aligned} \dot{C}(t) \quad &= \quad \mathscr{E}_2\left[\dot{C}(t;\tau)\right] \\ &= \quad \left(r_v - \delta_C - \delta X(t)\right)C(t) + \gamma\int_0^\infty A(t-\tau)d\bar{P}_2(\tau) \\ C(0) \quad &= \quad C_0\,, \end{aligned} \tag{2.2.2}$$

where C_0 is the initial condition for the total chronically infected cell population.

Next, we consider the delay between viral infection and viral production for the acutely infected cells $A(t)$. Again, it is unreasonable to expect the entire population of acutely infected cells to simultaneously commence viral production $\bar{\mu}_1$ $(\bar{\mu}_1 > 0)$ hours after infection. We suppose that the delay between infection and production (for acutely infected cells $A(t)$) varies across the population with probability distribution $\bar{P}_1$. When considering the viral population, we first partition the expected total viral population V into those virions V_A produced by acutely infected cells and those virions V_C produced by chronically infected cells so that

$$V = V_A + V_C\,.$$

We then denote by $V_A(t;\tau)$ the subpopulation of virus which are produced by an acutely infected cell τ hours after being infected. Thus, the rate of change in this subgroup of virions is governed by

$$\dot{V}_A(t;\tau) \quad = \quad -cV_A(t;\tau) + n_A A(t-\tau) - pV_A(t;\tau)T(t)\,.$$

To obtain the (expected) number of virus at time t that have been produced by acutely infected cells, we must integrate over the distribution $\bar{P}_1$, over all possible delays

$$V_A(t) = \mathscr{E}_1[V_A(t;\tau)] = \int_0^\infty V_A(t;\tau)d\bar{P}_1(\tau)\,,$$

which yields the governing equation for this larger subpopulation of virions

$$\begin{aligned}\dot{V}_A(t) \quad &= \quad \mathscr{E}_1[\dot{V}_A(t;\tau)] \\ &= \quad -cV_A(t) + n_A\int_0^\infty A(t-\tau)d\bar{P}_1(\tau) - pV_A(t)T(t)\,.\end{aligned}$$

To account for the chronically infected cells as a source of virions, we denote V_C as the subpopulation of virions produced by chronically infected cells. Thus the equation describing the rate of change in the size of this subpopulation is

$$\dot{V}_C(t) \quad = \quad -cV_C(t) + n_C C(t) - pV_C(t)T(t)\,,$$

where the expected value C of the total population of chronically infected cells is defined in

(2.2.1). Therefore, the governing equations for the total population of virus are described by

$$\begin{aligned}
\dot{V}(t) &= \mathscr{O}_1[\dot{V}_A(t;\tau)+\dot{V}_C(t)] \\
&= -c(V_A(t)+V_C(t))+n_A\int_0^\infty A(t-\tau)d\bar{P}_1(\tau)+n_C C(t)-p(V_A(t)+V_C(t))T(t) \\
&= -cV(t)+n_A\int_0^\infty A(t-\tau)d\bar{P}_1(\tau)d\tau+n_C C(t)-pV(t)T(t) \\
V(0) &= V_0\,,
\end{aligned}$$

where V_0 is the initial condition for the total virions population.

Moreover, we assume that the A and T subclasses have no subpopulation structures, and are therefore governed by

$$\dot{A}(t) = \big(r_v-\delta_A-\delta X(t)\big)A(t)-\gamma\int_0^\infty A(t-\tau)d\bar{P}_2(\tau)+pV(t)T(t) \tag{2.2.3}$$

$$A(0) = A_0 \tag{2.2.4}$$

$$\dot{T}(t) = (r_u-\delta_u-\delta X(t)-pV(t))\,T(t)+S \tag{2.2.5}$$

$$T(0) = T_0\,, \tag{2.2.6}$$

with initial conditions A_0 and T_0. Note that in (2.2.3), the rate term with the delay (representing the delayed conversion of A to C) is simply the negative of the delay rate term in (2.2.2).

Finally, we make the change of variables $P_i(\xi)=\bar{P}_i(-\xi)$ so that the distributions are now

defined on $(-\infty, 0]$ instead of $[0, \infty)$,[2] and obtain the system

$$\dot{V}(t) = -cV(t) + n_A \int_{-\infty}^{0} A(t+\tau) dP_1(\tau) + n_C C(t) - pV(t)T(t) \quad (2.2.7)$$

$$\dot{A}(t) = \big(r_v - \delta_A - \delta X(t)\big) A(t) - \gamma \int_{-\infty}^{0} A(t+\tau) dP_2(\tau) + pV(t)T(t) \quad (2.2.8)$$

$$\dot{C}(t) = \big(r_v - \delta_C - \delta X(t)\big) C(t) + \gamma \int_{-\infty}^{0} A(t+\tau) dP_2(\tau) \quad (2.2.9)$$

$$\dot{T}(t) = (r_u - \delta_u - \delta X(t) - pV(t)) T(t) + S\,. \quad (2.2.10)$$

Clearly the problem of how to mathematically represent these phenomena is decidedly nontrivial and includes issues such as how to account for intra-individual variability (e.g., inter-cellular variability arising within a single infected individual or laboratory assay) and/or inter-individual variability arising between individual subjects or data from multiple assays. We have attempted to account for these concerns here, but it is important to remember that this model, and all subsequent modifications, were designed with the primary goal of gaining a deeper understanding of *in vitro* experiments (such as those described in [82]). Thus, our model and discussions here deal exclusively with the simulation of and goodness of fit to *in vitro* data. Conversely, we do wish to develop approaches that may be used as an aid in understanding *in vivo* phenomena and thus we have endeavored to design our methods with sufficient flexibility to accommodate information (from HIV infected subjects) concerning the inter-individual and intra-individual delay time variability.

[2] We do this to be consistent with the notation of Section 3.1.2 which is standard in the functional differential equation (FDE) literature.

2.3 Delay Issues

As a central focus of our modeling effort has been on attempting to obtain reasonable mathematical representations of these delays, we now consider some of the practical implications of this approach. Also note that in the subsequent discussions in this section (and indeed the rest of this document), all numerical simulations for each of the systems of functional differential equations (FDE) given above were performed using the methods described in Section 3.1.2.

2.3.1 Relevance of Delay

Consider the system of equations (2.2.7)-(2.2.10) with P_1, P_2 representing the distributions of the delays between acute infection and viral production and between acute infection and chronic infection, respectively. For $\tau_1, \tau_2 > 0$, if we assume Heaviside distributions with unit jumps at $-\tau_1 < 0$ and $-\tau_1 - \tau_2 < 0$ for P_1, P_2, respectively, the system reduces to

$$\dot{V}(t) = -cV(t) + n_A \int_{-\infty}^{0} A(t+\tau)\delta_{-\tau_1}(\tau)d\tau + n_C C(t) - pV(t)T(t) \tag{2.3.1}$$

$$\dot{A}(t) = \big(r_v - \delta_A - \delta X(t)\big)A(t) - \gamma \int_{-\infty}^{0} A(t+\tau)\delta_{-\tau_1-\tau_2}(\tau)d\tau + pV(t)T(t) \tag{2.3.2}$$

$$\dot{C}(t) = \big(r_v - \delta_C - \delta X(t)\big)C(t) + \gamma \int_{-\infty}^{0} A(t+\tau)\delta_{-\tau_1-\tau_2}(\tau)d\tau \tag{2.3.3}$$

$$\dot{T}(t) = \big(r_u - \delta_u - \delta X(t) - pV(t)\big)T(t) + S\,, \tag{2.3.4}$$

where $\delta_{-\tau}$ is a Dirac delta "density" with atom at $-\tau$. The evaluation of these integrals results in a system of non-distributed delay differential equations

$$\begin{aligned}
\dot{V}(t) &= -cV(t) + n_A A(t-\tau_1) + n_C C(t) - pV(t)T(t) \\
\dot{A}(t) &= \big(r_v - \delta_A - \delta X(t)\big)A(t) - \gamma A(t-\tau_1-\tau_2) + pV(t)T(t) \\
\dot{C}(t) &= \big(r_v - \delta_C - \delta X(t)\big)C(t) + \gamma A(t-\tau_1-\tau_2) \\
\dot{T}(t) &= (r_u - \delta_u - \delta X(t) - pV(t))\,T(t) + S\,,
\end{aligned} \tag{2.3.5}$$

for $0 \le t \le t_f$ where t_f finite. We have made this simplification to emphasize the importance of the delay in accurately modeling the pathogenesis and thus illustrate this point in Figure 2.3.1, which depicts simulations of the system (2.3.5) with and without discrete delays (i.e., $\tau_1 = 24$ and $\tau_2 = 3$ in (2.3.5)). Both the undelayed system solutions and the delayed system solutions were computed for $N = 32$ (where N, a positive integer, is the index of approximation, with larger values corresponding to higher accuracy, as explained below in Section 3.1.2) with the parameters described in Tables 2.2, 4.1, and 4.2 and initial conditions matching the experiment from [82]. Clearly, the presence of nonzero delays has a dramatic effect upon the simulation, and indeed this plot was the first indication that our efforts regarding an accurate mathematical characterization of the delay were justified (further evidence in the form of a statistical significance argument is presented in Section 4.2).

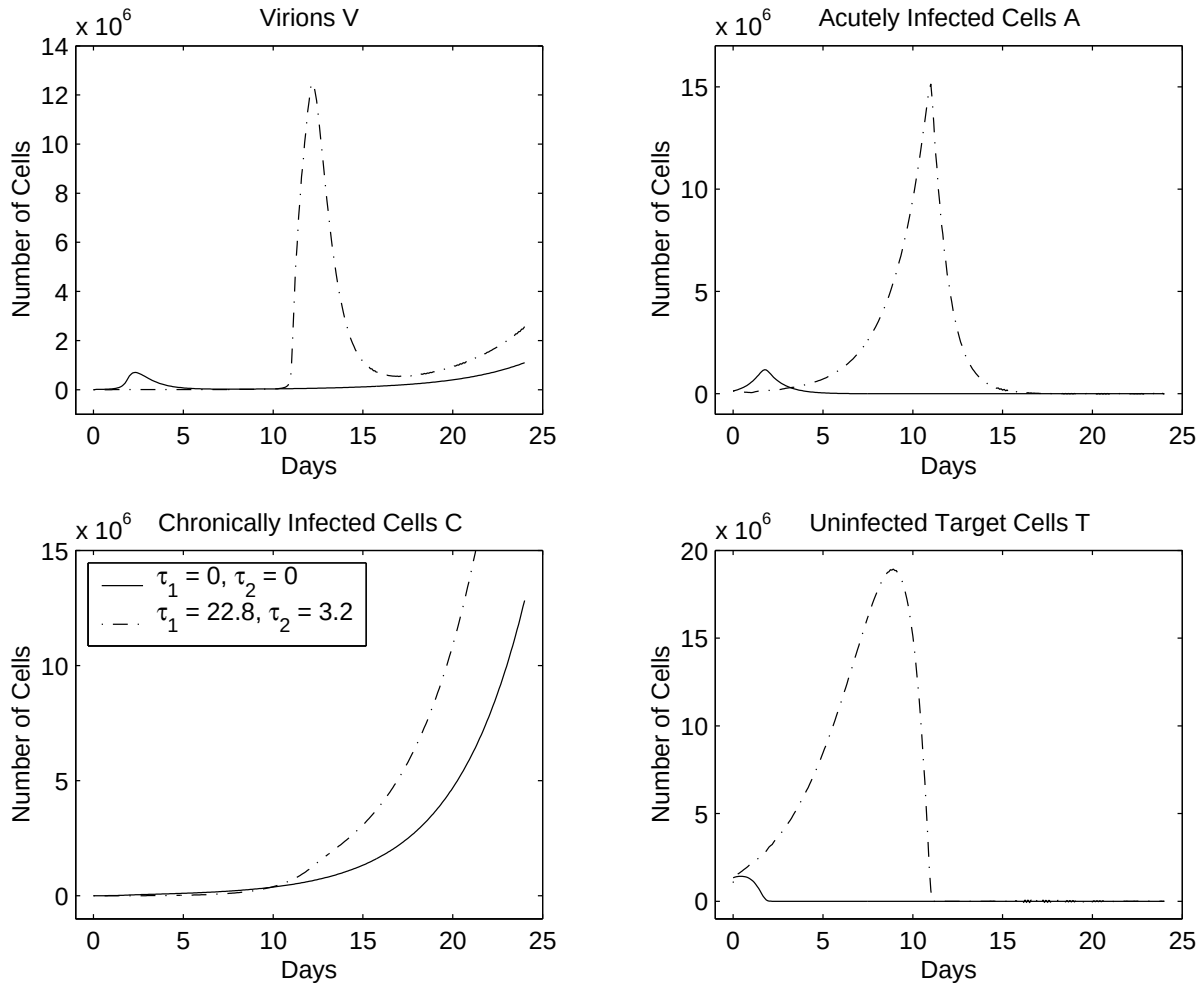

Figure 2.3.1: Simulations of system (2.3.5) with ($\tau_1 = 24$, $\tau_2 = 3$) and without ($\tau_1 = 0$, $\tau_2 = 0$) discrete delays.

2.3.2 Gamma Distribution Issues

If we assume that P_1, P_2 are $\mathscr{C}^1(-\infty, 0; \mathbb{R})$ with probability densities (also known as kernels) k_1, k_2, respectively, the system in (2.2.7)-(2.2.10) becomes

$$\dot{V}(t) = -cV(t) + n_A \int_{-\infty}^{0} A(t+\tau)k_1(\tau)d\tau + n_C C(t) - pV(t)T(t) \quad (2.3.6)$$

$$\dot{A}(t) = \big(r_v - \delta_A - \delta X(t)\big)A(t) - \gamma \int_{-\infty}^{0} A(t+\tau)k_2(\tau)d\tau + pV(t)(Tt) \quad (2.3.7)$$

$$\dot{C}(t) = \big(r_v - \delta_C - \delta X(t)\big)C(t) + \gamma \int_{-\infty}^{0} A(t+\tau)k_2(\tau)d\tau \quad (2.3.8)$$

$$\dot{T}(t) = (r_u - \delta_u - \delta X(t) - pV(t))\,T(t) + S. \quad (2.3.9)$$

We present the system in this form, as it helps us to elucidate some issues concerning other efforts to include delay mechanisms in HIV modeling. Specifically, the use of the scaled gamma function

$$k_\Gamma(\xi; b, n) = \frac{\xi^{n-1}}{(n-1)!b^n} \quad (2.3.10)$$

as the distribution of the times to viral production (for infected cells) is a particularly popular modeling choice. The advantage to using the gamma distribution is that with a clever change of variables, the distributed delay system can be rewritten as a non-delayed system of ODE's (and thus easily simulated using standard software packages, e.g., Matlab). This transformation is known as the *method of stages*, which we referred to in Section 1.2.2. A full derivation of the equivalent system of ODE's (where just the viral production delay is modeled with a gamma distribution) is presented in [66]. However, from our perspective, the use of a gamma function as a kernel with fixed parameters b, n is problematic (and somewhat misleading if one is trying

to introduce randomness) because it implies simple *deterministic* dynamics in the description of the internal variable model represented by the delay terms. These dynamics are easily seen as they manifest themselves in the $\dot{V}$ equation, which by introducing the internal variables $y = (y_1, \ldots, y_n)^T$ reduces equation (2.3.6) to the equivalent system

$$\begin{aligned} \dot{V}(t) &= -cV(t) + n_C C(t) + n_A y_n(t) - pV(t)T(t) \\ \dot{y}_1(t) &= \big(A(t) - y_1(t)\big)/b \\ \dot{y}_2(t) &= \big(y_1(t) - y_2(t)\big)/b \\ &\vdots \quad \vdots \quad \vdots \\ \dot{y}_n(t) &= \big(y_{n-1}(t) - y_n(t)\big)/b\,. \end{aligned} \tag{2.3.11}$$

If we write the vector version of $\dot{y}$, we find that

$$\begin{aligned} \dot{y}(t) &= \big(B_1 + B_2\big)\, y(t) + \tfrac{1}{b} \begin{pmatrix} A(t) \\ 0 \\ \vdots \\ 0 \end{pmatrix} \\ &= \big(B_1 + B_2\big)\, y(t) + F(t)\,, \end{aligned}$$

where

$$B_1 = \operatorname{diag}\left(-b^{-1}\right), \quad B_2 = \begin{pmatrix} 0 & \cdots & \cdots & \cdots & 0 \\ 1/b & \ddots & & & \vdots \\ 0 & \ddots & \ddots & & \vdots \\ \vdots & \ddots & \ddots & \ddots & \vdots \\ 0 & \cdots & 0 & 1/b & 0 \end{pmatrix}.$$

Note that if we were to use this method, an analogous system of equations are needed to represent the delays in (2.3.7) and (2.3.8). Furthermore, while this kernel does generate equations which are simple to simulate on a computer (an unnecessary simplification, given the well-developed numerical methods for delay systems developed in [8, 10] and described in Section 3.1.2), the resulting model is *equivalent* to a model with *completely identical deterministic internal dynamics* for each sub-population of cells. That is, the choice of the gamma kernel to describe the delay distribution yields a system that is equivalent to a completely deterministic system. Moreover, the use of this kernel and its purported connections with uncertainty across a population can readily lead to a false impression of the presence of randomness in the model. If one chooses to use this delay representation for the internal dynamics, one way to truly introduce randomness or uncertainty into the model is to make *b* or *n* or *both* random in (2.3.10) and hence in (2.3.11).

Remark 2.3.1. We note that the kernel (2.3.10) is a special case of a kernel that can be written in terms of the impulse response function $e^{(B_1+B_2)t}$. That is, in (2.3.11) we have that $y_n(t)$ is

given by the n^{th} component of the vector function

$$y(t) = \int_0^t e^{(B_1+B_2)(t-s)} F(s) ds .$$

Indeed any kernel that is generated by an n-dimensional linear system

$$\dot{y}(t) = B_3 y(t) + F(t)$$

for internal dynamics similar to the situation in (2.3.11) will result in an *apparently* stochastic dependent equation (2.2.7) which is in reality completely equivalent to a deterministic system. For a discussion of such representations in the context of internal dynamics and hysteresis in composite materials (which has the same form as the uncertainty in the present models), we refer the reader to [11].

2.3.3 Kernel Choice and Form

A primary advantage of our methodology and numerical scheme lies in the fact that for systems that are linear in the delay term (like (2.3.6)-(2.3.9)), we can consider arbitrary kernels and not just ones based upon the gamma function. Moreover, for distributions parameterized by their mean μ and variance σ^2, this flexibility will allow us to (in theory) independently identify μ and σ^2.

In order to use the method of stages (MOS) to simulate a system like (2.2.7)-(2.2.10), it is required that the distribution for any delay be represented by a gamma function, i.e., the use of

the MOS is impossible without this assumption. Moreover, for the gamma function, the mean μ and the variance σ^2, are described by b and n ($\mu = nb$ and $\sigma^2 = nb^2$), where b is a real and n is a positive integer. In the MOS implementation, n then corresponds to the order of the system of approximating ODE's (see equation (2.3.11)), while b is a coefficient in the system. In other words, in order to use the MOS to identify μ (using the given data in an NLS parameter identification framework), it is necessary identify the *number* of equations to be used in the approximation. This is a most challenging problem, since the NLS optimization would thus be trying to identify two reals using a real and an integer. Moreover, in any iterative procedure, the order of the underlying system could change with each iteration. If we used *our* numerical scheme and chose (for example) k_1 as the gamma function in (2.3.6), we do not encounter this issue, since we do not place any requirements on the shape of the distribution (it only needs to be $L_2(-r,0;\mathbb{R})$). However, we remark that a straightforward evaluation of the resulting convolution integral is problematic and results in floating point arithmetic under/overflow. The issues involved, along with an implementation of the convolution that accounts for the problem (while only incurring a minimal increase in simulation time), are explored in Appendix A.

For the HIV phenomena we are studying, it is theorized that the shape of the delay distributions is roughly unimodal and symmetric [28]. Therefore, in our initial studies we considered simulations using density functions consisting of a (normalized) triangular hat function, an inverted quadratic function, a gaussian function, and (of course) a gamma function. Since there is no quick change of variables for three of these systems that will reduce them to a system of ODE's, alternate numerical methods are required to simulate the dynamics of the modeled

system.

The numerical implementation for each of these kernels is of the form

$$k(s;\mu,\varsigma,s_1,s_2) \quad = \quad \frac{K(s;\mu,\varsigma)\chi_{[s_1,s_2]}(s)}{\int_{-\infty}^{0} K(\xi;\mu,\varsigma)\chi_{[s_1,s_2]}(\xi)d\xi} \tag{2.3.12}$$

with mean μ, width ς, support $[s_1,s_2] \subset \mathbb{R}$, indicator function $\chi_{[a,b]}$ for the interval $[a,b]$, and where the choice of K determines which kernel is under consideration. For example, the (normalized) hat and inverted quadratic kernels are described by

$$\widehat{k}(s;\mu,\varsigma,s_1,s_2) \quad = \quad \frac{\widehat{K}(s;\mu,\varsigma)\chi_{[s_1,s_2]}(s)}{\int_{-\infty}^{0} \widehat{K}(\xi;\mu,\varsigma)\chi_{[s_1,s_2]}(\xi)d\xi} \tag{2.3.13}$$

where

$$\begin{aligned}\widehat{K}(\xi;\mu,\varsigma) \quad = \quad & \left(\frac{2\xi}{\varsigma^2}+\frac{1}{\varsigma}\left(1-\frac{2\mu}{\varsigma}\right)\right)\chi_{[\mu-\frac{\varsigma}{2},\mu]}(\xi) \\ & +\left(-\frac{2\xi}{\varsigma^2}+\frac{1}{\varsigma}\left(1+\frac{2\mu}{\varsigma}\right)\right)\chi_{[\mu,\mu+\frac{\varsigma}{2}]}(\xi)\end{aligned}$$

and

$$\widetilde{k}(s;\mu,\varsigma,s_1,s_2) \quad = \quad \frac{\widetilde{K}(s;\mu,\varsigma)\chi_{[s_1,s_2]}(s)}{\int_{-\infty}^{0} \widetilde{K}(\xi;\mu,\varsigma)\chi_{[s_1,s_2]}(\xi)d\xi} \tag{2.3.14}$$

where

$$\widetilde{K}(\xi;\mu,\varsigma) \quad = \quad \frac{1}{(\xi-\mu)^2+\varsigma}$$

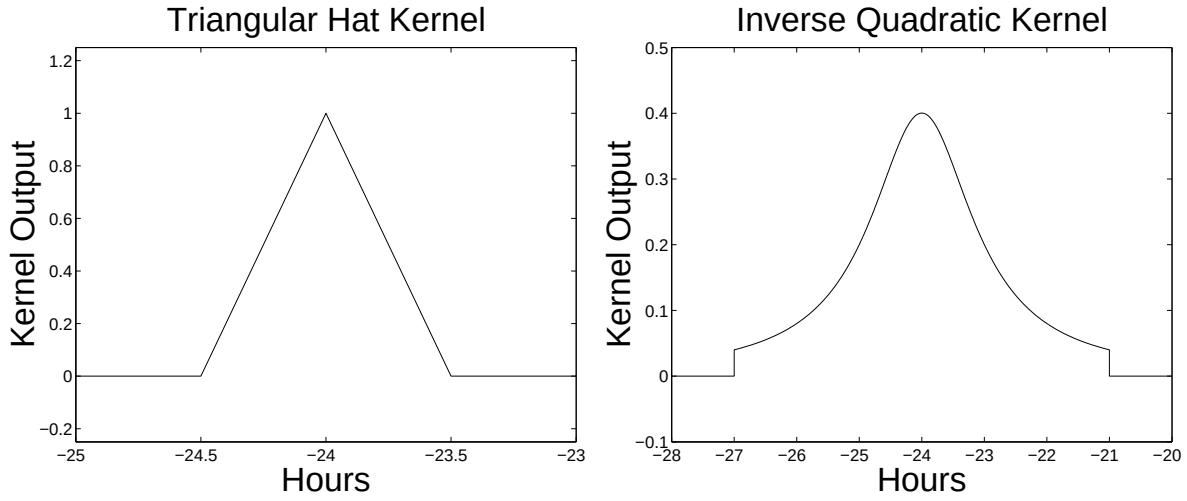

Figure 2.3.2: Sample graphs of the hat $\widehat{k}$ and inverted quadratic $\widetilde{k}$ kernels.

respectively. Note that except for the gaussian and gamma functions, the width ς is *not* equal to the standard deviation σ, it is merely an arbitrary parameter used to conveniently control the width of a kernel. Thus for both the hat and inverted quadratic kernels, the width ς and the variance σ^2 are related, but in a mathematically nontrivial way.

We depict in Figure 2.3.2 sample plots for $\widehat{k}$ and $\widetilde{k}$. Note that in order to preserve the normalization, the height of these kernels automatically scales with changes in the width ς. Moreover, if s_1, s_2 are chosen so that $s_1 < \mu - \frac{\varsigma}{2}$, $s_2 > \mu + \frac{\varsigma}{2}$, the support for the hat kernel $\widehat{k}$ will always be $[\mu - \frac{\varsigma}{2}, \mu + \frac{\varsigma}{2}]$ (which we have done in all the calculations reported on in this paper). We use the $\chi_{[s_1,s_2]}$ notation in the $\widehat{k}$ kernel only to have consistency in the notation when we compare kernels in Section 4.2.

Chapter 3

Mathematical Analysis

For those interested in the mathematical aspects of simulating an FDE system, Section 3.1 contains the necessary mathematical and numerical analysis foundations. In Section 3.1.1, we describe the conversion of the FDE system to an Abstract Evolution Equation (AEE) system as well as provide existence and uniqueness results for a solution to the Functional Differential Equation (FDE). As is discussed in Section 3.1.2, we then approximate the state for this FDE by and element in the space spanned by piece-wise linear splines (i.e., in a Galerkin approach) and numerically calculate the generalized Fourier coefficients of approximate solutions relative to the splines. With these coefficients, we recover an approximation to the solution of the FDE and then provide a convergence proof for this numerical approximation scheme.

Some of the parameters used in our modeling are not known to a high degree of accuracy and in order to identify them, we perform a nonlinear least squares (NLS) optimization and thus we must examine the well-posedness of this inverse problem. In Section 3.2.1 we describe the

space of admissible parameters, while in Section 3.2.2 we present well-posedness results for the forward problem. We complete our discussion in Section 3.2.3 by presenting arguments for the existence of a solution to the inverse problem and that that solution is continuously dependent upon the given data.

The last section in this chapter (Section 3.3) contains a discussion of the theoretical foundations for the sensitivity equations. In Section 3.3.1, we present justifications for the well-posedness of the sensitivity equations with respect to one parameter, while in Section 3.3.2 we discuss some of the practical issues regarding a simulation of the sensitivity system.

3.1 Functional Differential Equation Analysis

3.1.1 Existence and Uniqueness

Throughout the rest of this document $r \in \mathbb{R}$, is to be thought of as the largest possible hysteretic influence of the delay distributions. In other words, for the current time t, anything that happens in the system before $t - r$ does not affect the current dynamics. With this convention, we let

$$x(t) = \left[x_1(t), x_2(t), x_3(t), x_4(t)\right]^T = \left[V(t), A(t), C(t), T(t)\right]^T$$

and

$$x_t(\theta) = x(t+\theta)\,, -r \leq \theta \leq 0, r \in \mathbb{R}^+.$$

Thus our system, as described in (2.2.7)-(2.2.10), can then be written as

$$\begin{aligned} \dot{x}(t) &= L(x(t), x_t) + f_1(x(t)) + f_2(t) \quad \text{for } 0 \le t \le t_f \\ \left(x(0), x_0\right) &= (\Phi(0), \Phi) \in Z, \Phi \in \mathscr{C}\left(-r, 0; \mathbb{R}^4\right) \end{aligned} \tag{3.1.1}$$

where t_f is finite, $Z = \mathbb{R}^4 \times L_2(-r, 0; \mathbb{R}^4)$ is the state space, and for $(\eta, \phi) \in Z$,

$$\begin{aligned} L(\eta, \phi) &= \begin{bmatrix} -c & 0 & n_C & 0 \\ 0 & r_v - \delta_A & 0 & 0 \\ 0 & 0 & r_v - \delta_C & 0 \\ 0 & 0 & 0 & r_u - \delta_u \end{bmatrix} \eta + n_A \left[\delta_{(1,2)}\right]_{(4,4)} \int_{-r}^{0} \phi(\theta) dP_1(\theta) \\ &\quad + \gamma \left(\left[\delta_{(3,2)}\right]_{(4,4)} - \left[\delta_{(2,2)}\right]_{(4,4)} \right) \int_{-r}^{0} \phi(\theta) dP_2(\theta), \end{aligned}$$

$$f_1(\eta) = \begin{bmatrix} -p\eta_1\eta_4 \\ -\delta\left(\sum_{i=2}^{4} \eta_i\right)\eta_2 + p\eta_1\eta_4 \\ -\delta\left(\sum_{i=2}^{4} \eta_i\right)\eta_3 \\ -\delta\left(\sum_{i=2}^{4} \eta_i\right)\eta_4 - p\eta_1\eta_4 \end{bmatrix},$$

$$f_2(t) = [0, 0, 0, S]^T, \; 0 \le t \le t_f.$$

Here Φ is the initial time history of the system on $[-r, 0]$, P_1, P_2 are probability distributions, and $[\delta_{(i,j)}]_{(4,4)}$ denotes a 4 by 4 matrix with a one in the (i, j)th element and zeros elsewhere.

Following the discussion in [3] regarding the existence and uniqueness of a solution to (3.1.1), we consider the following definitions and lemmas.

We define the norm on the space Z as

$$\|(\eta,\phi)\|_Z = \left(|\eta|^2 + \int_{-r}^{0} |\phi(\theta)|^2 d\theta\right)^{1/2}, (\eta,\phi) \in Z.$$

Clearly, Z is a Hilbert space with inner product

$$\langle(\eta,\phi),(\zeta,\psi)\rangle_Z = \eta^T\zeta + \int_{-r}^{0} \phi(\theta)^T\psi(\theta)d\theta,$$

for $(\eta,\phi), (\zeta,\psi) \in Z$.

For the following discussion, we denote $|\cdot|$ as the norm on $\mathbb{R}^4$ (or the induced norm on $\mathbb{R}^{4\times4}$, depending on the context) and $\|\cdot\|$ as the norm on $L_2(-r,0;\mathbb{R}^4)$. Throughout, we restrict our attention to initial $(\eta,\phi) \in Z$ such that ϕ is at least piecewise continuous and hence Borel measurable. This ensures that the right side of (3.1.1) is well defined for probability distributions P_1, P_2.

As mentioned in Section 2.1, the nonlinearities exemplified by terms such as px_1x_4 are biologically unrealistic. However, these nonlinear terms in f_1 can be replaced by standard saturation limited nonlinearities such as

$$\begin{aligned} px_1x_4 \quad &\text{by} \quad p_1(x_1)x_4 \\ \text{and } \delta x_ix_j \quad &\text{by} \quad \delta_i(x_i)x_j \text{ (for } i,j = 2,3,4), \end{aligned}$$

where

$$p_1(x_1) \quad = \quad \begin{cases} 0 & x_1 < 0 \\ px_1 & 0 \le x_1 \le \bar{x}_1 \\ p\bar{x}_1 & \bar{x}_1 < x_1 \,, \end{cases} \tag{3.1.2}$$

and

$$\delta_i(x_i) = \begin{cases} 0 & x_i < 0 \\ \delta x_i & 0 \le x_i \le \bar{x}_i \\ \delta \bar{x}_i & \bar{x}_i < x_i \,, \end{cases} \tag{3.1.3}$$

(for finite upper bounds $\bar{x}_i \in \mathbb{R}^+, i = 1,2,3,4$), and where f_1 can be replaced by

$$\tilde{f}_1(\eta) \quad = \quad \begin{bmatrix} -p_1(\eta_1)\eta_4 \\ -\left(\sum_{i=2}^4 \eta_i\right) \delta_2(\eta_2) + p_1(\eta_1)\eta_4 \\ -\left(\sum_{i=2}^4 \eta_i\right) \delta_3(\eta_3) \\ -\left(\sum_{i=2}^4 \eta_i\right) \delta_4(\eta_4) - p_1(\eta_1)\eta_4 \end{bmatrix}, \eta \in \mathbb{R}^4. \tag{3.1.4}$$

Note that p_i and δ_i are globally bounded functions satisfying $p_1(x_1) \le p\bar{x}_1$ and $\delta_i(x_i) \le \delta\bar{x}_i$. Indeed they are piecewise differentiable, satisfying $p_1'(x_1) \le p$ and $\delta_i'(x_i) \le \delta$.

Now we can prove the global existence and uniqueness of a solution to

$$\begin{aligned} \dot{x}(t) \quad &= \quad L(x(t), x_t) + \tilde{f}_1(x(t)) + f_2(t) \qquad \text{for } 0 \le t \le t_f \,, \\ \big(x(0), x_0\big) \quad &= \quad (\Phi(0), \Phi) \in Z \end{aligned} \tag{3.1.5}$$

with t_f finite, through the following series of steps. We first define $\mathscr{F} = L + \tilde{f}_1$ on Z by

$$\mathscr{F}(\eta, \phi) = L(\eta, \phi) + \tilde{f}_1(\eta).$$

Lemma 3.1.1. *The function $\mathscr{F} = L + \tilde{f}_1 : Z \to \mathbb{R}^4$ is piecewise continuously differentiable.*

Proof. Given that all pertinent components of the equation (3.1.5) are piecewise continuously differentiable, we can conclude that the function $\mathscr{F}$ is as well. □

Lemma 3.1.2. *For all $(\eta, \phi), (\zeta, \psi) \in Z$ the function $\mathscr{F} = L + \tilde{f}_1$ satisfies a global Lipschitz condition*

$$|\mathscr{F}(\eta, \phi) - \mathscr{F}(\zeta, \psi)| \leq K_L \{|\eta - \zeta| + \|\phi - \psi\|\} \tag{3.1.6}$$

for some fixed constant $K_L > 0$.

Proof. Let

$$M = \begin{bmatrix} -c & 0 & n_C & 0 \\ 0 & r_v - \delta_A & 0 & 0 \\ 0 & 0 & r_v - \delta_C & 0 \\ 0 & 0 & 0 & r_u - \delta_u \end{bmatrix}$$

and observe that we have

$$|\mathscr{F}(\eta, \phi) - \mathscr{F}(\zeta, \psi)| \quad \leq \quad |L(\eta, \phi) - L(\zeta, \psi)| + \left|\tilde{f}_1(\eta) - \tilde{f}_1(\zeta)\right|. \tag{3.1.7}$$

The first term in the sum on the right side of (3.1.7) is easily bounded by

$$\begin{aligned} |L(\eta,\phi)-L(\zeta,\psi)| &= \Bigg| M(\eta-\zeta)+n_A\left[\delta_{(1,2)}\right]_{(4,4)}\int_{-r}^{0}(\phi(\theta)-\psi(\theta))\,dP_1(\theta) \\ &\qquad +\gamma\left(\left[\delta_{(3,2)}\right]_{(4,4)}-\left[\delta_{(2,2)}\right]_{(4,4)}\right)\int_{-r}^{0}(\phi(\theta)-\psi(\theta))\,dP_2(\theta)\Bigg| \\ &\leq \max\left\{|M|,\left|n_A\right|,2|\gamma|\right\}(|\eta-\zeta|+\|\phi-\psi\|)\,. \end{aligned}$$

To bound the second term, note that the multidimensional Mean Value Theorem implies that for $\eta,\zeta\in\mathbb{R}^4$

$$\tilde{f}_1(\eta)-\tilde{f}_1(\zeta) = \int_0^1 \left\langle \mathbf{D}\tilde{f}_1(\eta+\theta(\zeta-\eta)),\eta-\zeta\right\rangle d\theta\,,$$

where the 4×4 matrix valued function is given by

$$\mathbf{D}\tilde{f}_1=\left[\begin{array}{cccc} \partial_1\tilde{f}_1 & \partial_2\tilde{f}_1 & \partial_3\tilde{f}_1 & \partial_4\tilde{f}_1 \end{array}\right],$$

where $\partial_i\tilde{f}_1$ is the partial derivative of $\tilde{f}_1$ with respect to the ith component of its vector argument.

Define $\bar{\Omega}=\{x\in\mathbb{R}^4 : x_i\leq \bar{\chi}, i=1,2,3,4\}$ and recall the definition of $\tilde{f}_1$ in (3.1.4). For $x\in\bar{\Omega}$, $\mathbf{D}\tilde{f}_1$ is linear and $|\mathbf{D}\tilde{f}_1|\leq K_L^1(\bar{\Omega})$ for some constant $K_L^1>0$ that depends upon $\bar{\Omega}$. On $\mathbb{R}^4\setminus\bar{\Omega}$, $\mathbf{D}\tilde{f}_1$ is constant and hence $|\mathbf{D}\tilde{f}_1|\leq K_L^2(\bar{\Omega})$ for some constant $K_L^2>0$ that depends upon $\bar{\Omega}$.

By the properties of integrals and Cauchy-Schwarz we then know that

$$\begin{aligned} \left|\tilde{f}_1(\eta)-\tilde{f}_1(\zeta)\right| &\leq \int_0^1 \left|\left\langle \mathbf{D}\tilde{f}_1(\eta+\theta(\zeta-\eta)),\zeta-\eta\right\rangle\right| d\theta \\ &\leq \int_0^1 \left|\mathbf{D}\tilde{f}_1(\eta+\theta(\zeta-\eta))\right||\zeta-\eta|\, d\theta \\ &\leq \max\left\{K_L^1,K_L^2\right\}|\eta-\zeta|\,. \end{aligned}$$

Combining these results we obtain the global Lipschitz condition (3.1.6) for

$$K_L = \max\left\{|M|,\left|n_A\right|,2|\gamma|,K_L^1,K_L^2\right\}.$$

□

Remark 3.1.3. Note that in the above Lemma, K_L may not necessarily be the minimal Lipschitz constant; we merely wish to emphasize its existence for use in a subsequent theorem.

Following the standard arguments for the existence and uniqueness of the solution to an ODE on a finite interval $I=[0,t_f]$, we begin by noting that as a consequence of the Second Fundamental Theorem of Calculus, we can rewrite (3.1.5) as

$$\begin{aligned} x(t) &= \Phi(0)+\textstyle\int_0^t\left\{L(x(s),x_s)+\tilde{f}_1(x(s))+f_2(s)\right\}ds \quad t\in I, \\ &= \Phi(t) \qquad -r\leq t<0\,. \end{aligned} \tag{3.1.8}$$

We now make the following definition.

Definition 3.1.4. Let *successive approximations* to the solution of (3.1.8) on $[-r, t_f]$ be defined for $j = 0, 1, 2, \ldots$, as

$$\begin{aligned} y_0(t) &= \begin{cases} \Phi(0) & t \in I \\ \Phi(t) & -r \le t < 0 \end{cases} \\ y_{j+1}(t) &= \Phi(0) + \int_0^t \left\{ L(y_j(s), (y_j)_s) + \tilde{f}_1(y_j(s)) + f_2(s) \right\} ds \qquad t \in I, \\ &= \Phi(t) \qquad\qquad -r \le t < 0\,. \end{aligned} \tag{3.1.9}$$

Theorem 3.1.5. *Given a finite interval I, suppose $L + \tilde{f}_1$ satisfies both Lemma 3.1.1 and Lemma 3.1.2. Then there exists a unique solution to (3.1.5) on I, whenever Φ is at least piecewise continuous.*

Proof. The general idea of our proof is to show that the successive approximations defined in (3.1.9) converge to a unique solution of (3.1.8).

Let the residual function of two functions z, w be defined as

$$e(t; z, w) = |z(t) - w(t)| + \|z_t - w_t\|\,, \tag{3.1.10}$$

for $z, w \in \mathscr{C}(-2r, t_f : \mathbb{R}^4)$, $t \in I = [-r, t_f]$ and let $\mathscr{F}$ be defined as

$$\mathscr{F}(t; z) = L(z(t), z_t) + \tilde{f}_1(z(t))$$

for $z \in \mathscr{C}(-2r, t_f; \mathbb{R}^4)$, $t \in I$.

If we consider the residual for the functions y_{j+1} and y_j, we find that for $t \in I$ and $j > 0$

$$\begin{aligned} e(t;y_{j+1},y_j) &= \left| \int_0^t \left\{ \mathscr{F}(s;y_j) - \mathscr{F}(s;y_{j-1}) \right\} ds \right| \\ &\quad + \left\| \int_0^{t+\cdot} \left\{ \mathscr{F}(s;y_j) - \mathscr{F}(s;y_{j-1}) \right\} ds \right\| \\ &\leq K_L \int_0^t e(s;y_j,y_{j-1}) ds + \left\| K_L \int_0^{t+\cdot} e(s;y_j,y_{j-1}) ds \right\| \end{aligned}$$

and thus

$$e(t;y_{j+1},y_j) \leq 2K_L \max\left\{1,\sqrt{r}\right\} \int_0^t e(s;y_j,y_{j-1}) ds\,. \tag{3.1.11}$$

Note that the case for $j = 0$ (with $t \in I$) is special

$$\begin{aligned} e(t;y_1,y_0) &= \left| y_1(t) - y_0(t) \right| + \left\| \left(y_1\right)_t - \left(y_0\right)_t \right\| \\ &= \left| \int_0^t \left\{ \mathscr{F}(s;y_0) + f_2(s) \right\} ds \right| + \left\| \int_0^{t+\cdot} \left\{ \mathscr{F}(s;y_0) + f_2(s) \right\} ds \right\| \\ &\leq 2\max\left\{1,\sqrt{r}\right\} \int_0^t \left\{ K_L \left| e(s,y_0,0) \right| + |S| \right\} ds \\ &\leq 2\max\left\{1,\sqrt{r}\right\} \int_0^t \left\{ K_L \left(|\Phi(s) + \|\Phi\|| \right) + |S| \right\} ds \\ &\leq 2\max\left\{1,\sqrt{r}\right\} \left(K_L \left(|\Phi(0) + \|\Phi\|| \right) + |S| \right) |t|\,, \end{aligned}$$

and thus

$$e(t;y_1,y_0) \leq \max\left\{1,\sqrt{r}\right\} K_G\, |t|$$

where

$$K_G = 2\left(K_L \left(|\Phi(0)| + \|\Phi\| \right) + |S| \right).$$

We claim that from (3.1.11) and the $j = 0$ case, we have

$$e(t; y_{n+1}, y_n) \leq \frac{K_G}{2K_L} \frac{(2\max\{1, \sqrt{r}\} K_L |t|)^{n+1}}{(n+1)!}, t \in I. \tag{3.1.12}$$

Clearly, this is true for $n = 0$, and the general case follows easily from induction using (3.1.11). Using the estimate (3.1.12), we can then infer that

$$\begin{aligned} \sum_{j=0}^{\infty} e(t; y_{j+1}, y_j) &\leq \frac{K_G}{2K_L} \sum_{j=0}^{\infty} \frac{(2\max\{1, \sqrt{r}\} K_L |t|)^{(j+1)}}{(j+1)!} \\ &\leq \frac{K_G}{2K_L} e^{2\max\{1,\sqrt{r}\}K_L|t|}. \end{aligned}$$

Thus, by the comparison test, $\sum_{j=0}^{\infty} e(t; y_{j+1}, y_j)$ converges uniformly for $t \in I$, which proves that $\{y_j(t)\}$ converges uniformly for all $t \in I$. Denote $\lim_{j\to\infty} y_j(t)$ as $y(t)$. Since the y_j's are continuous and converge uniformly to y, we see that y is both continuous on I and satisfies (3.1.5) by taking limits in (3.1.9). Note that this also yields y absolutely continuous on $[0, t_f]$

To prove the uniqueness of our solution, suppose we have two distinct solutions $\{y, \tilde{y}\} \in \mathscr{C}(-r, t_f; \mathbb{R}^4)$ to (3.1.8). Using the same arguments as in establishing (3.1.11), we have

$$\begin{aligned} e(t; y, \tilde{y}) &\leq \left| \int_0^t \{\mathscr{F}(s; y) - \mathscr{F}(s; \tilde{y})\} ds \right| + \left\| \int_0^{t+\cdot} \{\mathscr{F}(s; y) - \mathscr{F}(s; \tilde{y})\} ds \right\| \\ &\leq 2\max\left\{1, \sqrt{r}\right\} K_L \int_0^t e(s; y, \tilde{y}) ds. \end{aligned}$$

Thus by Gronwall's inequality we have that

$$|y(t)-\tilde{y}(t)|+\|y_t-\tilde{y}_t\| \quad \leq \quad 0 \qquad \text{for } t \in I,$$

and thus $y(t)=\tilde{y}(t)$ for $t \in I$ and also for $t \in [-r,0]$ since both solutions satisfy the same initial condition.

We have therefore now proven that there exists a unique solution (for $[-r,t_f]$) to (3.1.8) and thus to (3.1.5), which is in fact absolutely continuous on $[0,t_f]$. Moreover, if the initial condition Φ is in $\mathscr{C}(-r,0;\mathbb{R}^4)$, we can also conclude that $x(t) \in \mathscr{C}(-r,t_f;\mathbb{R}^4)$. □

In our simulations, where the states do not exceed the predefined upper bounds in (3.1.2), (3.1.3), we know that these solutions solve (3.1.1) as well as (3.1.5). In any case (3.1.5) is the biologically meaningful system.

3.1.2 Abstract Evolution Equation Implementation

The system described by (3.1.5) can be written in a form that facilitates a discussion regarding its approximation which is developed fully in [10] and will only be summarized here.

Define the nonlinear operator $\mathscr{A} : \mathscr{D}(\mathscr{A}) \subset Z \to Z$ by

$$\begin{aligned} \mathscr{D}(\mathscr{A}) &= \left\{(\psi(0),\psi) \in Z : \psi \in H^1(-r,0;\mathbb{R}^4)\right\} \\ \mathscr{A}(\psi(0),\psi) &= \left(L(\psi(0),\psi)+\tilde{f}_1(\psi(0)), \tfrac{d}{d\theta}\psi\right). \end{aligned}$$

With this definition, we can then write (3.1.5) in the form

$$\begin{aligned} \dot{z}(t) &= \mathscr{A}z(t) + \big(f_2(t), 0\big) \\ z(0) &= z_0\,, \end{aligned} \tag{3.1.13}$$

where $(f_2(t), 0) \in Z$ and $z_0 \in Z$.

Let $\{Z^N, \mathbb{P}^N, \mathscr{A}^N\}$ be our approximation scheme for (3.1.13) satisfying the conditions of Theorem 3.1 in [10], where Z^N is a spline subspace of Z, $\mathbb{P}^N$ is the orthogonal projection of Z onto Z^N, and $\mathscr{A}^N$ is the approximating operator $\mathscr{A}^N = \mathbb{P}^N \mathscr{A} \mathbb{P}^N$. Thus, using $\{Z^N, \mathbb{P}^N, \mathscr{A}^N\}$ we can generate an approximation to the formulation described by (3.1.13), which we denote by

$$\begin{aligned} \dot{z}^N(t) &= \mathscr{A}^N z^N(t) + \mathbb{P}^N(f_2(t), 0) \\ z^N(0) &= \mathbb{P}^N(\eta, \phi)\,. \end{aligned} \tag{3.1.14}$$

As before, the second Fundamental Theorem of Calculus implies that an alternative description of (3.1.14) is

$$z^N(t) = \mathbb{P}^N(\eta, \phi) + \int_0^t \left\{ \mathscr{A}^N z^N(\sigma) + \mathbb{P}^N(f_2(\sigma), 0) \right\} d\sigma\,.$$

Theorem 3.1.6. *Given the systems described in (3.1.5) and (3.1.14) with* $(\eta, \phi) = (\psi(0), \psi)$, $\psi \in H^1(-r, 0; \mathbb{R}^4)$, *under the conditions of Lemmas 3.1.1 and 3.1.2, we have that* $z^N(t) \to x(t; \psi, f_2), x_t(\psi, f_2))$, *as* $N \to \infty$, *uniformly in* t *on the finite interval* I.

Proof. The function f_2 is clearly in $L_2(I)$ and thus Theorem 2.2 in [3] directly implies our desired conclusion. □

As in [10], we choose hat functions (piece-wise linear splines) as our basis for Z_1^N (the sub-

space of Z^N spanned by the hat functions). Thus, if we partition $[-r,0]$ by $t_j^N = -j(r/N)$, $j = 0,\ldots,N$, we can then define the basis $\hat{\beta}^N = (\beta^N(0),\beta^N)$ by

$$\beta^N = \left[e_0^N, e_1^N, \ldots, e_N^N\right] \otimes \mathbb{I}_n$$

where $\mathbb{I}_n$ is the $n \times n$ identity matrix and the e_j^N's are characterized by

$$e_j^N(t_i^N) = \delta_{ij};\ i,j = 0,\ldots,N\,.$$

Therefore, an element in Z_1^N can be written as

$$z^N = \hat{\beta}^N \alpha^N = \sum_{j=0}^{N} \left(e_j^N(0), e_j^N\right) a_j^N\,,\ \text{with } a_j^N \in \mathbb{R}^N\,.$$

Denote A^N as the matrix representation of $\mathscr{A}^N$ restricted to Z_1^N and let $w^N(t)$ and $F^N(t)$ be defined such that $z^N(t) = \hat{\beta}^N w^N(t)$ and $\mathbb{P}^N(f_2(t),0) = \hat{\beta}^N F^N(t)$ respectively. By construction we have that $\mathscr{A}^N \hat{\beta}^N = \hat{\beta}^N A^N$, which implies that solving (3.1.5) for $z^N(t)$ is equivalent to solving

$$\begin{aligned} \dot{w}^N(t) &= A^N w^N(t) + F^N(t) \quad t \in I\,, \\ w^N(0) &= w_0^N \end{aligned} \tag{3.1.15}$$

for $w^N(t)$, where $\hat{\beta}^N w_0^N = \mathbb{P}^N(\eta,\phi)$.

We remark that if we are able to obtain w^N, the product $\hat{\beta}^N w^N$ converges uniformly in t on

I to the solution of (3.1.5)

$$\lim_{N\to\infty} \hat{\beta}^N w^N(t, w_0^N, F^N) = \left(x(t;\eta,\psi,f_2), x_t(\eta,\psi,f_2)\right) .$$

For the numerical simulation of (3.1.15), it is necessary to compute $\mathbb{P}^N(\gamma,\psi)$ for any $(\gamma,\psi) \in Z$ and $A^N\alpha^N$ for $\alpha^N \in \mathbb{R}^n$. Since $\mathbb{P}^N(\gamma,\psi)$ is the orthogonal projection of $(\gamma,\psi) \in Z$ onto Z^N, $\mathbb{P}^N(\gamma,\psi)$ is uniquely determined by the $\mu^N \in \mathbb{R}^N$ such that

$$\left\langle \hat{\beta}^N \mu^N - (\gamma,\psi), \hat{\beta}^N \right\rangle_Z = 0$$

or equivalently,

$$\left\langle \hat{\beta}^N, \hat{\beta}^N \right\rangle_Z \mu^N = \left\langle \hat{\beta}^N, (\gamma,\psi) \right\rangle_Z . \tag{3.1.16}$$

Thus, solving (3.1.16) for μ^N yields $\mathbb{P}^N(\gamma,\psi) = \hat{\beta}^N\mu^N$ for any $(\gamma,\psi) \in Z$ and implies that $F^N(t)$ is uniquely defined by

$$F^N(t) = \left(\left\langle \hat{\beta}^N, \hat{\beta}^N \right\rangle_Z\right)^{-1} \left\langle \hat{\beta}^N, \left(f_2(t), 0\right) \right\rangle_Z .$$

To calculate $A^N\alpha^N$, first consider the action of $\mathscr{A}^N$ applied to $\hat{\beta}^N\alpha^N$, an element of Z^N. We know that for any $\alpha^N \in \mathbb{R}^n$

$$\begin{aligned} \mathscr{A}^N\hat{\beta}^N\alpha^N &= \mathbb{P}^N\left(\mathscr{A}\hat{\beta}^N\alpha^N\right) \\ &= \mathbb{P}^N\left(L((\beta^N(0)\alpha^N), \beta^N\alpha^N) + \tilde{f}_1(\beta^N(0)\alpha^N), D(\beta^N\alpha^N)\right) \end{aligned}$$

and that $\mathscr{A}^N \hat{\beta}^N \alpha^N = \hat{\beta}^N A^N \alpha^N$. Thus

$$0 \quad = \quad \hat{\beta}^N A^N \alpha^N - \mathbb{P}^N \left\{ L((\beta^N(0)\alpha^N), \beta^N \alpha^N) + \tilde{f}_1 \left(\beta^N(0)\,\alpha^N\right), \frac{d}{d\theta}\left(\beta^N \alpha^N\right) \right\}$$

and

$$0 \quad = \quad \left\langle \hat{\beta}^N, \hat{\beta}^N A^N \alpha^N - \left\{ L(\beta^N(0)\alpha^N), \beta^N \alpha^N) + \tilde{f}_1(\beta^N(0)\alpha^N), \frac{d}{d\theta}\left(\beta^N \alpha^N\right) \right\} \right\rangle_Z$$

which implies that

$$\left\langle \hat{\beta}^N, \hat{\beta}^N \right\rangle_Z \left(A^N \alpha^N\right) = \left\langle \hat{\beta}^N, \left\{ L(\beta^N(0)\alpha^N), \beta^N \alpha^N) + \tilde{f}_1(\beta^N(0)\alpha^N), \frac{d}{d\theta}\left(\beta^N \alpha^N\right) \right\} \right\rangle_Z .$$

Therefore, for any $\alpha^N \in \mathbb{R}^n$, the action of A^N on α^N is defined by

$$\left(\left\langle \hat{\beta}^N, \hat{\beta}^N \right\rangle_Z \right)^{-1} \left\langle \hat{\beta}^N, \left\{ L(\beta^N(0)\alpha^N), \beta^N \alpha^N) + \tilde{f}_1(\beta^N(0)\alpha^N), \frac{d}{d\theta}\left(\beta^N \alpha^N\right) \right\} \right\rangle_Z .$$

With these characterizations, we can now calculate $w^N(t)$ and thus $z^N(t)$ (on I), and thus a numerical approximation to the solution of (3.1.5). We note that the characterization of the FDE system allows us to include both discrete and distributed delays in any modeling and simulation investigations.

3.2 Inverse Problem

Before performing our NLS optimization to identify certain parameters in our model, we need to verify the well-posedness of this inverse problem. Therefore, in this section we extend the definition of the solution x and the right side $\mathscr{F}$ to also be dependent upon upon the fixed parameters or distributions (depending upon the parameter of interest). We are interested in identifying only a specific subset of them, since some of their values are already well established. In particular we are most interested in the delay distributions and as such, they are primary focus of our efforts.

3.2.1 Parameter Space

We begin our study of the inverse problem by remarking that typically, one would only be interested in identifying $q \in Q_{ad}$, where q is a vector (e.g., $[\gamma, p, \delta]$) and Q_{ad} is the domain of admissible parameters. However, we are most interested in the delay distributions, and thus we let $Q_r = [-r, 0]$, $\mathbb{S}$ be the class of all Borel subsets of Q_r (the Borel σ-algebra), and $\mathscr{P}(Q_r)$ be the space of probability measures on $(Q_r, \mathbb{S})$. Moreover, to establish the theoretical framework necessary to identify both probability distributions P_1 and P_2 from (3.1.1), we denote

$$\Pi_{ad} = \mathscr{P}(Q_r) \times \mathscr{P}(Q_r) ,$$

where $\pi \in \Pi_{ad}$, means that $\pi = (P_1, P_2)$, for $P_1, P_2 \in \mathscr{P}(Q_r)$.

In the following discussion, we make use of a construct from advanced probability theory,

the Prohorov metric (denoted ρ). As is discussed in [14, 35], convergence in the Prohorov metric is equivalent to weak convergence (and actually weak* convergence, when considering $\mathscr{P} \subset \mathscr{C}^*$). We describe a topology for Π_{ad} by defining the following metric. For $\bar{\pi}, \hat{\pi} \in \Pi_{ad}$, let

$$\rho_\Pi(\bar{\pi}, \hat{\pi}) = \rho(\bar{P}_1, \hat{P}_1) + \rho(\bar{P}_2, \hat{P}_2)\,.,$$

where $\overline{\pi} = (\overline{P}_1, \overline{P}_2)$ and $\widehat{\pi} = (\widehat{P}_1, \widehat{P}_2)$. Given our data $\widehat{X} \in \mathbb{R}^{10}$, the goal of the inverse problem is to find a solution to

$$\min_{\pi \in \Pi_{ad}} J(\pi, \widehat{X}) = \min_{\pi \in \Pi_{ad}} \frac{1}{10} \sqrt{\sum_{i=1}^{10} \left(X(t_i, \pi) - \widehat{X}_i \right)^2}, \tag{3.2.1}$$

where X is the total cell compartment (see Table 2.1). Note that in general, J may not necessarily have a unique minimizer, in which case the corresponding solution (denoted by $\Pi^*(\widehat{X})$) could be a set of pairs and not just one pair of probability distribution functions. In this case, we define the distance between two of these sets $\Pi^*(\overline{X})$ and $\Pi^*(\widehat{X})$ (for data $\overline{X}, \widehat{X}$) to be

$$d_H(\Pi^*(\overline{X}), \Pi^*(\widehat{X})) \quad = \quad \inf \left\{ \rho_\Pi(\overline{\pi}, \widehat{\pi}); \overline{\pi} \in \Pi^*(\overline{X}), \widehat{\pi} \in \Pi^*(\widehat{X}) \right\},$$

the Hausdorff distance (see [49] for more information on Hausdorff distances).

As mentioned in Section 3.1.1, we have a uniformly convergent (in t on finite intervals for fixed π) numerical scheme which generates an approximate solution x^N to (3.1.1), and thus to $X(t_i, \pi)$. However, we have not yet shown that as $N \to \infty$, $x^N(\pi^N) \to x(\pi)$ as $\pi^N \to \pi$ in the ρ_Π metric. This is the focus of the next section and forms the theoretical basis for our attempt

to numerically solve

$$\min_{\pi\in\Pi_{ad}} J^N(\pi,\widehat{X}) \quad = \quad \min_{\pi\in\Pi_{ad}} \frac{1}{10}\sqrt{\sum_{i=1}^{10}\left(X^N(t_i,\pi)-\widehat{X}_i\right)^2}, \tag{3.2.2}$$

where N is a problem dependent index of approximation.

3.2.2 Well-posedness of the Forward Problem

In order to consider calculating a solution to (3.2.2), we must establish the well posedness of this optimization problem. Thus we must prove that the solution to (3.1.1) is continuous in the delay and that there exists a solution to both (3.2.1) and then to (3.2.2). Following the development in [7], with inspiration from [4, 5] for extending those results to Π_{ad} from $\mathscr{P}(Q_r)$, we will examine both the problem stability and the method stability.

We say that the *forward problem is well-posed* if the unique solution to the model (in our case x) is continuously dependent upon the parameter π which we are trying to identify. Recall the original system described in Section 3.1.1 and that within our definition of $\mathscr{F}$, we have *a priori* defined the delay distributions P_1 and P_2. Let us fix $t\in[0,t_f]$ and consider the continuity of a solution to (3.1.1) with respect to these delay distributions. Thus we interpret the solution x as the mapping $x(t,\cdot):\Pi_{ad}\to\mathbb{R}^4$, parameterized by the time t. Similarly, we interpret the right side of the differential equation $\mathscr{F}$ as the mapping $\mathscr{F}:\Pi_{ad}\times\mathbb{R}^4\times\mathscr{C}(-r,0;\mathbb{R}^4)\to\mathbb{R}^4$. We note that in fact our only interest is in initial conditions that are at least piecewise continuous so that throughout we may use the L_2 norm even though $\Phi\in\mathscr{C}$.

Lemma 3.2.1. *For all* $(\bar{\pi},(\eta,\phi)),(\hat{\pi},(\zeta,\psi))\in\Pi_{ad}\times\mathbb{R}^4\times\mathscr{C}(-r,0;\mathbb{R}^4)$ *the function* $\mathscr{F}=$

$L+\tilde{f}_1$ satisfies the following condition

$$|\mathscr{F}(\bar{\pi},(\eta,\phi))-\mathscr{F}(\hat{\pi},(\zeta,\psi))| \quad \leq \quad K_L\left(|\eta-\zeta|+\|\phi-\psi\|\right)+\mathscr{T}(\psi,\bar{\pi},\hat{\pi}),$$

where

$$K_L \quad = \quad \max\{|M|,\left|n_A\right|,2|\gamma|,K_L^1,K_L^2\}$$

from Lemma 3.1.2 and $\mathscr{T}$ is a function such that $\mathscr{T}(\psi,\bar{\pi},\hat{\pi})\to 0$ as $\rho_\Pi(\bar{\pi},\hat{\pi})\to 0$.

Proof. Consider

$$|\mathscr{F}(\bar{\pi},(\eta,\phi))-\mathscr{F}(\hat{\pi},(\zeta,\psi))| \quad \leq \quad |L((\eta,\phi),\bar{\pi})-L((\zeta,\psi),\hat{\pi})|+\left|\tilde{f}_1(\eta)-\tilde{f}_1(\zeta)\right|.$$

The bounding of the last term on the right side by $|\eta-\zeta|$ is described in detail in the proof of Lemma 3.1.2. Thus, let us examine the first term in the sum

$$\begin{aligned}
|L((\eta,\phi),\bar{\pi})-L((\zeta,\psi),\hat{\pi})| \quad &\leq \quad |M(\eta-\zeta)|+\left|n_A\right|\left|\int_{-r}^{0}\phi(\theta)d\bar{P}_1(\theta)-\int_{-r}^{0}\psi(\theta)d\hat{P}_1(\theta)\right| \\
&\quad +2|\gamma|\left|\int_{-r}^{0}\phi(\theta)d\bar{P}_2(\theta)-\int_{-r}^{0}\psi(\theta)d\hat{P}_2(\theta)\right| \\
&\leq \quad |M|\,|\eta-\zeta|+\left|n_A\right|\left(\left|\int_{-r}^{0}\{\phi(\theta)-\psi(\theta)\}\,d\bar{P}_1(\theta)\right|\right. \\
&\quad \left.+\left|\int_{-r}^{0}\psi(\theta)d\bar{P}_1(\theta)-\int_{-r}^{0}\psi(\theta)d\hat{P}_1(\theta)\right|\right) \\
&\quad +2|\gamma|\left(\left|\int_{-r}^{0}\{\phi(\theta)-\psi(\theta)\}\,d\bar{P}_2(\theta)\right|\right.
\end{aligned}$$

$$+\left|\int_{-r}^{0}\psi(\theta)d\bar{P}_2(\theta)-\int_{-r}^{0}\psi(\theta)d\hat{P}_2(\theta)\right|\Bigg).$$

The sum

$$\left|\int_{-r}^{0}\psi(\theta)d\bar{P}_1(\theta)-\int_{-r}^{0}\psi(\theta)d\hat{P}_1(\theta)\right|+\left|\int_{-r}^{0}\psi(\theta)d\bar{P}_2(\theta)-\int_{-r}^{0}\psi(\theta)d\hat{P}_2(\theta)\right| \tag{3.2.3}$$

is bounded by a function $\mathscr{T}$ which converges to zero when $\bar{P}_1,\bar{P}_2$ converge to $\hat{P}_1,\hat{P}_2$ in the Prohorov metric respectively. This result is well known in probability and measure theory and discussions as well as convergence proofs are available in multiple references [13, 14, 33, 35, 60, 86] (sometimes being referred to as the Helly-Bray theorem). Moreover, combined with the bounds for the other term (from Lemma 3.1.2), the bounding of (3.2.3) by the $\mathscr{T}$ function yields the Lemma. □

Now we are prepared to prove the continuity of the solution with respect to π.

Theorem 3.2.2. *Given $t\in[0,t_f]$ and $\pi\in\Pi_{ad}$, the resultant solution to (3.1.1) is point-wise continuous at $\pi\in\Pi_{ad}$.*

Proof. Since ρ_Π is a metric topology, it suffices to argue that $x(t,\pi^n)\to x(t,\pi)$ for any sequence $\{\pi^n\}_{n=1}^{\infty}$ where as $n\to\infty$, $\pi^n\to\pi$ in ρ_Π. Consider the first term in the sum on the right side in (3.1.10)

$$|x(t,\pi^n)-x(t,\pi)|\le\int_0^t|\mathscr{F}(\pi^n,(x(s,\pi^n),x_s(\pi^n)))-\mathscr{F}(\pi,(x(s,\pi),x_s(\pi)))|\,ds.$$

By Lemma 3.2.1, we have that

$$|x(t,\pi^n) - x(t,\pi)| \leq \int_0^t K_L e(s, x_s(\pi^n), x_s(\pi)) ds + \max_{s\in[0,t_f]} \{\mathscr{T}(x_s(\pi),\pi^n,\pi)\} |t_f|, \qquad (3.2.4)$$

where e is the residual of two functions evaluated at a fixed time t (as defined in (3.1.10)). Now consider the second term in (3.1.10)

$$\begin{aligned} \|x_t(\pi^n) - x_t(\pi)\| &\leq \left\| \int_0^{t+\cdot} |\mathscr{F}(\pi^n, (x(s,\pi^n), x_s(\pi^n))) - \mathscr{F}(\pi, (x(s,\pi), x_s(\pi)))| \, ds \right\| \\ &\leq \sqrt{r} \int_0^t |\mathscr{F}(\pi^n, (x(s,\pi^n), x_s(\pi^n))) - \mathscr{F}(\pi, (x(s,\pi), x_s(\pi)))| \, ds, \end{aligned}$$

which has the same bound as in (3.2.4), but multiplied by $\sqrt{r}$. Combining these two bounds gives us

$$\begin{aligned} e(t, x_t(\pi^n), x_t(\pi)) &\leq 2\max\left\{1,\sqrt{r}\right\} K_L \int_0^t e(s, x_s(\pi^n), x_s(\pi)) ds \\ &\quad + 2\max\left\{1,\sqrt{r}\right\} \max_{s\in[0,t_f]} \{\mathscr{T}(x_s(\pi),\pi^n,\pi)\} t_f, \end{aligned}$$

and an application of Gronwall's inequality yields

$$\begin{aligned} e(t, x_t(\pi^n), x_t(\pi)) &\leq 2\max\left\{1,\sqrt{r}\right\} \max_{s\in[0,t_f]} \{\mathscr{T}(x_s(\pi),\pi^n,\pi)\} t_f e^{\int_0^t 2\max\{1,\sqrt{r}\} K_L ds} \\ &\leq 2\max\left\{1,\sqrt{r}\right\} \max_{s\in[0,t_f]} \{\mathscr{T}(x_s(\pi),\pi^n,\pi)\} t_f e^{2\max\{1,\sqrt{r}\} K_L t_f}, \end{aligned}$$

from which it follows immediately that $|x(t,\pi^n) - x(t,\pi)| \to 0$ as $\pi^n \to \pi$. Therefore we have

pointwise continuity of the solution x (and thus X and J) with respect to the optimization variable of interest π. □

Similar arguments can be used to prove that for fixed N, the approximations x^N (and hence X^N and J^N defined above in (3.2.2)) are continuous in π on Π_{ad}. However, the convergence of $|x^N(t,\pi^n) - x^N(t,\pi)| \to 0$ as $N,n \to \infty$ is not as obvious (but still true), and is proven in the following lemma.

Lemma 3.2.3. *For $t \in [0,t_f]$, $\pi \in \Pi_{ad}$, and $\{\pi^n\} \in \Pi_{ad} \ni \lim_{n\to\infty} \rho_\Pi(\pi^n,\pi) = 0$, if $x^N(t,\pi^n)$ is the solution to (3.1.14), then $|x^N(t,\pi^n) - x^N(t,\pi)| \to 0$ as $N,n \to \infty$.*

Proof. Consider for $t \in [0,t_f]$ and $\mathbb{P}_1^N$ the first component of the orthogonal projection operator $\mathbb{P}^N$

$$\begin{aligned}
e(t,x_t^N(\pi^n),x_t^N(\pi)) &= \left|x^N(t,\pi^n) - x^N(t,\pi)\right| + \left\|x_t^N(\pi^n) - x_t^N(\pi)\right\| \\
&\leq 2\max\left\{1,\sqrt{r}\right\} \max_{\theta\in[-r,0]} \left|x^N(t+\theta,\pi^n) - x^N(t+\theta,\pi)\right| \\
&\leq 2\max\left\{1,\sqrt{r}\right\} \int_0^t \left|\mathbb{P}_1^N \mathscr{F}(\pi^n, x^N(s,\pi^n), x_s^N(\pi^n)) \right. \\
&\qquad \left. - \mathbb{P}_1^N \mathscr{F}(\pi, x^N(s,\pi), x_s^N(\pi))\right| ds \\
&\leq 2K_Z \int_0^t \left|\mathscr{F}(\pi^n, x^N(s,\pi^n), x_s^N(\pi^n)) - \mathscr{F}(\pi, x^N(s,\pi), x_s^N(\pi))\right|,
\end{aligned}$$

where $K_Z = \max\{1,\sqrt{r}\}$. By Lemma 3.2.1, we then know that

$$\begin{aligned}
e(t,x_t^N(\pi^n),x_t^N(\pi)) &\leq 2K_L K_Z \int_0^t \left\{\left|x^N(s,\pi^n) - x^N(s,\pi)\right| + \left\|x_s^N(\pi^n) - x_s^N(\pi)\right\|\right\} ds \\
&\qquad + K_Z \int_0^t \mathscr{T}(x_s^N(\pi),\pi^n,\pi) ds
\end{aligned}$$

$$\leq \quad 2K_L K_Z \int_0^t e(s, x_s^N(\pi^n), x_s^N(\pi))ds + K_Z \max_{s\in[0,t_f]} \mathscr{T}(x_s^N(\pi), \pi^n, \pi)\,.$$

From (3.2.3), it is easily argued that if $x_s^N(\pi) \to x_s(\pi)$ *uniformly in s*, then $\mathscr{T}(x_s^N, \pi^n, \pi) \to 0$ as $N, n \to \infty$. Moreover, an application of Gronwall's inequality gives us that

$$e(t, x_t^N(\pi^n), x_t^N(\pi)) \to 0$$

as $N, n \to \infty$ and $\pi^n \to \pi$ in the ρ_Π metric, and thus we conclude that $|x^N(t,\pi^n) - x^N(t,\pi)| \to 0$ as well. □

Corollary 3.2.4. *Given the same conditions in Lemma 3.2.3, then* $|x^N(t,\pi^N) - x(t,\pi)| \to 0$ *as* $N \to \infty$ *for* $\pi^N \to \pi$ *in the* ρ *metric.*

Proof. Consider

$$\left|x^N(t,\pi^N) - x(t,\pi)\right| \quad \leq \quad \left|x^N(t,\pi^N) - x^N(t,\pi)\right| + \left|x^N(t,\pi) - x(t,\pi)\right|\,.$$

The first term converges because of Lemma 3.2.3, while the second term converges as a result of our numerical scheme. □

With this corollary, we are now prepared to prove our inverse problem existence theorem in the next section.

3.2.3 Problem Convergence and Method Stability

As mentioned at the beginning of the last section, in order to fully justify our claim regarding the well posedness of the inverse problem, we need to examine questions concerning the existence of a solution to (3.2.1) and (3.2.2) as well as the dependence of those solutions upon given data.

Theorem 3.2.5. *There exists a solution to the inverse problem as described in (3.2.1) and (3.2.2). Moreover, one can find solutions to the family of problems (3.2.2) that converge to a solution to (3.2.1) as $N \to \infty$.*

Proof. From results in [14], we know that if Q_r is compact, (Π_{ad}, ρ_Π) is also compact. The Weierstrass theorem (in finite dimensional spaces) states that a continuous function on a compact set has a maximum and a minimum. A simple extension of this theorem (using [61, Theorem 1, page 40] as a guide) to a semicontinuous functional on a compact subset of a metric space (as opposed to a normed linear space) indicates that the functional will attain a minimum on the metric space. By Theorem 3.2.2 and Lemma 3.2.3, we have that both $\pi \mapsto x(t,\pi)$ and $\pi \mapsto x^N(t,\pi)$, for fixed $t \in [0, t_f]$, are continuous and thus both J and J^N are continuous with respect to π. Therefore, we know that there exist minimizers for the original and approximate cost functionals J and J^N, respectively.

Let $\{\pi^{*N}\} \in \Pi_{ad}$ be any sequence of solutions to (3.2.2) and $\{\pi^{*N_k}\}$ a convergent (in ρ_Π) subsequence of minimizers (this is possible since Π_{ad} is a compact metric space). Recall that minimizers are not necessarily unique, but one can always select a convergent subsequence of minimizers in Π_{ad}. Denote the limit (in ρ_Π) of this subsequence as π^*. By the minimizing

properties of $\pi^{*N_k} \in \Pi_{ad}$, we then know that

$$J^{N_k}(\pi^{*N_k}) \leq J^{N_k}(\pi);\ \forall \pi \in \Pi_{ad}. \tag{3.2.5}$$

By Corollary 3.2.4, we have the convergence of $x^N(t,\pi^N) \to x(t,\pi)$ and thus $J^N(\pi^N) \to J(\pi)$ as $N \to \infty$ when $\rho_\Pi(\pi^N,\pi) \to 0$. Therefore in the limit as $N_k \to \infty$, the inequality in (3.2.5) goes to

$$J(\pi^*) \leq J(\pi);\ \forall \pi \in \Pi_{ad}, \tag{3.2.6}$$

with π^* as the (not necessarily unique) minimizer of (3.2.1). □

We have proven not only that there is a solution to the original and approximate inverse problems, but also that as we increase the accuracy of the approximate solution, in some sense, it approaches a solution to the original inverse problem.

Next we need to describe more fully the space over which we will be optimizing. Let

$$Q_M \quad = \quad \left\{q_j^M\right\}_{j=1}^M$$

for $M = 1,2,\ldots$ and

$$Q_D = \bigcup_{M=1}^{\infty} Q_M$$

where the sequences are chosen such that Q_D is dense in Q_r. For each $M \in \mathbb{Z}^+$, let

$$\Pi_{ad}^M \quad = \quad \left\{ \pi \in \Pi_{ad} : \pi = (\sum_{j=1}^M p_{1j}\chi_{q_j^M}, \sum_{j=1}^M p_{2j}\chi_{q_j^M}); q_j^M \in Q_M;\right.$$

$$p_{1j}, p_{2,} \in \mathbb{R}; p_{1j}, p_{2j} \geq 0; \sum_{j=1}^{M} p_{1j} = \sum_{j=1}^{M} p_{2j} = 1 \Bigg\}$$

where χ is the indicator function, and define

$$\Pi_D = \bigcup_{M=1}^{\infty} \Pi_{ad}^M .$$

Clearly Q_r is a complete, separable metric space and thus it is easily shown that using Theorem 3.1 from [5] that Π_D is dense in Π_{ad}. We can thus directly conclude that any element $\pi \in \Pi_{ad}$ can be approximated by a sequence $\{\pi_{M_j}\}$, $\pi_{M_j} \in \Pi_{ad}^{M_j}$ such that as $M_j \to \infty$, $\rho_\Pi(\pi_{M_j}, \pi) \to 0$.

Following the discussion concerning Theorem 4.1 in [5], we now state our theorem regarding the continuous dependence of the inverse problem upon the given data.

Theorem 3.2.6. *Let Q_r be $[-r, 0]$, assume that for fixed $t \in [0, t_f]$, $\pi \mapsto x(t, \pi)$ is continuous on Π_{ad}, and let Q_D be a countable dense subset of Q_r as defined above. Suppose the observed data $\widehat{X}_m, \widehat{X} \in \mathbb{R}^n$ (n a positive integer) are such that $\widehat{X}_m \to \widehat{X}$ as $m \to \infty$. Moreover, suppose that $\Pi_N^{*M}(\widehat{X}_m)$ is the set of minimizers for $J^N(\pi; \widehat{X}_m)$ over $\pi \in \Pi_{ad}^M$ corresponding to the data $\widehat{X}_m$. Similarly, suppose that $\Pi^*(\widehat{X})$ is the set of minimizers of $J(\pi; \widehat{X})$ over $\pi \in \Pi_{ad}$ corresponding to the data $\widehat{X}$. Then, $d_H(\Pi_N^{*M}(\widehat{X}_m), \Pi^*(\widehat{X})) \to 0$ as $N, M, m \to \infty$ and $\widehat{X}_m \to \widehat{X}$.*

Proof. Combine arguments of Theorem 3.2.5 and Corollary 3.2.4 and note that in Theorem 4.1 in [5], the cost function is being optimized over a space of probability distributions. Thus by

using this theorem we can claim that

$$\begin{aligned} d_H(\Pi_N^{*M}(\widehat{X}_m), \Pi^*(\widehat{X})) &= \inf\left\{\rho_\Pi(\pi_{N,m}^M, \pi); \pi_{N,m}^M \in \Pi_N^{*M}(\widehat{X}_m), \pi \in \Pi^*(\widehat{X})\right\} \\ &= \inf\big\{\rho(P_{N,m,1}^M, P_1) + \rho(P_{N,m,2}^M, P_2); \\ &\qquad \pi_{N,m}^M = (P_{N,m,1}^M, P_{N,m,2}^M) \in \Pi_N^{*M}(\widehat{X}_m), \\ &\qquad \pi = (P_1, P_2) \in \Pi^*(\widehat{X})\Big\} \to 0, \end{aligned}$$

since each of the terms in the sum converge to zero as $N, M, m \to \infty$ and $\widehat{X}_m \to \widehat{X}$. □

Combining the results of these two theorems, we can claim both that there exists a solution to the inverse problem and that it is continuously dependent upon the given data. We have established well-posedness of the forward problem in Section 3.2.2. In this section, we have shown problem stability and method stability of our inverse problem. Therefore we can conclude well-posedness of our inverse problem.

Lastly, we note that the theoretical results of this section only apply to the identification of two parameter distributions. However, the extension to the other parameters (i.e., the ones not associated with the delay) follows readily from considering the NLS optimization over $Q_{ad} \times \Pi_{ad}$ where (as before) Q_{ad} is the domain of admissible values for the deterministic parameters.

3.3 Sensitivity Analysis

The first step in the sensitivity analysis is to derive the *sensitivity equations* by formally taking derivatives (with respect to a parameter of interest) on both sides of the original equation(s). The solution to this new system (assuming for the moment that it is well-posed) contains information regarding the sensitivity of the original system to perturbations in the chosen parameter (around some *a priori* fixed value of that parameter). Hereafter we will refer to the solution to the sensitivity equations as a *sensitivity function*.

Note that a full and thorough sensitivity analysis can include not only derivatives with respect to the scalar parameters (e.g., γ or δ_A), but also Fréchet derivatives with respect to the delay distributions (e.g., P_1 or P_2). The following sections include discussions regarding the well-posedness of the sensitivity equations as well as analysis of an example system of sensitivity equations. Moreover, while we choose to focus on one particular parameter, we could have easily chosen any parameter to illustrate the ideas.

In earlier sections, we used the L_2 norm because the state space was $\mathbb{R}^4 \times L_2(-r,0;\mathbb{R}^4)$. In this section, we will use $\mathbb{R}^4 \times \mathscr{C}(-r,0;\mathbb{R}^4)$, along with the corresponding norm $\|\cdot\|_\infty$ on $[-r,0]$. We do this both because the estimates are easier to calculate[1] and because the initial conditions for the sensitivity equations are always zero in our analysis (and hence continuous). This was not the situation for general solutions to the delay equations treated in earlier sections.

[1] Note that the use of the L_2-norm would not change any of the results.

3.3.1 Well-posedness of the Sensitivity Equations

Here will only consider distributions P_1, P_2 that are both differentiable and parameterizable by a mean μ and a standard deviation σ (i.e., for $i = 1,2$, $p_i(\theta) = \frac{\partial}{\partial\theta}P_i(\theta)$ and $P_i(\theta) = P_i(\theta,\mu_i,\sigma_i)$ for $\theta \in [-r,0]$). Moreover, we will further assume that the resulting densities p_i are $\mathscr{C}^1$ in μ_i and σ_i, respectively.

To illustrate the sensitivity procedure, we will consider the sensitivity of our HIV population system with respect to μ_1 (mean delay time between viral infection and the initiation of viral production) of the solution x to (3.1.1). Let us fix the forms of the distributions P_1, P_2 and consider for $t \in [-r,t_f]$, the derivative of $x(t,\mu_1)$ with respect to μ_1 (where μ_1 is the parameter corresponding to the mean of p_1). If we let $(\eta,\phi) \in \mathbb{R}^4 \times \mathscr{C}(-r,0;\mathbb{R}^4)$, $t \in [0,t_f]$, $\mu_1 > 0$, then from results established in Section 3.1.1, we note that $\mathscr{F}(t,\eta,\phi,\mu_1) = L(\eta,\phi;\mu_1) + f_1(\eta) + f_2(t)$ is $\mathscr{C}^1$ in t, η, ϕ, and μ_1 under the smoothness assumptions (from the same Section) on $\mathscr{F}$, L, f_1, and f_2. For our specific case, to prove that the derivative of x with respect to μ_1 exists and is continuous in t, we will make use of the following lemma.

Lemma 3.3.1. *There exists a solution to the linear (variational) system*

$$\begin{aligned} \dot{y}(t) &= g_1(x(t,\mu_1);y(t)) + g_2(\mu_1;y_t) + g_3(x_t(\mu_1),\mu_1;1) \\ (y(0),y_0) &= (\Psi(0),\Psi) \in \mathbb{R}^4 \times \mathscr{C}(-r,0;\mathbb{R}^4), \end{aligned} \tag{3.3.1}$$

for $0 \le t \le t_f$, $x(t,\mu_1)$ the solution to (3.1.1), and where for $\mu,\xi \in \mathbb{R}$, $\eta,\zeta \in \mathbb{R}^4$, $\phi,\psi \in$

$\mathscr{C}(-r,0;\mathbb{R}^4)$,

$$
\begin{aligned}
g_1(\eta;\zeta) &= M_\eta \zeta\,, \\
g_2(\mu;\psi) &= n_A \left[\delta_{(1,2)}\right]_{(4,4)} \int_{-r}^{0} \psi(\theta) p_1(\theta,\mu,\sigma_1) d\theta \\
&\quad + \gamma(\left[\delta_{(3,2)}\right]_{(4,4)} - \left[\delta_{(2,2)}\right]_{(4,4)}) \int_{-r}^{0} \psi(\theta) p_2(\theta,\mu_2,\sigma_2) d\theta \\
g_3(\phi,\mu;\xi) &= n_A \left[\delta_{(1,2)}\right]_{(4,4)} \int_{-r}^{0} \phi(\theta) \left(\frac{\partial}{\partial \mu_1} p_1(\theta,\mu,\sigma_1)\right)(\xi) d\theta\,,
\end{aligned}
$$

and where

$$
M_\eta = \begin{bmatrix}
-c - p\eta_4 & 0 & n_C & -p\eta_1 \\
p\eta_4 & r_v - \delta_A - \delta\left(2\eta_2+\eta_3+\eta_4\right) & -\delta\eta_2 & -\delta\eta_2 + p\eta_1 \\
0 & -\delta\eta_3 & r_v - \delta_C - \delta - \delta\left(\eta_2+2\eta_3+\eta_4\right) & -\delta\eta_3 \\
-p\eta_4 & -\delta\eta_4 & -\delta\eta_4 & r_u - \delta_u - \delta\left(\eta_2+\eta_3+2\eta_4\right) - p\eta_1
\end{bmatrix}
$$

Proof. On the right side of (3.3.1), the function $g_1+g_2+g_3$ satisfies both the differentiability condition (Lemma 3.1.1) and the global Lipschitz condition (Lemma 3.1.2). Following the reasoning in the proof of Theorem 3.1.5, by defining a convergent sequence of successive approximations, it can then easily be shown that a solution exists and is unique. □

Remark 3.3.2. Note that Lemma 3.3.1 guarantees the existence of a solution to a system of equations with a *general* initial condition Ψ. Recall that in equation (3.1.4), the initial condition Φ is independent of μ_1 and thus the next step will be to argue that system (3.3.1) combined with the trivial initial condition $\Psi = 0$ comprises the sensitivity equations.

Theorem 3.3.3. *The solution x of (3.1.1) has a derivative with respect to the parameter* μ_1 *and for* $\mu_1 = \mu > 0$*, this derivative* $v(t) = \frac{\partial}{\partial \mu_1} x(t,\mu)$ *satisfies (3.3.1) with the initial condition* $(\Psi(0), \Psi) = (0,0) \in \mathbb{R}^4 \times \mathscr{C}(-r, 0; \mathbb{R}^4)$.

Proof. To prove the existence of a derivative of x with respect to the parameter μ_1, we fix μ_1 at $\mu > 0$, let $\varepsilon \in \mathbb{R}$ be a perturbation of μ, and for all $t \in [-r, t_f]$, define

$$h(t,\mu,\varepsilon) = x(t,\mu+\varepsilon) - x(t,\mu)\,.$$

The overall structure of the proof is thus to show that

$$\frac{\partial}{\partial \mu_1} x(t,\mu) = \lim_{|\varepsilon| \to 0} \frac{h(t,\mu,\varepsilon)}{\varepsilon}$$

exists and is continuous for $t \in [-r, t_f]$. We begin by considering h

$$\begin{aligned} h(t,\mu,\varepsilon) &= \int_0^t \{\mathscr{F}(s, x(s,\mu+\varepsilon), x_s(\mu+\varepsilon), \mu+\varepsilon) - \mathscr{F}(s, x(s,\mu), x_s(\mu), \mu)\}\, ds \\ &= \int_0^t \{\mathscr{F}(s, x(s,\mu+\varepsilon), x_s(\mu+\varepsilon), \mu+\varepsilon) - \mathscr{F}(s, x(s,\mu), x_s(\mu+\varepsilon), \mu+\varepsilon) \\ &\quad + \mathscr{F}(s, x(s,\mu), x_s(\mu+\varepsilon), \mu+\varepsilon) - \mathscr{F}(s, x(s,\mu), x_s(\mu), \mu+\varepsilon) \\ &\quad + \mathscr{F}(s, x(s,\mu), x_s(\mu), \mu+\varepsilon) - \mathscr{F}(s, x(s,\mu), x_s(\mu), \mu)\}\, ds\,. \end{aligned}$$

According to the Mean Value Theorem [56], we have

$$\begin{aligned} h(t,\mu,\varepsilon) \quad = \quad & \int_0^t \int_0^1 \big\{ D_x \mathscr{F}(s, x(s,\mu) + s'h(s,\mu,\varepsilon), x_s(\mu+\varepsilon), \mu+\varepsilon)(h(s,\mu,\varepsilon)) \\ & + D_{x_t} \mathscr{F}(s, x(s,\mu), x_s(\mu) + s'h_s(\mu,\varepsilon), \mu+\varepsilon)(h_s(\mu,\varepsilon)) \\ & + D_{\mu_1} \mathscr{F}(s, x(s,\mu), x_s(\mu), \mu + s'\varepsilon)(\varepsilon) \big\} \, ds' ds, \end{aligned}$$

where $D_x\mathscr{F}$, $D_{x_t}\mathscr{F}$, $D_{\mu_1}\mathscr{F}$ are the Fréchet derivatives of $\mathscr{F}$ with respect to its second, third, and fourth arguments respectively. Since $\mathscr{F}$ is $\mathscr{C}^1$ in all its arguments, we then know that there exists linear functions $\Delta^1_{s',\varepsilon}$, $\Delta^2_{s',\varepsilon}$, $\Delta^3_{s',\varepsilon}$ (each parameterized by s' and ε) such that

$$\begin{aligned} h(t,\mu,\varepsilon) \quad = \quad & \int_0^t \int_0^1 \Big\{ D_x \mathscr{F}(s, x(s,\mu), x_s(\mu), \mu)(h(s,\mu,\varepsilon)) + \Delta^1_{s',\varepsilon}(h(s,\mu,\varepsilon)) \\ & + D_{x_t} \mathscr{F}(s, x(s,\mu), x_s(\mu), \mu)(h_s(\mu,\varepsilon)) + \Delta^2_{s',\varepsilon}(h_s(\mu,\varepsilon)) \\ & + D_{\mu_1} \mathscr{F}(s, x(s,\mu), x_s(\mu), \mu)(\varepsilon) + \Delta^3_{s',\varepsilon}(\varepsilon) \Big\} \, ds' ds, \end{aligned}$$

where $|\Delta^1_{s',\varepsilon}|, |\Delta^2_{s',\varepsilon}|, |\Delta^3_{s',\varepsilon}| \to 0$ uniformly in s' as $|\varepsilon| \to 0$. Thus for $s \in [0,t]$, $\nu, \xi \in \mathbb{R}$, $\eta, \zeta \in \mathbb{R}^4$, $\phi, \psi \in \mathscr{C}(-r, 0; \mathbb{R}^4)$, and g_1, g_2, g_3 as defined in Lemma 3.3.1,

$$\begin{aligned} D_x \mathscr{F}(s,\eta,\phi,\nu)(\zeta) \quad &= \quad g_1(\eta;\zeta) \\ D_{x_t} \mathscr{F}(s,\eta,\phi,\nu)(\psi) \quad &= \quad g_2(\nu;\psi) \\ D_{\mu_1} \mathscr{F}(s,\eta,\phi,\nu)(\xi) \quad &= \quad g_3(\phi,\nu;\xi). \end{aligned}$$

Then the equation for h is

$$\begin{aligned} h(t,\mu,\varepsilon) &= \int_0^t \left\{ g_1(x(s,\mu);h(s,\mu,\varepsilon)) + g_2(\mu;h_s(\mu,\varepsilon)) + g_3(x_s(\mu),\mu;\varepsilon) \right\} ds \\ &\quad + \int_0^t \int_0^1 \left\{ \Delta^1_{s',\varepsilon}(h(s,\mu,\varepsilon)) + \Delta^2_{s',\varepsilon}(h_s(\mu,\varepsilon)) + \Delta^3_{s',\varepsilon}(\varepsilon) \right\} ds' ds \,. \end{aligned}$$

Moreover, since g_1, g_2, g_3 are all linear in their last arguments, the equation for h can be used to obtain

$$\begin{aligned} |h(t,\mu,\varepsilon)| &\leq \|h_t(\mu,\varepsilon)\|_\infty \\ &\leq \max_{\tau\in[t-r,t]} \int_0^\tau \left\{ \left| g_1(x(s,\mu);\cdot) + \int_0^1 \left|\Delta^1_{s',\varepsilon}\right| ds' \right| |h(s,\mu,\varepsilon)| \right. \\ &\quad + \left| g_2(\mu;\cdot) + \int_0^1 \left|\Delta^2_{s',\varepsilon}\right| ds' \right| \|h_s(\mu,\varepsilon)\|_\infty \\ &\quad \left. + \left| g_3(x_s(\mu),\mu;\cdot) + \int_0^1 \left|\Delta^3_{s',\varepsilon}\right| ds' \right| |\varepsilon| \right\} ds \,. \end{aligned}$$

Thus for constants $K_1, K_2 > 0$, we know that

$$\|h_t(\mu,\varepsilon)\|_\infty \leq K_1 \int_0^t \|h_s(\mu,\varepsilon)\|_\infty ds + K_2 t_f |\varepsilon| \,,$$

and a simple application of Gronwall's inequality implies that

$$\|h_t(\mu,\varepsilon)\|_\infty \leq K_2 \left| t_f \right| |\varepsilon| \, e^{K_1 t_f} \,, \tag{3.3.2}$$

which will be useful in the next step.

Now, if we divide both sides of the equation for h by ε so that

$$\begin{aligned}\frac{h(t,\mu,\varepsilon)}{\varepsilon} &= \int_0^t \left\{ g_1(x(s,\mu);\frac{h(s,\mu,\varepsilon)}{\varepsilon}) + g_2(\mu;\frac{h_s(\mu,\varepsilon)}{\varepsilon}) + g_3(x_s(\mu),\mu;\frac{\varepsilon}{\varepsilon}) \right\} ds \\ &\quad + \int_0^t \int_0^1 \left\{ \Delta^1_{s',\varepsilon}(\frac{h(s,\mu,\varepsilon)}{\varepsilon}) + \Delta^2_{s',\varepsilon}(\frac{h_s(\mu,\varepsilon)}{\varepsilon}) + \Delta^3_{s',\varepsilon}(\frac{\varepsilon}{\varepsilon}) \right\} ds' ds,\end{aligned}$$

we note that the form of the integrand is strikingly similar to the right side of the equation in (3.3.1). For equation (3.3.1), we denote the solution generated using $\mu_1 = \mu$ and initial condition $(\Psi(0),\Psi) = (0,0) \in \mathbb{R}^4 \times \mathscr{C}\{-r,0;\mathbb{R}^4\}$ as $v(t)$ for $t \in [-r,t_f]$. Moreover, we claim that this solution v is equal to the limit of h/ε as $|\varepsilon| \to 0$.

By Lemma 3.3.1, we know that v exists and is continuous for $t \in [-r,t_f]$. Clearly v and h/ε are identically zero for $t \in [-r,0]$ for all $\varepsilon > 0$, and thus we consider for $t \in [0,t_f]$

$$\begin{aligned}\left| v(t) - \frac{h(t,\mu,\varepsilon)}{\varepsilon} \right| &\leq \left\| v_t - \frac{h_t(\mu,\varepsilon)}{\varepsilon} \right\|_\infty \\ &\leq \max_{\tau\in[t-r,t]} \left| \int_0^\tau \left\{ g_1(x(s,\mu);v(s) - \frac{h(s,\mu,\varepsilon)}{\varepsilon}) + g_2(\mu;v_s - \frac{h_s(\mu,\varepsilon)}{\varepsilon}) \right.\right. \\ &\qquad \left. + g_3(x_s(\mu),\mu;1-\frac{\varepsilon}{\varepsilon}) \right\} ds - \int_0^\tau \int_0^1 \left\{ \Delta^1_{s',\varepsilon}(\frac{h(s,\mu,\varepsilon)}{\varepsilon}) \right. \\ &\qquad \left.\left. + \Delta^2_{s',\varepsilon}(\frac{h_s(\mu,\varepsilon)}{\varepsilon}) + \Delta^3_{s',\varepsilon}(\frac{\varepsilon}{\varepsilon}) \right\} d\tau ds \right| \\ &\leq \max_{\tau\in[t-r,t]} \left\{ \int_0^\tau \left\{ \left| g_1(x(s,\mu);\cdot) \right| \left| v(s) - \frac{h(s,\mu,\varepsilon)}{\varepsilon} \right| \right.\right. \\ &\qquad + \left| g_2(\mu;\cdot) \right| \left\| v_s - \frac{h_s(\mu,\varepsilon)}{\varepsilon} \right\|_\infty + \left| g_3(x_s(\mu),\mu;\cdot) \right| |0| \\ &\qquad \left. + \int_0^1 \left\{ \left| \Delta^1_{s',\varepsilon} \right| \left| \frac{h(s,\mu,\varepsilon)}{\varepsilon} \right| + \left| \Delta^2_{s',\varepsilon} \right| \left\| \frac{h_s(\mu,\varepsilon)}{\varepsilon} \right\|_\infty + \left| \Delta^3_{s',\varepsilon} \right| |1| \right\} ds' \right\} ds \right\}\end{aligned}$$

$$\begin{aligned} &\leq \int_0^t \left(\left|g_1(x(s,\mu);\cdot)\right| + \left|g_2(\mu;\cdot)\right|\right) \left\| v_s - \frac{h_s(\mu,\varepsilon)}{\varepsilon} \right\|_\infty ds \\ &\quad + \int_0^t \int_0^1 \left\{ \left|\Delta^1_{s',\varepsilon}\right| \left| \frac{h(s,\mu,\varepsilon)}{\varepsilon} \right| + \left|\Delta^2_{s',\varepsilon}\right| \left\| \frac{h_s(\mu,\varepsilon)}{\varepsilon} \right\|_\infty + \left|\Delta^3_{s',\varepsilon}\right| |1| \right\} ds' ds . \end{aligned}$$

By equation (3.3.2), we know that

$$\begin{aligned} \left\| v_t - \frac{h_t(\mu,\varepsilon)}{\varepsilon} \right\|_\infty &\leq \int_0^t \left\{ \left|g_1(x(s,\mu);\cdot)\right| + \left|g_2(\mu;\cdot)\right| \right\} \left\| v_s - \frac{h_s(\mu,\varepsilon)}{\varepsilon} \right\|_\infty ds + \\ &\quad + \int_0^t \int_0^1 K_2 \left|t_f\right| \exp(K_1 t_f) \left\{ \left|\Delta^1_{s',\varepsilon}\right| + \left|\Delta^2_{s',\varepsilon}\right| \right\} \frac{|\varepsilon|}{|\varepsilon|} + \left|\Delta^3_{s',\varepsilon}\right| |1| \, ds' ds \\ &\leq K_1 \int_0^t \left\| v_s - \frac{h_s(\mu,\varepsilon)}{\varepsilon} \right\|_\infty ds \\ &\quad + t_f \int_0^1 \left\{ K_2 t_f \exp(K_1 t_f) \left\{ \left|\Delta^1_{s',\varepsilon}\right| + \left|\Delta^2_{s',\varepsilon}\right| \right\} + \left|\Delta^3_{s',\varepsilon}\right| \right\} ds' \\ &\leq K_1 \int_0^t \left\| v_s - \frac{h_s(\mu,\varepsilon)}{\varepsilon} \right\|_\infty ds + K_3(t_f) \int_0^t \left\{ \left|\Delta^1_{s',\varepsilon}\right| + \left|\Delta^2_{s',\varepsilon}\right| + \left|\Delta^3_{s',\varepsilon}\right| \right\} ds' , \end{aligned}$$

where $K_3(t_f) = t_f \max\{K_2 t_f \exp(K_1 t_f), 1\}$. By Gronwall's inequality, we then have that

$$\left| v(t) - \frac{h(t,\mu,\varepsilon)}{\varepsilon} \right| \leq K_3(t_f) \int_0^1 \left\{ \left|\Delta^1_{s',\varepsilon}\right| + \left|\Delta^2_{s',\varepsilon}\right| + \left|\Delta^3_{s',\varepsilon}\right| \right\} ds' e^{K_1 t_f} .$$

Since $|\Delta^1_{s',\varepsilon}|, |\Delta^2_{s',\varepsilon}|, |\Delta^3_{s',\varepsilon}| \to 0$ uniformly in s' as $|\varepsilon| \to 0$, we can then conclude that for $t \in [-r, t_f]$, $h/\varepsilon \to v$ as $|\varepsilon| \to 0$. Therefore, the partial derivative of x with respect to μ_1 (evaluated at $\mu_1 = \mu > 0$) exists and satisfies (3.3.1) with the initial condition $(\Psi(0), \Psi) = (0,0) \in \mathbb{R}^4 \times \mathscr{C}(-r, 0; \mathbb{R}^4)$, which completes the proof. □

The line of reasoning presented here in Lemma 3.3.1 and Theorem 3.3.3 concerns the existence and continuity (in t) of the derivative of a solution to (3.1.1) with respect to the specific

parameter μ_1.Similar arguments (again with minimal changes to g_3) establish the existence and continuity (in t) of derivatives with respect to μ_2, σ_1, and σ_2. For the parameters that appear in (3.1.1) as linear coefficients, g_1 and g_2 are slightly altered (dependent upon the parameter under consideration), while $g_3 \equiv 0$. However, these differences do not change the conclusion that the derivative of the solution $x(t)$ (with respect to any parameter appearing on the right side of (3.1.1)) exists and is continuous in time. One can also establish differentiability of solutions with respect to discrete delays (i.e., when P_1 or P_2 is a Dirac measure) and well-posedness of the appropriate sensitivity equations. The arguments, while in the spirit of those given above, are somewhat more tedious and will not be given here.

3.3.2 Analysis

In this section we examine some applications of the theory developed in the previous section. Note that the simulation presented here was performed with our Matlab implementation of the numerical scheme from Section 3.1.2. As can be inferred from equation (3.3.1), in order to solve sensitivity equations, one needs the solution x of the original system. As mentioned in the previous section, for illustrative purposes, we fix the forms of the delay distributions and thus assume them to be parameterized by $\mu_1, \sigma_1, \mu_2, \sigma_2$. This step eliminates the need to worry about identifying the entire distributions from Section 3.2.1. We choose to employ discrete delays (Dirac measures) for the distributions, and in a later section (Section 4.1), we will present the results and the reasoning that led to this decision. For the interested reader, both the experimental data and the numerical best fit solution x^N (using parameters from Table

4.2), are depicted in Figure 4.2.1 in the next chapter. It is this x^N which we use when simulating the solutions to sensitivity equations.

By Theorem 3.3.3, we can legitimately consider the derivative of both sides of (3.1.1) with respect to any appropriate parameter. We first consider the derivative of $x(t)$ with respect to μ_1 at $\mu_1 = \mu$

$$\begin{aligned} \tfrac{d}{d\mu_1}\dot{x}(t,\mu) &= \tfrac{d}{d\mu_1}L(x(t,\mu),x_t(\mu);\mu) + \tfrac{d}{d\mu_1}f_1(x(t,\mu)) + \tfrac{d}{d\mu_1}f_2(t) \\ \tfrac{d}{d\mu_1}(x(0,\mu),x_0(\mu)) &= \tfrac{d}{d\mu_1}(\Phi(0),\Phi) \in \mathbb{R}^4 \times \mathscr{C}(-r,0;\mathbb{R}^4)\,. \end{aligned} \tag{3.3.3}$$

for $0 \le t \le t_f$. If we denote $v(t) = \frac{d}{d\mu_1}x(t,\mu)$ (for some specific value of $\mu_1 = \mu > 0$), we obtain the sensitivity equations

$$\begin{aligned} \dot{v}(t) &= g_1(x(t,\mu);v(t)) + g_2(\mu;v_t) + g_3(x_t(\mu),\mu;1) \quad \text{for } 0 \le t \le t_f \\ (v(0),v_0) &= (0,0) \in \mathbb{R}^4 \times \mathscr{C}(-r,0;\mathbb{R}^4)\,, \end{aligned} \tag{3.3.4}$$

where g_1, g_2, g_3 are as defined in Lemma 3.3.1. As before, due to the complexity of the right side of (3.3.4), we cannot solve exactly for the solution $v(t)$. Moreover, we do not have x which appears in the terms g_1 and g_3; we only have an approximation x^N to x. Therefore, we must propose a viable numerical scheme to calculate an approximation v^N that satisfies (3.3.4) with x replaced by x^N and such that $\lim_{N\to\infty} v^N = v$.

Hence we consider v^N an approximate solution to (3.3.4) with $x = x^N$ in the coefficients.

This is a linear nonautonomous system of the form

$$\begin{aligned} \dot{v}^N(t) &= \mathscr{A}^N(t)v^N(t) + g_2(v_t^N) + g_3(x_t^N) \\ \left(v^N(0), v_0^N\right) &= (0,0) \in \mathbb{R}^4 \times \mathscr{C}(-r,0;\mathbb{R}^4)\,, \end{aligned} \tag{3.3.5}$$

which for N fixed and x^N given, is a special case of the systems treated in [6], where existence and uniqueness is guaranteed. To obtain convergence of v^N to v (the unique solution to (3.3.4)), we turn to [3]. A straightforward extension of the theory presented there to treat nonautonomous linear systems such as (3.3.5) will yield, (under the approximation scheme described in [6]), the desired convergence.

If we were to plot simulations of (3.3.4) (or actually, the approximate solution defined by (3.3.5)), interpretations of these plots would suggest specific effects that changes in μ_1 would have on the solution x. Moreover, if we were to also perform the analogous derivation for the infection rate p, a plot of that sensitivity function would depict the effect that changes in p would have on x. Since μ_1 and p differ in their units, the sensitivity functions for μ_1 and p would also have different units, thus rendering any comparison nonsensical. We turn to the sensitivity analysis literature to resolve this issue. To enable a comparison of the effects that parameters with different units have on the solution, we simply multiply by the parameter under consideration, e.g.,

$$\left[\frac{\partial}{\partial\mu_1}x_1(t,\mu), \frac{\partial}{\partial\mu_1}x_2(t,\mu), \frac{\partial}{\partial\mu_1}x_3(t,\mu), \frac{\partial}{\partial\mu_1}x_4(t,\mu)\right]^T \cdot \mu\,.$$

This form of the sensitivity function is known as the *semirelative* or *semilogarithmic* or *unnormalized* sensitivity function [30, 31]. Moreover, this form is actually the differential of x with respect to μ_1 at μ in the direction μ

$$D_{\mu_1} x_i(t,\mu)[\mu] = \left(\frac{\partial}{\partial \mu_1} x_i(t,\mu)\right) \cdot \mu$$

for $i = 1,2,3,4$. With this weighting, we now have the tools to rank the parameters with regard to their influence over the solution.

3.3.3 Discussion

As discussed in Section 1.2.4, the taking of a derivative (with respect to parameters) of the equations governing a system is not a new idea and indeed has been around (in some form) for at least 170 years. Within control theory and engineering applied to physical systems, the forms of the fundamental mathematical models often are, for the most part, relatively well established and not so open to debate. For example, in some investigations, it may not be fruitful to question the significance of the viscosity parameter in the Navier-Stokes equations (although sensitivity of flow patterns to viscosity is sometimes very important, see [84]). However, the constitutive parameters and forms of the mathematical models employed in the biological sciences are frequently not as well agreed upon, and indeed (as is evidenced by the literature) open to considerable debate. Since the current approach to sensitivity was originally developed in the context of control theory, the cited literature is (understandably) biased toward that field; a considerable proportion of the papers are devoted to analyzing the sensitivity of transfer func-

tions and eigenvalues. Thus the application of mathematically rigorous sensitivity analyses to dynamical systems designed to model biological phenomena does not seem to be common practice. Indeed, many sensitivity analysis studies involve copious simulations. As such, there are many possibilities that have not been fully examined.

In the analysis presented above, we only considered first derivatives of the parameters. In theory, we could have examined derivatives with respect to multiple parameters, e.g., $\frac{\partial^2 x}{\partial n_A \partial \delta_A}$ (joint sensitivities), an analysis of which could be used to ascertain the independent identifiability of parameters. We could have also taken a derivative with respect to the initial conditions, which (as is intuitive) would suggest the influence of the initial conditions over the solution (and can be an extremely useful tool in understanding certain biological systems). Finally, we could have considered the derivative of the least squares functional (3.2.1) with respect to a parameter (as was explored in [55]), which could then be used as part of a jacobian in an optimization algorithm (as part of a parameter estimation scheme).

The process of taking the derivative of a system with respect to a parameter is usually not an exceedingly challenging task and it is important to remember that the sensitivity function only reveals the local behavior (since it is a derivative) around the fixed parameter value. However, this idea can yield useful insights into the solution of complex systems (even those with nonlinearities and delays) such as (3.1.1). Effectively, the technique of using simulation sensitivity functions presented here is a more mathematically rigorous (and quicker) way to attain insight into a system than manually adjusting a parameter and observing the effect on the solution through massive simulation efforts.

Chapter 4

Numerical Results

Clearly, the number of data points in Figure 2.1.1 is insufficient to carry out (with any degree of confidence) rigorous inverse problem investigations or to perform a legitimate statistical analysis with models such as those discussed above. However, our goal is to illustrate our methodology, and thus in this chapter, we perform the inverse problem calculations (fully aware of their inadequacies) to obtain an estimate of the delays and then compare these calculated values with the experimentally accepted ones.

In Section 4.1, we report results on a numerical simulation experiment in which we compare the effect of different kernel choices (for the delay distribution) upon the solution.

Based upon discussions with S. E. Holte and M. Emerman we chose to use our inverse problem methodology to identify a subset of the parameters in Table 2.2. The choices, along with the best fit values are collected in Table 4.2 (in Section 4.2). With the results from these inverse problem calculations, we perform a test for the statistical significant of the mechanism

in the FDE which accounts for the delays.

In the last section of this chapter (Section 4.3) we present results from a sample sensitivity analysis on the parameters over which we performed the inverse problem.

4.1 Kernel Investigation

We examined the nature of the delay by numerically simulating our system using the method described in Section 3.1.2 and the different kernels described in Section 2.3.3. Specifically, we studied the effect of different μ's, different ς's (or σ's depending on the kernel choice), and kernel smoothness upon the system, and present a representative selection of our findings from these investigations. Note that if a gamma is chosen to represent the distributed delay, the calculation of the convolution term is nontrivial and Appendix A contains a discussion of the numerical issues, as well as a possible way to resolve the problem.

To examine the effects of kernels with different smoothness properties, we fixed $\mu_1 = -22.8$, $\sigma_1^2 = 1$, $\mu_2 = -26$, $\sigma_2^2 = 1$ and then ran the numerical simulations of (2.3.6)-(2.3.9) using the normalized hat kernel $\widehat{k}$, inverted quadratic kernel $\widetilde{k}$, gamma kernel, and gaussian kernel. Note that the choice of μ_1 and μ_2 is motivated by results that appear in the next section. The results using three of the kernels are depicted in Figure 4.1.1. The width ς was chosen so that the variance for $\widehat{k}$ and $\widetilde{k}$ was approximately one (corresponding to $\varsigma = 4.9$ for $\widehat{k}$ and $\varsigma = 0.05$ for $\widetilde{k}$). If we compare these behaviors with that of the discrete delay system depicted in Figure 2.3.1, we observe that kernel shape/smoothness does not appear to have a significant effect upon the simulation (for unimodal, symmetric kernels). Other simulations (not presented

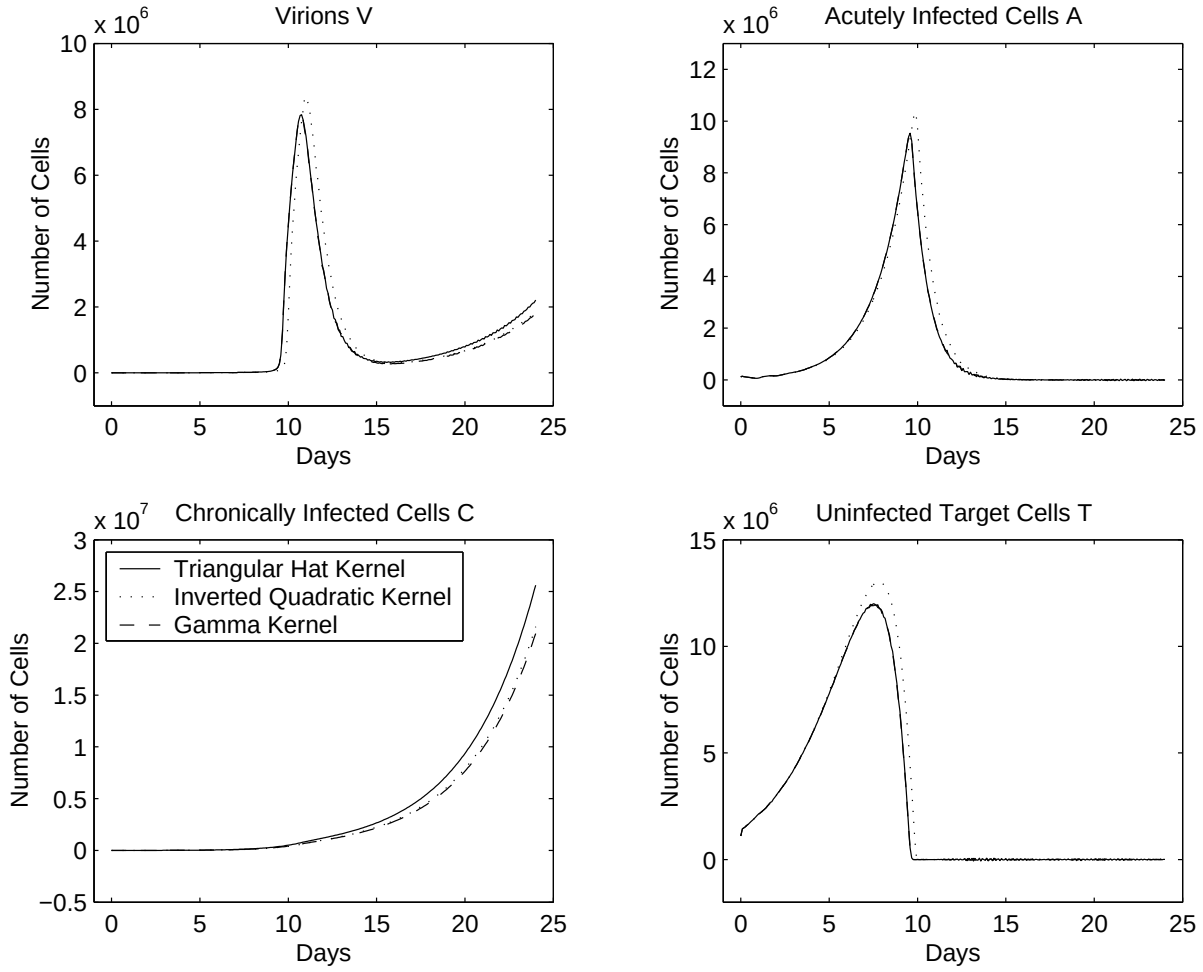

Figure 4.1.1: Simulations of (3.1.14) with the $\widehat{k}$, $\widetilde{k}$, and k_Γ kernels.

here) also confirmed that the qualitative behavior of solutions does not vary greatly between the discrete delay systems and systems with the continuous kernels $\widetilde{k}$, $\widehat{k}$ with mean equal to the discrete delay.

Next, we studied the influence that s_1 and s_2 have upon the solution, since they determine the kernel support (at least in the case of $\widetilde{k}$). Note that it is not useful to study the support independent of ς when using $k_1(s) = \widehat{k}(s;\mu,\varsigma,s_1,s_2)$, and thus we only examine the ramifications of varying the support of $k_1 = \widetilde{k}$. Our interests were focused upon parameter ranges in which

$k_1(\mu+\frac{\sigma}{2}) \gg k_1(s_2)$ and $k_1(\mu-\frac{\sigma}{2}) \gg k_1(s_1)$ to prevent interference between σ and the domain of the kernel support. Over a wide range of values for s_1 and s_2 (that satisfied our criteria) there were negligible differences between the simulations, and thus we do not present a plot of the results.

To assess the effect of the mean μ_1 on the kernel k_1 (the kernel from the $\dot{V}$ equation), we let k_1 be the hat kernel $\widehat{k}$, fixed the other parameters, and performed simulations of (3.1.1) for a variety of means μ_1, the results of which are depicted in Figure 4.1.2. For this simulation, we let the second kernel $k_2 = \widehat{k}$, but kept its mean fixed at $\mu_2 = \mu_1 - 3.2$. Note that as the mean varies, we observe a dramatic temporal shift in the peaks of various compartments. The simulations run using the inverted quadratic, gaussian, and gamma kernels exhibited virtually identical sensitivity to the perturbation of μ_1 (and are thus not depicted here).

To assess the effect of the mean μ_2 on the kernel k_2 (the kernel from the $\dot{A}$ and $\dot{C}$ equations), we let the kernels be exactly as described in the previous paragraph, except we set μ_1 to -22.8 and then varied μ_2. The results are depicted in Figure 4.1.3, and as you can see, while there is some change, it is not nearly as dramatic as that which occurs when varying μ_1.

Lastly, we studied the effect of varying the width ς (or standard deviation σ, depending on the choice) of the kernel on the solution. We let $k_1(t) = \widehat{k}(t;-22.8,\varsigma_1,-48,0)$, $k_2(t) = \widehat{k}(t;-26,1,-48,0)$ and then plotted the resulting x^N for a variety of (biologically reasonable) values for ς_1 in Figure 4.1.4. The obvious interpretation of the plots is that the width ς_1 does not seem to have much influence over the numerical simulation. Furthermore, varying ς_2 also has no visible effect on the simulations and as before, the use of the other kernels results in

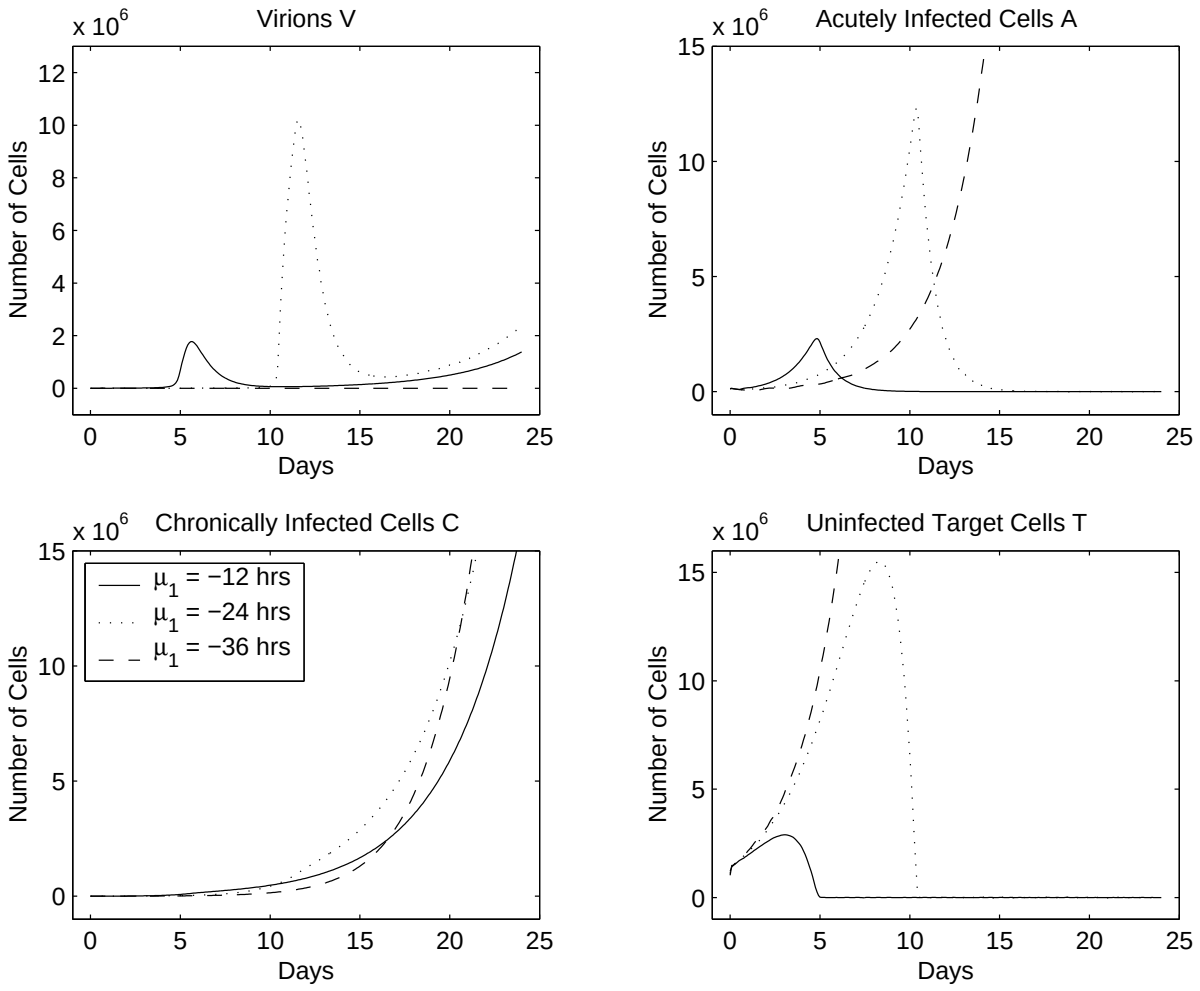

Figure 4.1.2: Simulations of (3.1.14) using $\widehat{k}$ for k_1 and k_2 for several values of μ_1 (with $\mu_2 = \mu_1 - 3.2$, $\varsigma_1 = \varsigma_2 = 1$, and $[s_1, s_2] = [-48, 0]$).

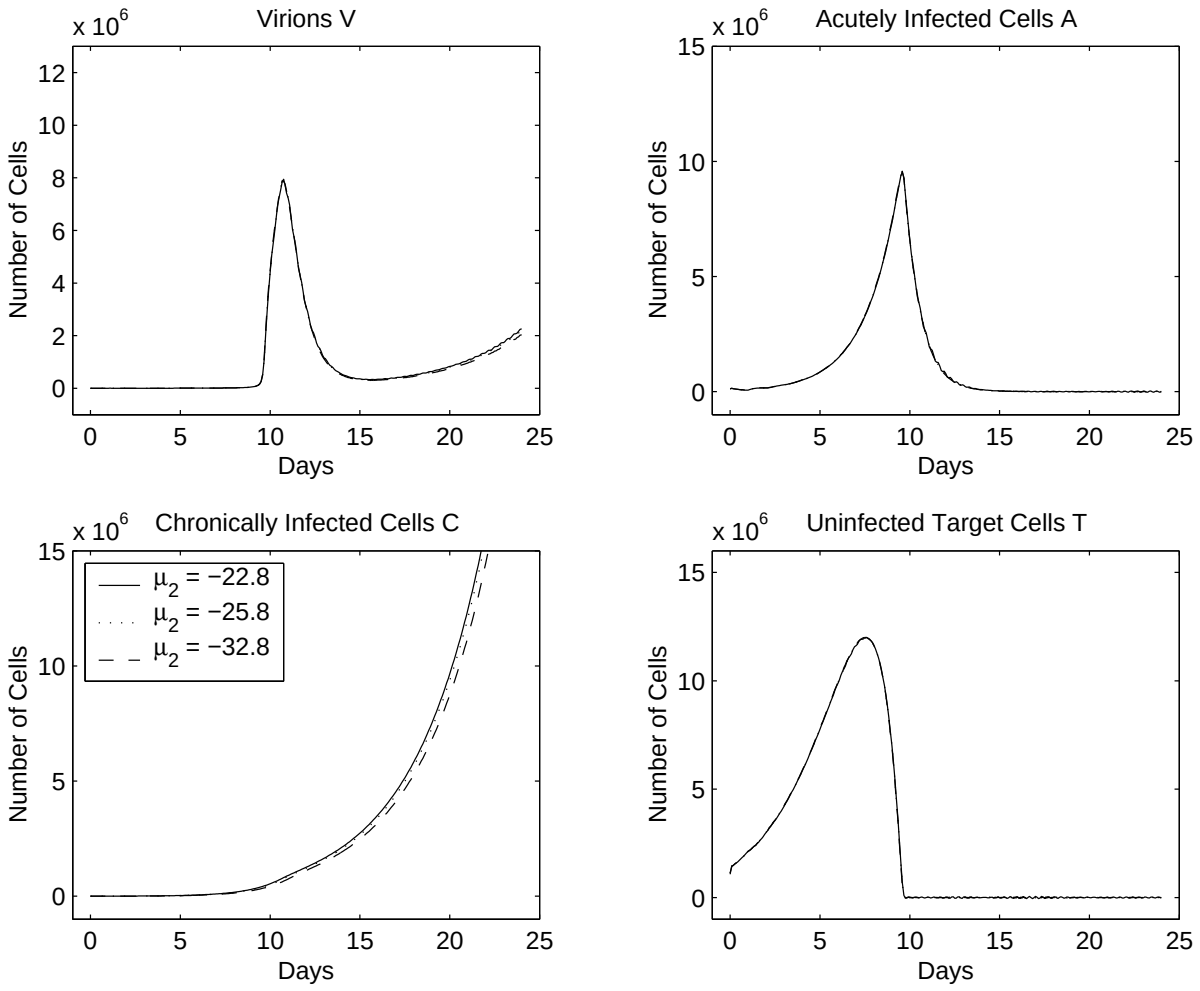

Figure 4.1.3: Simulations of (3.1.14) using $\widehat{k}$ for k_1 and k_2 for several values of μ_2 (with $\mu_1 = -22.8$, $\varsigma_1 = \varsigma_2 = 1$, and $[s_1, s_2] = [-48, 0]$).

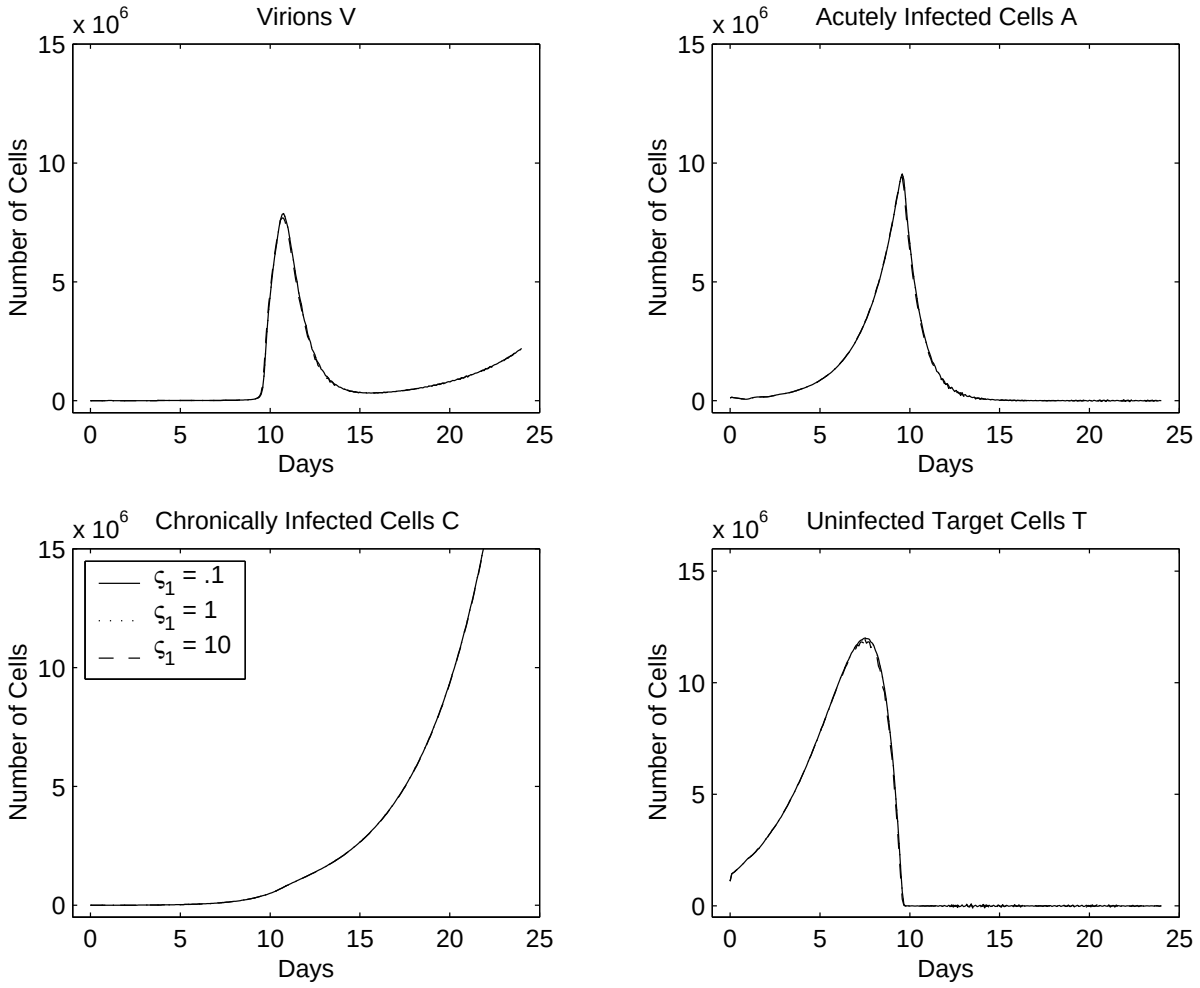

Figure 4.1.4: Simulations of (3.1.14) using $\widehat{k}$ for k_1 and k_2 for several values of ς_1 (with $\mu_1 = -22.8$, $\mu_2 = -26$, $\varsigma_2 = 1$, and $[s_1, s_2] = [-48, 0]$).

identical conclusions.

Clearly, if the width is too large, the solutions will not lie on top of one another. However, for reasonable values of ς_1 (or σ_1), using a Heaviside distribution to represent the kernel (i.e., a discrete delay) seems to adequately capture the dynamics for these simulations. Thus, since the simulations calculated with the discrete delay (like (2.3.5)) take less time to run than the ones with distributed delays, we use them in all the other simulations in this dissertation (unless

Parameter	Value	Units
V_0	0	virions
A_0	$1.5E+5$	cells
C_0	0	cells
T_0	$1.35E+6$	cells
c	0.12	(virion hours)$^{-1}$
r_v	0.035	(cell hours)$^{-1}$
r_u	0.035	(cell hours)$^{-1}$
S	0	cells

Table 4.1: Initial conditions and fixed parameters.

otherwise specified).

Among all the changes we made to the kernels (i.e., varying the smoothness and the parameters μ_1, ς_1, s_1, and s_2), the mean of the delay between viral infection and the initiation of viral production μ_1 seems to be the dominant parameter. Indeed this is the conclusion from our other, more mathematically rigorous investigations presented below.

4.2 Inverse Problem

The initial conditions (from [82]) for all our simulations are depicted in Table 4.1, along with the values of the parameters over which we did not optimize. Furthermore, all of the plots presented in this dissertation are from simulations run with $N = 32$ basis elements.

The results from our numerical experiments in Section 4.1 suggest that for these initial conditions and for values of the parameters within biologically reasonable ranges, the variance of the delay distribution is insignificant. Therefore, we chose to fix the delay distributions with unit jumps at μ_1 and μ_2 (and thus implicitly setting $\sigma_1 = \sigma_2 = 0$). Our intention is to identify

the parameters by minimizing the cost functional

$$J(q) = \frac{1}{10}\sqrt{\sum_{i=1}^{10}\left(X(t_i,q) - \widehat{X}_i\right)^2}, \tag{4.2.1}$$

where $\widehat{X}$ is the data from [82]. However, we do not have direct access to the solution x and thus (as is explained in Section 3.2) we numerically minimize

$$J^N(q) = \frac{1}{10}\sqrt{\sum_{i=1}^{10}\left(X^N(t_i,q) - \widehat{X}_i\right)^2}, \tag{4.2.2}$$

where $X^N = A^N + C^N + T^N$ is an approximation to X and N is an integer describing the accuracy of the numerical simulation. The optimization was performed using the Nelder-Mead nonlinear iterative routine in Matlab (*fminsearch*). Both the experimental results and the numerical best fit solution x^N (using parameters from Table 4.2) are depicted in Figure 4.2.1. Clearly, the simulation appears to be a very good fit to the experimental measurements. However, as mentioned before, we should be wary of drawing decisive conclusions given the sparsity of the experimental observations.

4.2.1 Statistical Significance of the Delays

In this section, we employ the ideas given in the discussions regarding a statistical testing methodology for model comparisons in inverse problems in [9]. We examine the statistical significance of the presence of both types of delays in fitting the models (2.3.5) to experimental data provided by Dr. Michael Emerman [82]. We used the data consisting of the total cells X

Parameter	Value	Units
n_A	0.112	hours^{-1}
n_C	0.011	hours^{-1}
γ	$9E-4$	hours^{-1}
δ_A	0.078	hours^{-1}
δ_C	0.025	hours^{-1}
δ_u	0.017	hours^{-1}
δ	$1E-12$	(cell hours)$^{-1}$
p	$1.3E-6$	(cell hours)$^{-1}$
μ_1	-22.8	hours
μ_2	-26	hours

Table 4.2: Optimal *in vitro* model parameter values.

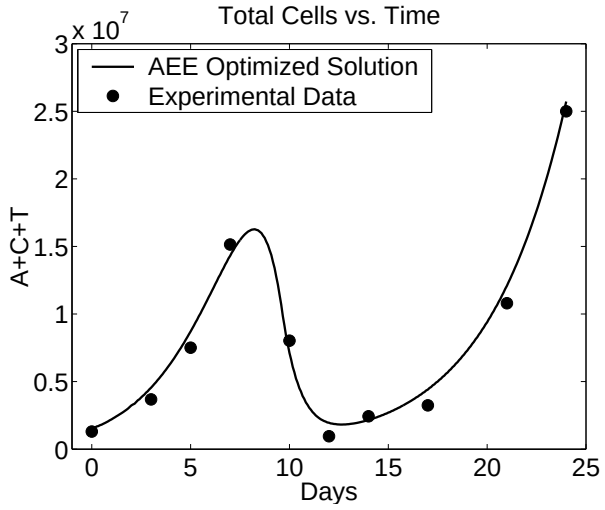

Figure 4.2.1: Data from [82] and best fit simulation x^N of (3.1.1) using parameters from Table 4.2.

Optimization Variables	p^*	τ_1^*	τ_2^*	J^{N*}
$q=(p,0,0)$	$4.28E-8$	-	-	$8.53E+5$
$q=(p,\tau_1,0)$	$1.28E-6$	23.4	-	$2.57E+5$
$q=(p,\tau_1,\tau_2)$	$1.33E-6$	22.8	3.2	$2.37E+5$

Table 4.3: Results from the inverse problem.

(sampled at time-points t_i; $i=1,2,\ldots,10$, denoted by the vector $\widehat{X}$, and depicted in Figure 2.1.1). We then carried out inverse problems for estimating the parameters p, p and τ_1, and p, τ_1, and τ_2, using the least squares criterion of (4.2.1) (or more precisely (4.2.2)). That is, we first estimate p holding $\tau_1=\tau_2=0$, then estimate p and τ_1 with $\tau_2=0$, and finally estimated p, τ_1, and τ_2 simultaneously. Note that we used delta distributions for both delays (in the appropriate simulations) in solving the inverse problem, although the methods apply readily to more general distributions.

As mentioned before, we optimized J^N using the Nelder-Mead nonlinear iterative routine in Matlab (*fminsearch*). The results of the inverse problems are summarized in Table 4.3, with the optimal parameter values denoted by p^*, τ_1^*, τ_2^* and the corresponding fit with the value $J^N(q^*)$ by J^{N*}.

We then investigated the statistical significance by using the test described on page 523 of [9]. The reader should be aware that the statistics we used here are only asymptotically χ^2 as the sample size becomes infinite. With only the ten data points we have to use here, one can rightfully question the legitimacy of our use of the tests given in [9]. None the less, we use these tests here to give some indications of the relevance of improved fits to data. We first considered a null hypothesis of *no dela*y in the acutely infected to viral production step. This

generated a test statistic of

$$U_{10}^{N}\left((p^*,0,0),(p^*,\tau_1^*,0)\right) = 10\frac{J(4.275E-8,0,0)-J(1.279E-6,23.4,0)}{J(1.279E-6,23.4,0)} \cong 23.2\,.$$

With this test statistics, we can use a $\chi^2(1)$ test to reject the hypothesis at all (useful) confidence levels. This suggests that the presence of a delay in the model is statistically significant. That is, the improved fit to data obtained by including the delay is not simply due to the increased degrees of freedom in the model. We also calculated the statistic to determine the significance of both delays versus no delay and found

$$U_{10}^{N}\left((p^*,0,0),(p^*,\tau_1^*,\tau_2^*)\right) \cong 26$$

and the significance of two delays versus one delay, obtaining

$$U_{10}^{N}\left((p^*,\tau_1^*,0),(p^*,\tau_1^*,\tau_2^*)\right) \cong 0.84\,.$$

As expected, the presence of two delays also appears to be statistically significant. However, it is interesting to note that for a null hypothesis of only *one delay* (i.e., $\tau_2 = 0$), the improvement in the fit to data due to the addition of a second delay to the inverse problem is not significant (i.e., we can only reject the hypothesis $\tau_2 = 0$ at 94% or lower confidence levels). This suggests that the modeling of the delay between infection and production is somewhat more critical than modeling a delay between acute productivity and chronic infection in developing an accurate

mathematical representation (which concurs with the conclusions from both the previous and the next section).

4.3 Sensitivity Analysis

In Section 3.3.2, we developed a mathematical framework that allows us to study the sensitivity of solutions to equations of the form (3.1.1) with respect to changes in its constitutive parameters. By Theorem 3.3.3 and the subsequent discussion, we know that there is a solution to the sensitivity equations (with respect to any appropriate parameter) and (by arguments presented in Section(3.3.2)) that we can numerical simulate an approximation to the sensitivity function.

We begin by considering the sensitivity of the solution x to changes in the mean delay between viral infection and the initiation of viral production μ_1.Thus (as described fully in Section 3.3.2), we take a derivative of the system with respect to μ_1 and obtain (3.3.3). Figure 4.3.1 depicts the approximation v^N of the solution v to the (3.3.4) (at $\mu = -22.8$), with each compartment multiplied by μ. It is important to realize that while the y-axis in Figure 4.3.1 has units of cells or virions respectively, it should still be thought of as a plot reflecting changes in the state with respect to changes in μ_1. In other words, we interpret the upper-left plot of Figure 4.3.1 to suggest that for a (positive) change in the mean delay, the virion compartment V will be dramatically smaller just before day 10 and then larger around day 12 (relative to $V(t,-22.8)$). Likewise for a change in μ_1, the acutely infected cell compartment A will be slightly smaller around day 9 and dramatically larger around day 10 (relative to $A(t,-22.8)$). All the plots depicted in Figure 4.3.1 suggest that there will be dramatic changes in the solution for changes

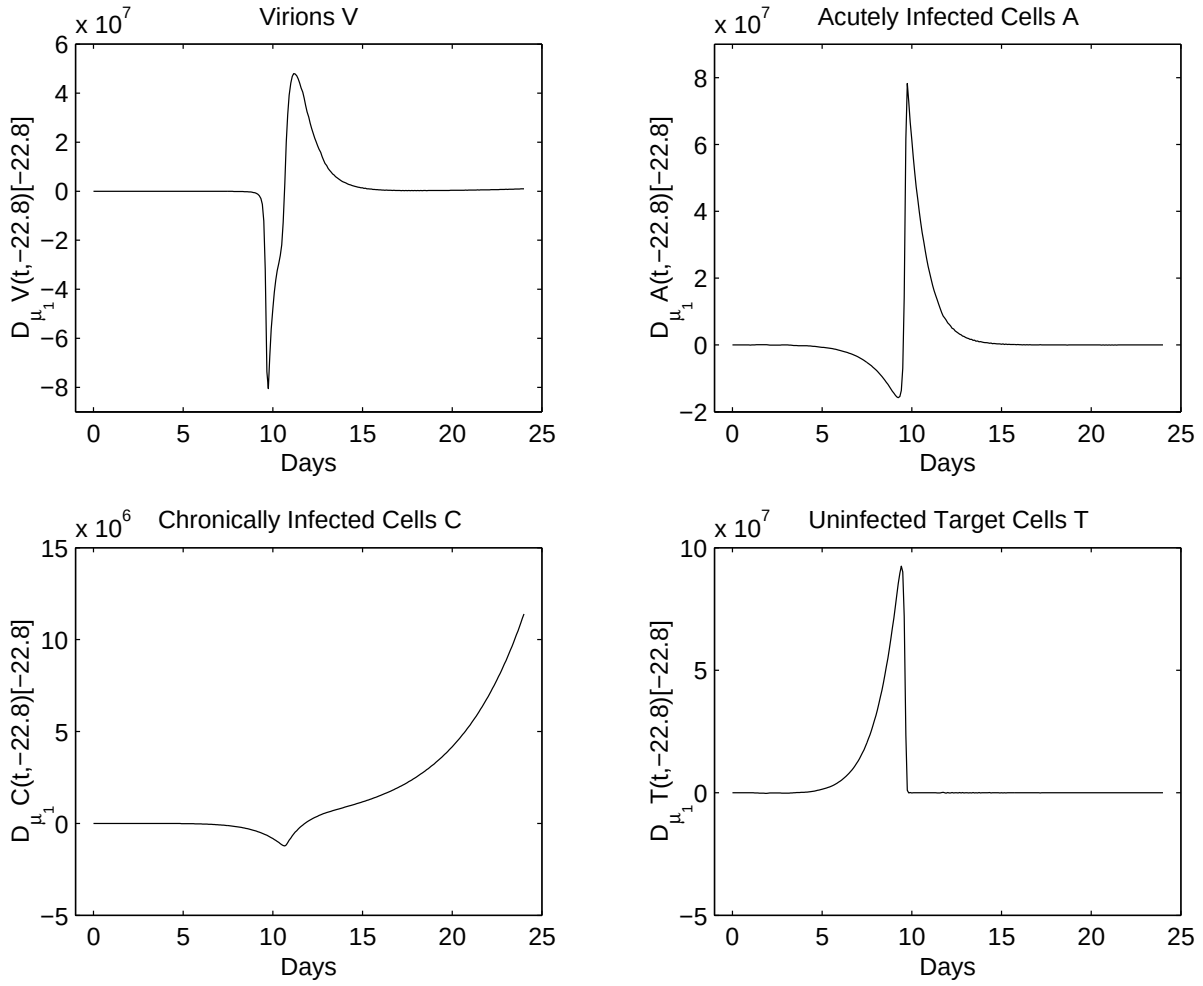

Figure 4.3.1: Simulation of the semirelative sensitivity solution with respect to μ_1 at $\mu_1 = \mu = -22.8$.

in μ_1, and indeed Figure 4.3.2 supports this claim (as well as the specific predictions suggested by the interpretation of Figure 4.3.1). For this simulation, it is important to note that there is practically no indication that the solution x will exhibit any sensitive to μ_1 until around day 5. In other words, for simulations on a short time interval (i.e., $t \in [-r, 120]$ hours), one could easily conclude that the solution x is insensitive to μ_1 (in the neighborhood of $\mu_1 = \mu = -22.8$ hours).

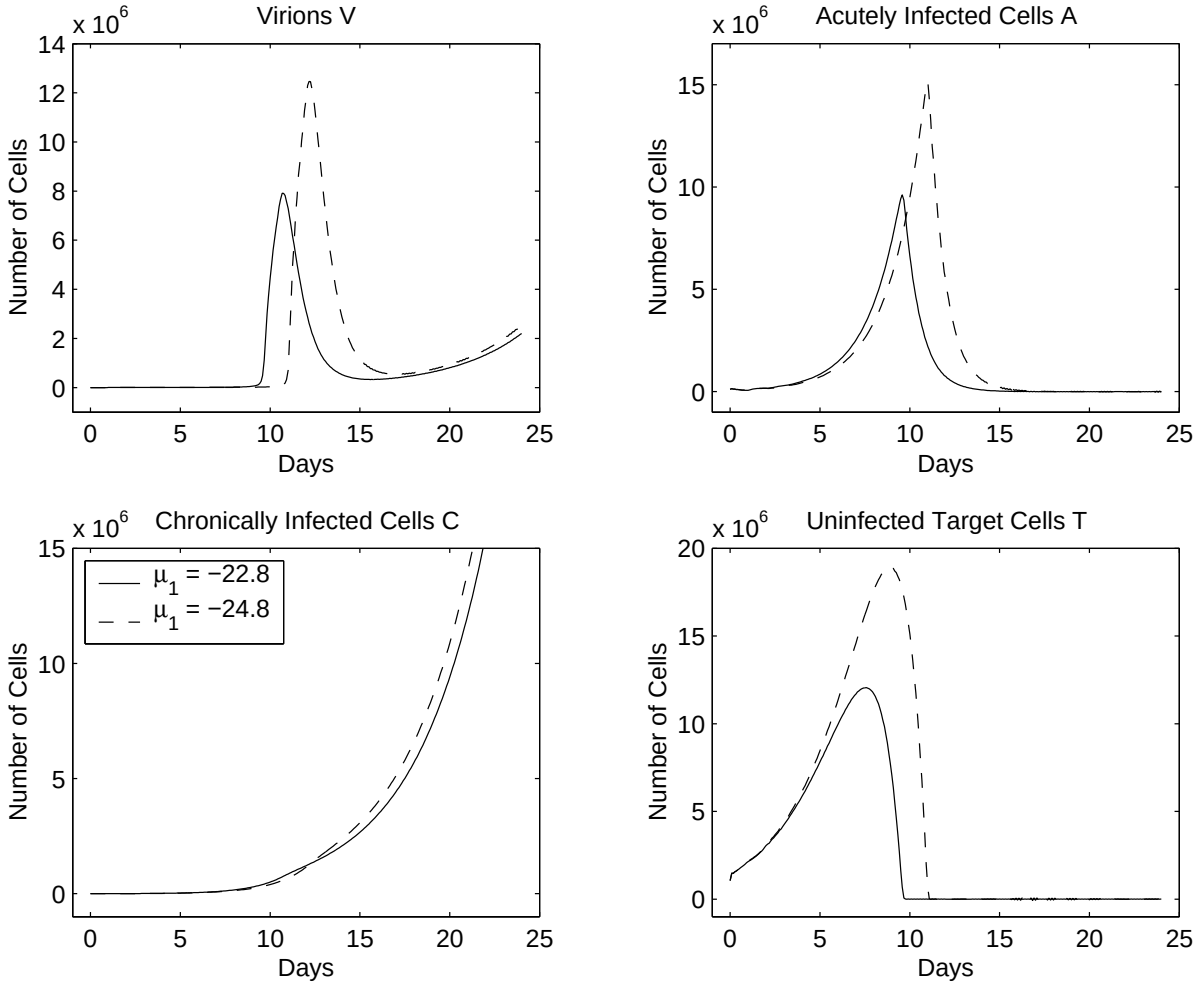

Figure 4.3.2: Simulations of $x^N(t;-24.8)$ and $x^N(t;-22.8)$.

As another example, let us consider the solution parameterized with respect to the infection rate p, i.e., $x(t) = x(t,p)$. Thus the derivative of (3.1.1) with respect to p at $\tilde{p} = 1.3E-6$ is for $0 \leq t \leq t_f$

$$\begin{aligned} \frac{d}{dp}\dot{x}(t,\tilde{p}) &= \frac{d}{dp}L(x(t,\tilde{p}),x_t(\tilde{p})) + \frac{d}{dp}f_1(x(t,\tilde{p}),\tilde{p}) + \frac{d}{dp}f_2(t) \\ \\ \frac{d}{dp}(x(0,\tilde{p}),x_0(\tilde{p})) &= \frac{d}{dp}(\Phi(0),\Phi) \in \mathbb{R}^4 \times \mathscr{C}(-r,0;\mathbb{R}^4)\,. \end{aligned}$$

As mentioned in the last part of Section 3.3.1, the sensitivity equations with respect to different parameters will be slightly different than (3.3.4), but unique solutions still exist and are continuous (for each system of sensitivity equations). Figures 4.3.4 and 4.3.3 depict the semirelative sensitivity functions for p and μ_2, respectively . A comparison of the scales on the vertical axis in Figure 4.3.1 versus the axis in Figures 4.3.4 and 4.3.3 suggests that changes in μ_1 have a more significant influence in the solution x than changes in μ_2 or p (and in one of the compartments by over four orders of magnitude). This result coincides nicely with one of the primary conclusions from Section 4.2.1 in which we concluded that when fitting the data, adding the second delay between than acute and chronic infection was not as significant as inclusion of the delay between viral infection and viral production.

Now that we have established the framework for calculating semirelative sensitivity functions, let us consider how to rank the influence that changes in the individual parameters have upon the solution x. Clearly, there are many options, but for simplicity, we will rank the parameters according to the magnitude of the ∞-norm, e.g., for the virion compartment and the

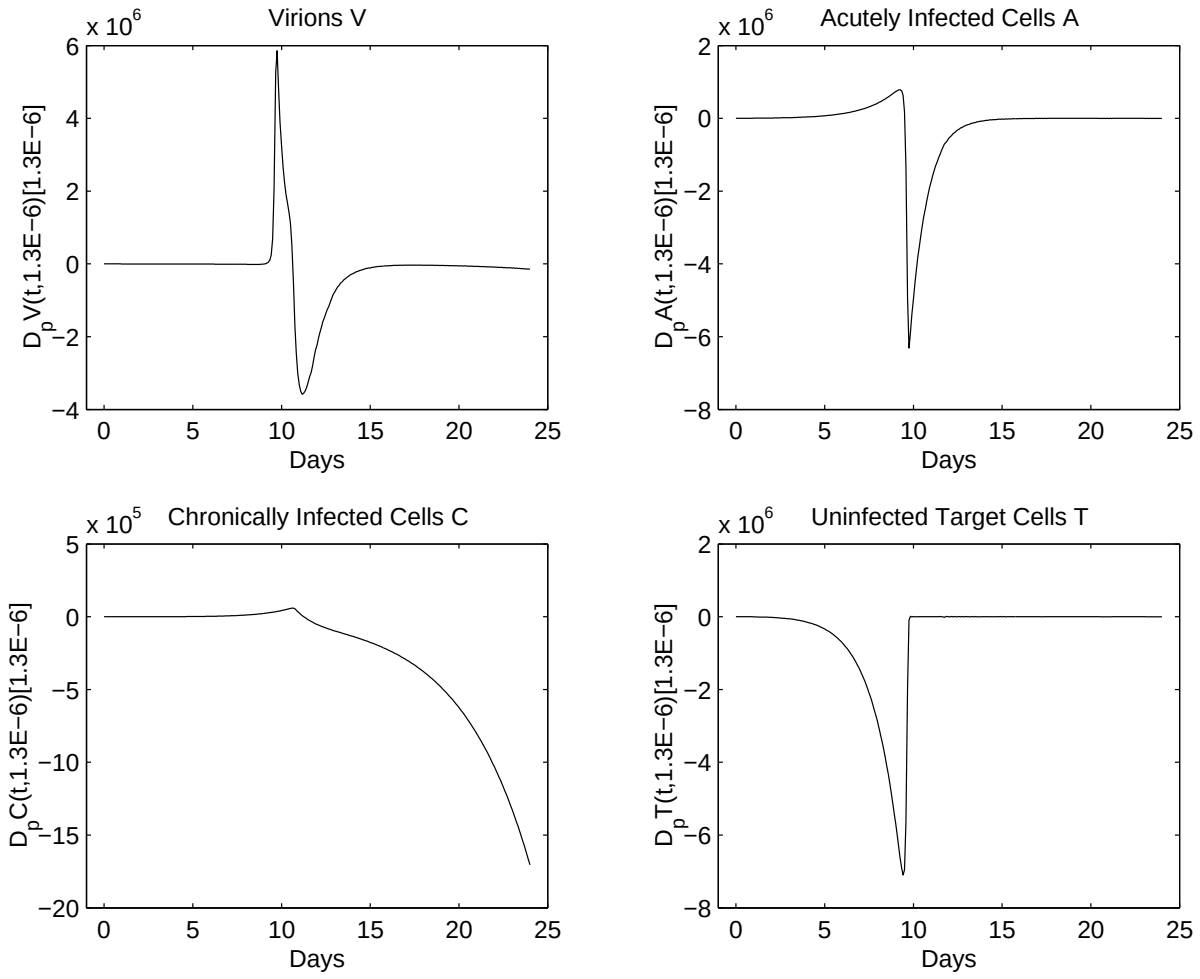

Figure 4.3.3: Simulation of semirelative sensitivity solution with respect to the infection rate p for $\tilde{p} = 1.3E-6$.

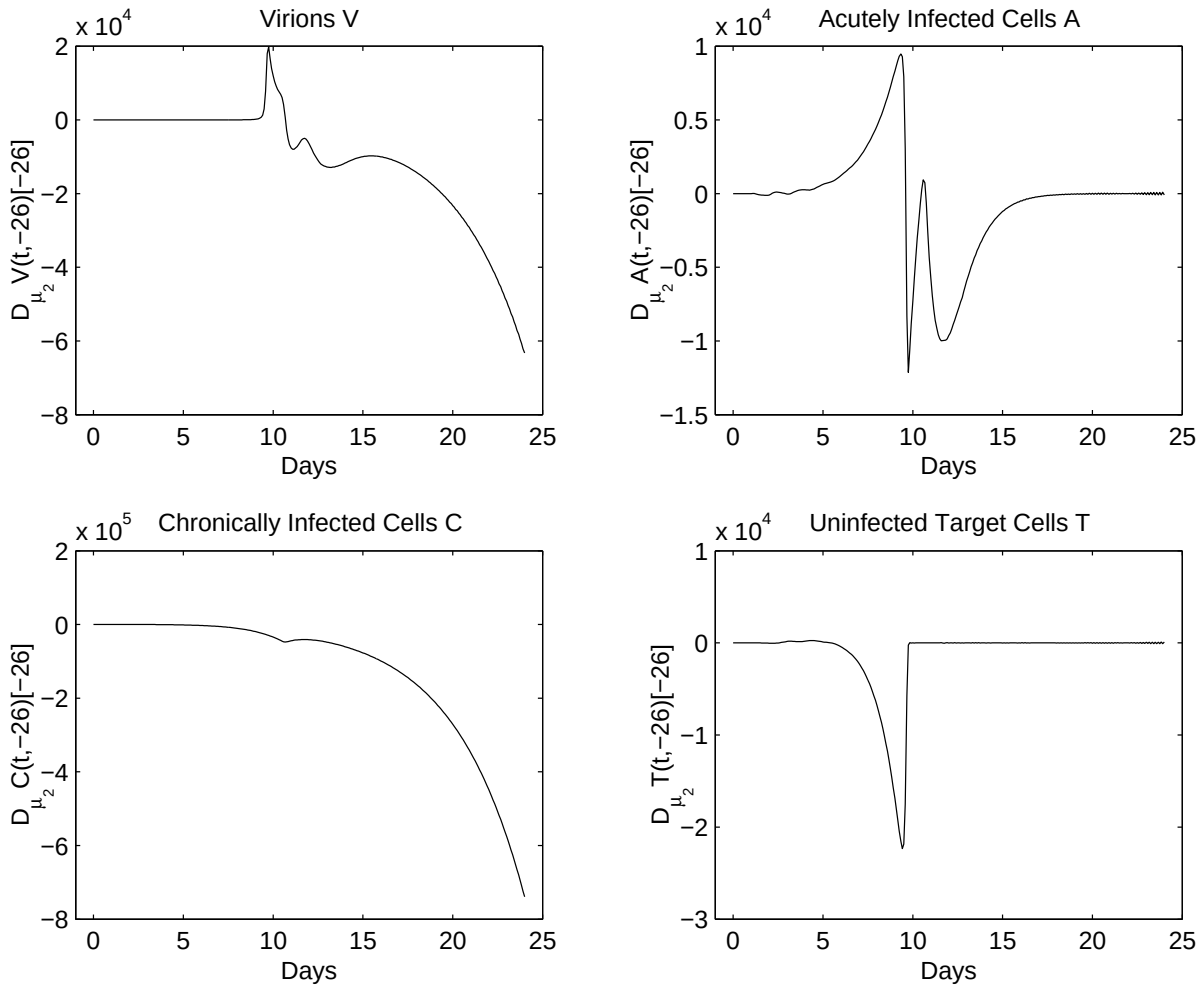

Figure 4.3.4: Simulation of semirelative sensitivity solution with respect to the mean delay between acute and chronic infection μ_2 for $\tilde{\mu}_2 = -26$.

sensitivity with respect to δ_A, we consider

$$\max_{t\in[0,t_f]} \left| D_{\delta_A} V(t, 0.0776)[0.0776] \right| .$$

To illustrate our reasoning, we will focus on just the Virion compartment V. Of the parameters over which we performed our NLS in Section 4.2, the chosen metric was largest for the parameters μ_1, n_A, δ_A, and δ_u. Figure 4.3.5 depicts (for the compartment V), the absolute values of the semirelative sensitivity functions with respect to μ_1, n_A, δ_A, and δ_u, for $t \in [8.5, 15]$ (the domain where there is the most activity in the sensitivity functions). The interpretation of this figure strongly suggests that δ_A and n_A have the strongest influence over the solution in the Virion compartment (in the chosen ∞-norm). Therefore, for the use of equation (3.1.1) (as a model to simulate HIV pathogenesis), both the viral production rate and the death rate for acutely infected cells (n_A and δ_A respectively), should be given high priority for determination with a high degree of accuracy. In other words, these parameters play an important role in the model and obtaining good values for them is more important to the system response than other parameters to which solutions are less sensitive.

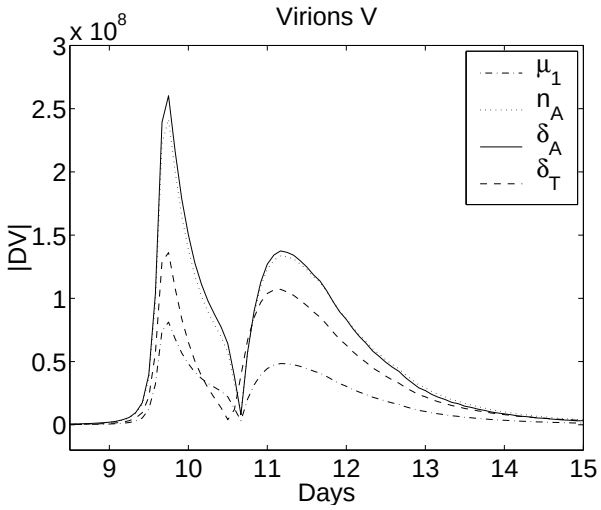

Figure 4.3.5: Absolute value of simulations of semirelative sensitivity solutions for several parameters (V compartment only).

Chapter 5

Conclusions and Future Directions

5.1 Concluding Remarks

A primary focus of this dissertation has been to showcase the power and utility of a variety of mathematical tools when used as an aid in understanding the viral dynamics exhibited by HIV in an *in vitro* experiment. However, it is important to realize that the tools and techniques presented here are not by any means specific to HIV pathogenesis. Indeed, we have attempted to present the ideas in a manner that allows them to be readily adapted for studying other physical systems.

In the first chapter, we offer a basic overview of HIV and its pathogenesis and present a survey of mathematical methods that have been used to study the virus. We also briefly discuss the history of delay differential equations and sensitivity analyses as they have been applied in the biological and physical sciences.

In Chapter 2, we develop a mathematical model to describe the cellular population dy-

namics of an *in vitro* HIV experiment [82]. An important and decidedly nontrivial aspect of modeling the HIV pathogenesis was deciding how to mathematically describe the delay between viral infection and production and indeed, we devote all of Section 2.3 to this topic.

In Chapter 3, we present the theoretical foundations for a rigorous mathematical analysis including: an existence and uniqueness proof for a solution to the model (Section 3.1.1), a numerical scheme based upon an Abstract Evolution Equation approach (Section 3.1.2), and well-posedness results for the inverse problem (Section 3.2) as well as the sensitivity equations (Section 3.3).

With this mathematical framework, we then present in Chapter 4 the results of applying these tools toward understanding the aforementioned *in vitro* experiment. For biologically plausible initial conditions and parameters, our results suggest that the difference between the system with distributed delays and the system with discrete delays is negligible. In other words, it is reasonable to simply use the discrete delay to model the system. The results of our statistical significance test (admittedly based upon sparse data) suggest that the presence of at least one delay is crucial for accurate modeling of the system. Finally, our illustration of a sample sensitivity analysis indicates that (locally) changes in the viral production rate n_A and the death rate δ_A for acutely infected cells will have the most significant influence in the simulation of the viral compartment.

5.2 Future Directions

As this dissertation has focused on the illustration of advanced mathematical and numerical analysis techniques, there are numerous research directions that have not been fully explored. The most pressing need is to acquire more data, against which we can then test our model and our statistical significance results.

The ultimate goal of studying most *in vitro* system is to be able to understand the corresponding *in vivo* system. Therefore, another obvious direction for research would be to test the effectiveness of our methodology on modeling *in vivo* systems. One area in which our techniques easily could be applied would be in designing drug therapy strategies. With the development of anti-retroviral drugs, there has been considerable debate regarding the proper treatment regimens. Recent research suggests that a series of structured treatment interruptions (STI) may help patients maintain suppression of their viral loads [17]. This situation is an excellent opportunity for the application of control theory, and indeed (for an appropriate formulation of the system), there even are tools in the sensitivity analysis literature (such as the gain sensitivity) that could prove to be extremely useful.

In Section 2.1, although we chose to use a random variable to model the variability across the population of cells, there are other ways to incorporate uncertainty. We could have used a stochastic process in modeling the delays, which would have resulted in the viral/cellular population dynamics being described by a stochastic differential equation (SDE). Much like delay equations and sensitivity analyses, there already exists a large body of knowledge about SDE's (containing both analytical results and computational techniques) and as such, this framework

could readily be adapted to study HIV pathogenesis.

There do exist freely available software packages that can simulate both delay equations and integro-differential equations (such as B. Ermentrout's XPPAUT [29]). However, to our knowledge, there does not exist publicly available software which can simulate functional differential equations that are linear in the delay term and can accept an initial condition/history in $\mathbb{R}^n \times L_2(-r, 0; \mathbb{R}^n)$ (as ours can). Therefore, we could consider making the software freely available for download, possibly under a copyleft license such as the GNU General Public License [32].

List of References

[1] H. M. Adelman and R. T. Haftka. Sensitivity analysis of discrete structural systems. *A.I.A.A. Journal*, 24:823–832, 1986.

[2] L. C. Andrews. *Special Functions for engineers and applied mathematicians*. McGraw-Hill, New York, NY, 1992.

[3] H. T. Banks. Identification of nonlinear delay systems using spline methods. In V. Lakshmikantham, editor, *Nonlinear Phenomena in Mathematical Sciences*, pages 47–55. Academic Press, Inc., New York, NY, 1982.

[4] H. T. Banks. Incorporation of uncertainty in inverse problems. Technical Report CRSC-TR02-08, Center for Research in Scientific Computation, North Carolina State University, Raleigh, NC, March 2002.

[5] H. T. Banks and K. L. Bihari. Modeling and estimating uncertainty in parameter estimation. *Inverse Problems*, 17:95–111, 2001.

[6] H. T. Banks, D. M. Bortz, and S. E. Holte. Incorporation of variability into the mathematical modeling of viral delays in HIV infection dynamics. Technical Report CRSC-

TR01-25, Center for Research in Scientific Computation, North Carolina State University, Raleigh, NC, September 2001.

[7] H. T. Banks, M. W. Buksas, and T. Lin. *Electromagnetic Material Interrogation Using Conductive Interfaces and Acoustic Wavefronts*. Number 21 in Frontiers in Applied Mathematics. SIAM, Philadelphia, 2000.

[8] H. T. Banks and J. A. Burns. Hereditary control problems: Numerical methods based on averaging approximations. *SIAM Journal of Control and Optimization*, 16:169–208, 1978.

[9] H. T. Banks and B. G. Fitzpatrick. Statistical methods for model comparison in parameter estimation problems for distributed systems. *Journal of Mathematical Biology*, 28:501–527, 1990.

[10] H. T. Banks and F. Kappel. Spline approximations for functional differential equations. *Journal of Differential Equations*, 34:496–522, 1979.

[11] H. T. Banks, G. A. Pinter, L. K. Potter, M. J. Gaitens, and L. C. Yanyo. Modeling of nonlinear hysteresis in elastomers. *Journal of Intelligent Material Systems and Structures*, 10:116–134, 1999. Tech. Report CRSC-TR99-09, Center for Research in Scientific Computation, North Carolina State University, Raleigh, NC February 1999.

[12] R. Bellman and K. L. Cooke. *Differential-Difference Equations*, volume 6 of *Mathematics in Science and Engineering*. Academic Press, Inc., New York, NY, 1963.

[13] H. Bergström. *Weak Convergence of Measures*. Probability and Mathematical Statistics. Academic Press, Inc., New York, NY, 1982.

[14] P. Billingsley. *Convergence of Probability Measures*. John Wiley & Sons, New York, NY, 1968.

[15] Bitkeeper - The Scalable Distributed Software Configuration Management System. http://www.bitkeeper.com.

[16] H. W. Bode. *Network Analysis and Feedback Amplifier Design*. Van Nostrand, New York, NY, 1945.

[17] S. Bonhoeffer, M. Rembiszewski, G. M. Ortiz, and D. F. Nixon. Risks and benefits of structured antiretroviral drug therapy interruptions in HIV-1 infection. *AIDS*, 14:2313–2322, 2000.

[18] D. M. Bortz, R. Guy, J. Hood, K. Kirkpatrick, V. Nguyen, and V. Shimanovich. Modeling HIV infection dynamics using delay equations. Technical Report CRSC-TR00-24, Center for Research in Scientific Computation, North Carolina State University, Raleigh, NC, October 2000. in: P. A. Gremaud, Z. Li, R. C. Smith, and H. T. Tran (Ed.). Proceedings of the 2000 Industrial Mathematics Modeling Workshop for Graduate Students.

[19] D. S. Callaway and A. S. Perelson. HIV-1 infection and low steady state viral loads. *Bulletin of Mathematical Biology*, 64:29–64, 2002.

[20] S. H. Christie. The Bakerian Lecture: Experimental determination of the laws of

magneto-electric induction in different masses of the same metal, and of its intensity in different metals. *Philosophical Transactions of the Royal Society of London*, 123:95–142, 1833.

[21] D. R. Cox and H. D. Miller. *The Theory of Stochastic Processes*. Chapman and Hall, London, 1965.

[22] J. B. Cruz, editor. *System Sensitivity Analysis*. Dowden, Hutchinson & Ross, Inc., Stroudsburg, PA, 1973.

[23] R. V. Culshaw and S. Ruan. A delay-differential equation model of HIV infection of CD4+ T-cells. *Mathematical Biosciences*, 165:27–39, 2000.

[24] J. M. Cushing. *Integrodifferential Equations and Delay Models in Population Dynamics*, volume 20 of *Lecture Notes in Biomathematics*. Springer-Verlag, New York, NY, 1977.

[25] O. Diekmann, S. A. van Gils, S. M. Verduyn Lunel, and H. O. Walther. *Delay Equations: Functional-, Complex-, and Nonlinear Analysis*, volume 110 of *Applied Mathematical Sciences*. Springer-Verlag, New York, NY, 1995.

[26] R. D. Driver. *Ordinary and Delay Differential Equations*, volume 20 of *Applied Mathematical Sciences*. Springer-Verlag, New York, NY, 1977.

[27] M. Emerman. HIV, Vpr, and the cell cycle. *Current Biol.*, 6:1096–1103, 1996.

[28] M. Emerman, November 2000. personal communication.

[29] B. Ermentrout. *Simulating, Analyzing, and Animating Dynamical Systems: A Guide to XPPAUT for Researchers and Students*. Society for Industrial and Applied Mathematics, Philadelphia, PA, 2002.

[30] M. Eslami. *Theory of Sensitivity in Dynamic Systems: An Introduction*. Springer-Verlag, Berlin, 1994.

[31] P. M. Frank. *Introduction to System Sensitivity Theory*. Academic Press, Inc., New York, NY, 1978.

[32] Free Software Foundation, Inc., 59 Temple Place - Suite 330, Boston, MA 02111-1307, USA. *GNU General Public License, Version 2*, June 1991. See http://www.fsf.org/licenses/licenses.html for details.

[33] A. Friedman. *Foundations of Modern Analysis*. Dover Publications, Inc., New York, NY, 1982.

[34] F. Frisch and H. Holme. The characteristic solution of a mixed difference and differential equation occurring in economic dynamics. *Econometrica*, 3:225–239, 1935.

[35] B. Fristedt and L. Gray. *A Modern Approach to Probability Theory*. Probability and its Applications. Birkhäuser, Boston, MA, 1997.

[36] W. C. Goh, M. E. Rogel, C. M. Kinsey, S. F. Michael, P. N. Fultz, M. A. Nowak, B. H. Hahn, and M. Emerman. HIV-1 Vpr increases viral expression by manipulation of the cell cycle: A mechanism for selection of Vpr *in vivo*. *Nature Medicine*, 4:65–71, 1998.

[37] H. Górecki, S. Fuksa, P. Grabowski, and A. Korytowski. *Analysis and Synthesis of Time Delay Systems*. John Wiley & Sons, New York, NY, 1989.

[38] Z. Grossman, M. Feinberg, V. Kuznetsov, D. Dimitrov, and W. Paul. HIV infection: how effective is drug combination treatment? *Immunology Today*, 19:528–532, 1998.

[39] Z. Grossman, M. Polis, M. B. Feinberg, Z. Grossman, I. Levi, S. Jankelevich, R. Yarchoan, J. Boon, F. de Wolf, J. M. A. Lange, J. Goudsmit, D. S. Dimitrov, and W. E. Paul. Ongoing HIV dissemination during HAART. *Nature Medicine*, 5:1099–1104, 1999.

[40] A. B. Gumel, P. N. Shivakumar, and B. M. Sahai. A mathematical model for the dynamics of HIV-1 during the typical course of infection. *Nonlinear Analysis*, 47:1773–1783, 2001.

[41] J. K. Hale and S. M. Verduyn Lunel. *Introduction to Functional Differential Equations*, volume 99 of *Applied Mathematical Sciences*. Springer-Verlag, New York, NY, 1993.

[42] A. V. M. Herz, S. Bonhoeffer, R. M. Anderson, R. M. May, and M. A. Nowak. Viral dynamics *in vivo*: limitations on estimates of intracellular delay and virus decay. *Proceedings of the National Academy of Sciences, USA*, 93:7247–7251, 1996.

[43] D. D. Ho, A. U. Neumann, A. S. Perelson, W. Chen, J. M. Leonard, and M. Markowitz. Rapid turnover of plasma virions and CD4 lymphocytes in HIV-1 infection. *Nature*, 373:123–126, 1995.

[44] S. Holte and M. Emerman. A competition model for viral inhibition of host cell proliferation. *Mathematical Biosciences*, 166:69–84, 2000.

[45] G. E. Hutchinson. Circular causal systems in ecology. *Annals of the New York Academy of Sciences*, 50:221–246, 1948.

[46] R. L. Iman and J. C. Helton. An investigation of uncertainty and sensitivity analysis techniques for computer models. *Risk Analysis*, 8:71–90, 1988.

[47] A. Jensen. An elucidation of Erlang's statistical works through the theory of stochastic processes. In E. Brockmeyer, H. L. Halstrøm, and A. Jensen, editors, *The life and works of A. K. Erlang*, pages 23–100. The Copenhagen Telephone Company, Copenhagen, 1948.

[48] A. Kamina, R. W. Makuch, and H. Zhao. Stochastic modeling of early HIV-1 population dynamics. *Mathematical Biosciences*, 170:187–198, 2001.

[49] J. L. Kelley. *General Topology*. Van Nostrand-Reinhold, Princeton, NJ, 1955.

[50] D. Kirschner, S. Lenhart, and S. Serbin. Optimal control of chemotherapy of HIV. *Journal of Mathematical Biology*, 35:775–792, 1997.

[51] M. Kleiber, H. Antúnez, T. D. Hien, and P. Kowalczyk. *Parameter Sensitivity in Nonlinear Mechanics: Theory and Finite Element Computations*. John Wiley & Sons, New York, NY, 1997.

[52] D. E. Knuth. *The Texbook*. Addison-Welsey Publishing Company, Inc., Reading, MA, 1986.

[53] I. Kramer. Modeling the dynamical impact of HIV on the immune system: Viral clearance, infection, and AIDS. *Mathematical and Computer Modelling*, 29:95–112, 1999.

[54] Y. Kuang. *Delay Differential Equations With Applications in Population Dynamics*. Number 191 in Mathematics in Science and Engineering. Academic Press, Inc., New York, NY, 1993.

[55] S. Kubiak, H. Lehr, T. Moeller, A. Parker, and E. Swim. Modeling control of HIV infection through structured treatment interruptions with recommendations for experimental protocol. In *Proceedings of the 2001 Industrial Mathematics Modeling Workshop for Graduate Students*, number CRSC-TR01-27 in Center for Research in Scientific Computation Techical Report, North Carolina State University, Raleigh, NC, November 2001.

[56] S. Lang. *Analysis II*. Addison-Welsey Publishing Company, Inc., Reading, MA, 1969.

[57] Linux Home Page at Linux Online. http://www.linux.org.

[58] A. L. Lloyd. The dependence of viral parameter estimates on the asumed viral load life cycle: limitations of studies of viral load data. *Proceedings of the Royal Society of London Series B*, 268:847–854, 2001.

[59] A. L. Llyod. Destabilization of epidemic models with the inclusion of realistic distri-

butions of infectious periods. *Proceedings of the Royal Society of London Series B*, 268:985–993, 2001.

[60] M. Loève. *Probability Theory*. The University Series in Higher Mathematics. D. Van Nostrand Company, Inc., Princeton, NJ, 1960.

[61] D. G. Luenberger. *Optimization by Vector Space Methods*. John Wiley & Sons, New York, NY, 1969.

[62] LyX - The Document Processor. http://www.lyx.org.

[63] R. M. May. *Stability and Complexity in Model Ecosystems*. Princeton University Press, Princeton, NJ, 2001. (orignially published 1973).

[64] N. Minorsky. Self-excited oscillations in a dynamical system possessing retarded actions. *Journal of Applied Mechanics*, 9:65–71, 1942.

[65] J. E. Mittler, M. Markowitz, D. D. Ho, and A. S. Perelson. Improved estimates for HIV-1 clearance rate and intracellular delay. *AIDS*, 13:1415–1417, 1999.

[66] J. E. Mittler, B. Sulzer, A. U. Neumann, and A. S. Perelson. Influence of delayed viral production on viral dynamics in HIV-1 infected patients. *Mathematical Biosciences*, 152:143–163, 1998.

[67] H. A. Monteiro, C. H. O. Gonçalves, and J. R. C. Piqueira. A condition for successful escape of a mutant after primary HIV infection. *Journal of Theoretical Biology*, 203:399–406, 2000.

[68] J. D. Murray. *Mathematical Biology,* volume 19 of *Biomathematics*. Springer-Verlag, New York, NY, 1989.

[69] J. M. Murray, G. Kaufmann, A. D. Kelleher, and D. A. Cooper. A model of primary HIV-1 infection. *Mathematical Biosciences*, 154:57–85, 1998.

[70] P. W. Nelson, J. E. Mittler, and A. S. Perelson. Effect of drug efficacy and the eclipse phase of the viral life cycle on estimates of HIV viral dynamic parameters. *Journal of Acquired Immune Deficiency Syndromes*, 26:405–412, 2001.

[71] P. W. Nelson, J. D. Murray, and A. S. Perelson. A model of HIV-1 pathogenesis that includes an intracellular delay. *Mathematical Biosciences*, 163:201–215, 2000.

[72] P. W. Nelson and A. S. Perelson. Mathematical analysis of delay differential equation models of HIV-1 infection. *Mathematical Biosciences*, 179:73–94, 2002.

[73] M. A. Nowak, S. Bonhoeffer, G. M. Shaw, and R. M. May. Anti-viral drug treatment: Dynamics of resistance in free virus and infected cell populations. *Journal of Theoretical Biology*, 184:203–217, 1997.

[74] M. A. Nowak and R. M. May. *Virus Dynamics: Mathematical Principles of Immunology and Virology*. Oxford University Press, Inc., New York, NY, 2000.

[75] A. S. Perelson. Modeling viral and immune system dynamics. *Nature Reviews Immunology*, 2:28–36, 2002.

[76] A. S. Perelson, P. Essunger, Y. Cao, M. Vesanen, A. Hurley, K. Saksela, M. Markowitz, and D. D. Ho. Decay characteristics of HIV-1-infected compartments during combination therapy. *Nature*, 387:188–191, 1997.

[77] A. S. Perelson and P. W. Nelson. Mathematical analysis of HIV-1 dynamics *in vivo*. *SIAM Review*, 41:3–44, 1999.

[78] A. S. Perelson, A. U. Neumann, M. Markowitz, J. M. Leonard, and D. D. Ho. HIV-1 dynamics *in vivo*: virion clearance rate, infected cell life-span, and viral generation time. *Science*, 271:1582–1586, 1996.

[79] A. N. Phillips. Reduction of HIV concentration during acute infection: Independence from a specific immune response. *Science*, 271:497–499, 1996.

[80] E. Pisani, B. Schwartländer, S. Cherney, and A. Winter, editors. *Global Summary of the HIV/AIDS Epidemic, end 1999*. Joint United Nations Programme on HIV/AIDS, June 2000.

[81] B. Ramratnam, S. Bonhoeffer, J. Binley, A. Hurley, L. Zhang, J. E. Mittler, M. Markowitz, J. P. Moore, A. S. Perelson, and D. D. Ho. Rapid production and clearance of HIV-1 and hepatitis C virus assessed by large volume plasma apheresis. *The Lancet*, 354:1782–1785, 1999.

[82] M. E. Rogel, L. I. Wu, and M. Emerman. The human immunodeficiency virus type 1 vpr gene prevents cell proliferation during chronic infection. *Journal of Virology*, 69:882–888, 1995.

[83] M. A. Stafford, L. Corey, Y. Cao, E. S. Daar, D. D. Ho, and A. S. Perelson. Modeling plasma virus concentration during primary HIV infection. *Journal of Theoretical Biology*, 203:285–301, 2000.

[84] L. G. Stanley. *Computational Methods for Sensitivity Analysis with Applications for Elliptic Boundary Value Problems*. Ph.D. dissertation, Virginia Polytechnic Institute and State University, Blacksburg, VA, 1999.

[85] N. I. Stilianakis, K. Dietz, and D. Schenzle. Analysis of a model for the pathogenesis of AIDS. *Mathematical Biosciences*, 145:27–46, 1997.

[86] D. W. Stroock. *Probability Theory, An Analytical View*. Cambridge University Press, New York, NY, 1993.

[87] J. Tam. Delay effect in a model for virus replication. *IMA Journal of Mathematics Applied to Medicine and Biology*, 16:29–37, 1999.

[88] W. Tan and H. Wu. Stochastic modeling of the dynamics of CD4+ T-cell infection by HIV and some monte carlo studies. *Mathematical Biosciences*, 147:173–205, 1998.

[89] W. Tan and Z. Xiang. Some state space models of HIV pathogenesis under treatment by anti-viral drugs in HIV-infected individuals. *Mathematical Biosciences*, 156(69):69–94, 1999.

[90] R. Tomović. *Sensitivity Analysis of Dynamic Systems*. McGraw-Hill Electronic Sciences Series. McGraw-Hill Book Company, Inc., New York, NY, 1963.

[91] R. Tomović and M. Vukobratović. *General Sensitivity Theory*. Number 35 in Modern Analytic and Computational Methods in Science and Mathematics. American Elsevier Publishing Company, Inc., New York, NY, 1972.

[92] H. C. Tuckwell and E. Le Corfec. A stochastic model for early HIV-1 population dynamics. *Journal of Theoretical Biology*, 195:451–463, 1998.

[93] D. Verotta and F. Schaedeli. Non-linear dynamics models characterizing long-term virological data from AIDS clinical trials. *Mathematical Biosciences*, 176:163–183, 2002.

[94] X. Wei, S. K. Ghosh, M. E. Taylor, V. A. Johnson, E. A. Emini, P. Deutsch, J. D. Lifson, S. Bonhoeffer, M. A. Nowak, B. H. Hahn, M. S. Saag, and G. M. Shaw. Viral dynamics in human immunodeficiency virus type 1 infection. *Nature*, 373:117–122, 1995.

[95] L. M. Wein, R. M. D'Amato, and A. S. Perelson. Mathematical analysis of antiretroviral therapy aimed at HIV-1 eradication or maintenance of low viral loads. *Journal of Theoretical Biology*, 192:81–98, 1998.

[96] L. M. Wein, S. A. Zeinos, and M. A. Nowak. Dynamic multidrug therapies for HIV: A control theoretic approach. *Journal of Theoretical Biology*, 185:15–29, 1997.

[97] D. Wick and S. G. Self. Early HIV infection *in vivo*: Branching-process model for studying timing of immune responses and drug therapy. *Mathematical Biosciences*, 165:115–134, 2000.

[98] A. Wierzbicki. *Models and Sensitivity of Control Systems*, volume 5 of *Studies in Automation and Control*. Elsevier Science Publishing Company, Inc., New York, NY, 1984.

[99] D. Wodarz and V. A. A. Jansen. The role of T cell help for anti-viral CTL responses. *Journal of Theoretical Biology*, 211:419–432, 2001.

[100] D. Wodarz, A. L. Lloyd, V. A. A. Jansen, and M. A. Nowak. Dynamics of macrophage and t cell infection by HIV. *Journal of Theoretical Biology*, 196:101–113, 1999.

[101] H. Wu, A. A. Ding, and V. de Gruttola. Estimation of HIV dynamic parameters. *Statistics in Medicine*, 17:2463–2485, 1998.

[102] S. Zhang and J. Jin. *Computation of Special Functions*. John Wiley & Sons, New York, NY, 1996.

APPENDICES

Appendix A

Gamma Convolution Implementation

We wish to evaluate a term of the form

$$\int_{-r}^{0} A(t+s)\, k_{\Gamma}(s;\mu,\sigma)\, ds, \tag{A.0.1}$$

where $r > 0$, A is an unknown function in $\mathscr{C}(-r,0;\mathbb{R})$, and

$$k_{\Gamma}(s;\mu,\sigma) = \frac{(-s)^{\left(\frac{\mu}{\sigma}\right)^2-1} e^{\left(\frac{s\mu}{\sigma^2}\right)}}{\Gamma\left(\left(\frac{\mu}{\sigma}\right)^2\right)\left(\frac{\sigma^2}{\mu}\right)^{\left(\frac{\mu}{\sigma}\right)^2}}, \tag{A.0.2}$$

where $\Gamma(\cdot)$ is the Gamma function. The problem with evaluating (A.0.2) (for finite values of s) is one of insufficient computational resources. On currently available 32 bit computers, the largest floating point number is about $2E+308$. Thus for $(\mu/\sigma)^2$ greater than about 171, the function $\Gamma((\mu/\sigma)^2)$ returns infinity. The term $(\sigma^2/\mu)^{((\mu/\sigma)^2)}$ will (in theory) cancel out $\Gamma((\mu/\sigma)^2)$. However, since the smallest representable number (on 32 bit computers) is about

$2E-308$, the computer rounds off the numerator to zero. Thus, numerical evaluation of the integral (A.0.1) is simply not possible for many reasonable values of μ and σ (in particular it's not possible for values in which we are interested).

Upon examination of (A.0.1), we observe that without the A, (A.0.1) is merely a normalized Gamma function. However, references on special functions (such as [2, 102]) do not suggest any methods for dealing with this form of the integral (A.0.1).

To resolve the computational issues generated by (A.0.2), let us consider the exponential of the natural log of $k_\Gamma(s;\mu,\sigma)$ for $s \leq 0$

$$\begin{aligned}\exp\left\{\ln\left(k_\Gamma(s;\mu\,\sigma)\right)\right\} &= \exp\left\{\left(\left(\frac{\mu}{\sigma}\right)^2-1\right)\ln(-s)+\frac{s\mu}{\sigma^2}-\left(\frac{\mu}{\sigma}\right)^2\ln\left(\frac{\sigma^2}{\mu}\right)\right. \\ &\qquad \left.-\ln\left(\Gamma\left(\left(\frac{\mu}{\sigma}\right)^2\right)\right)\right\}.\end{aligned}$$

The first three terms inside the exponential

$$\left(\left(\frac{\mu}{\sigma}\right)^2-1\right)\ln(-s)+\frac{s\mu}{\sigma^2}-\left(\frac{\mu}{\sigma}\right)^2\ln\left(\frac{\sigma^2}{\mu}\right)$$

can easily be evaluated (for values of s in our domain of interest) on 32 bit computers. For the last term, we make use of the Weierstrass form of the Gamma function [102],

$$\begin{aligned}\ln\left(\Gamma\left(\left(\frac{\mu}{\sigma}\right)^2\right)\right) &= \ln\left(\frac{e^{-\gamma\mu^2/\sigma^2}}{\mu^2/\sigma^2}\lim_{n\to\infty}\prod_{i=1}^{n}\left\{\frac{e^{\mu^2/(\sigma^2 i)}}{1+\frac{\mu^2}{\sigma^2 i}}\right\}\right) \\ &= -\gamma\left(\frac{\mu}{\sigma}\right)^2-2\ln\left(\frac{\mu}{\sigma}\right)+\sum_{i=1}^{\infty}\left\{\frac{\mu^2}{\sigma^2 i}-\ln\left(1+\frac{\mu^2}{\sigma^2 i}\right)\right\},\end{aligned}$$

where

$$\gamma = -\int_0^\infty e^{-x} \ln(x)\, dx \approx 0.577216,$$

the Euler-Mascheroni constant. Clearly the term $-\gamma(\mu/\sigma)^2 - 2\ln(\mu/\sigma)$ can be numerically evaluated for parameters in our domain of interest. Thus, let us consider the infinite series

$$\sum_{i=1}^{\infty} \left\{ \frac{\mu^2}{\sigma^2 i} - \ln\left(1 + \frac{\mu^2}{\sigma^2 i}\right) \right\},$$

and note that we can analytically evaluate for $a, b \in \mathbb{R}$,

$$\int_a^\infty \left\{ \frac{b}{x} - \ln\left(1 + \frac{b}{x}\right) \right\} dx = -b + (a+b)\ln\left(\frac{a+b}{a}\right).$$

For large n we know that

$$\begin{aligned} \sum_{i=1}^{\infty} \left\{ \frac{\mu^2}{\sigma^2 i} - \ln\left(1 + \frac{\mu^2}{\sigma^2 i}\right) \right\} \quad &\approx \quad \sum_{i=1}^{n} \left\{ \frac{\mu^2}{\sigma^2 i} - \ln\left(1 + \frac{\mu^2}{\sigma^2 i}\right) \right\} \\ &\quad + \int_n^\infty \left\{ \frac{\mu^2}{\sigma^2 \xi} - \ln\left(1 + \frac{\mu^2}{\sigma^2 \xi}\right) \right\} d\xi, \end{aligned}$$

and if we use the substitutions and approximations from above, we can then compute (A.0.2) by

$$\begin{aligned} k_\Gamma(s; \mu, \sigma) \quad &\approx \quad \exp\left\{ \left(\left(\frac{\mu}{\sigma}\right)^2 - 1 \right) \ln(t) - \frac{t\mu}{\sigma^2} - \left(\frac{\mu}{\sigma}\right)^2 \ln\left(\frac{\sigma^2}{\mu}\right) + \gamma\left(\frac{\mu}{\sigma}\right)^2 + \ln\left(\left(\frac{\mu}{\sigma}\right)^2 \right) \right. \\ &\quad \left. - \sum_{i=1}^{n} \left\{ \frac{\mu^2}{\sigma^2 i} - \ln\left(1 + \frac{\mu^2}{\sigma^2 i}\right) \right\} + \frac{\mu^2}{\sigma^2} - \left(n + \frac{\mu^2}{\sigma^2}\right) \ln\left(\frac{n + \mu^2/\sigma^2}{n}\right) \right\}. \end{aligned}$$

Therefore, it is possible to evaluate (A.0.2) in our specific regime of interest, and thus numerically integrate (A.0.1) when called for in our calculations. For $n = 10^6$, this approximation yields 5 digits of accuracy and only requires about 1 second of evaluation time on a Pentium III (866 MHz) workstation. Since we can only be confident of about 5 digits of accuracy in the simulations, this is a reasonable approximation for our purposes.